



**WYDZIAŁ BIOLOGII
i OCHRONY ŚRODOWISKA**
Uniwersytet Łódzki

InterDOC-START
Interdyscyplinarne Studia Doktoranckie

Agata Zakrzewska

Wykorzystanie danych termalnych pozyskanych z pułapu lotniczego do określania stanu zdrowotnego wybranych gatunków drzew

Usage of thermal infrared data obtained from the
airborne level to determine the trees' health status
of selected species

Praca doktorska

wykonana w Katedrze Biogeografii,
Paleoekologii i Ochrony Przyrody

Promotor:

- Dr hab. Dominik Kopec
prof. nadzw. UŁ

Promotor pomocniczy:

- Dr inż. Adrian Ochtyra

*Składam serdeczne podziękowania dla
dr. hab. Dominika Kopcia, prof. UŁ, za zaproszenie mnie
do realizacji studiów doktoranckich pod jego opieką,
pomoc i poświęcony czas w trakcie przygotowywania
niniejszej rozprawy doktorskiej.*

*Dziękuję również dr inż. Adrianowi Ochtyrze
za opiekę merytoryczną i pomoc
w powstawaniu niniejszej rozprawy.*

*Dziękuję również moim rodzicom
za nieustanne wsparcie i pomoc
w realizowaniu celów.*

Spis treści

Źródła finansowania.....	3
Dorobek naukowy	4
1. Wstęp.....	6
1.1. Ocena stanu zdrowotnego drzew.....	6
1.2. Wykorzystanie teledetekcyjnych danych termalnych do szacowania stanu zdrowotnego drzew	7
2. Cel pracy	8
3. Materiały i metody	9
3.1. Opis terenów badań i gatunków	9
3.2. Zbiór i przetwarzanie danych teledetekcyjnych	10
3.3. Pozyskanie naziemnych danych referencyjnych.....	11
3.4. Wyznaczanie temperatur koron drzew	13
3.5. Analizy statystyczne.....	13
4. Omówienie wyników prac wchodzących w skład rozprawy doktorskiej	14
4.1. Zmienność temperatury koron wybranych gatunków drzew rosnących w lesie i poza lasem z wykorzystaniem lotniczych danych termalnych (3,6–4,9 μm)	14
4.2. Oszacowanie uszkodzeń w indywidualnych koronach drzew świerka pospolitego spowodowane przez kornika drukarza przy użyciu fuzji danych termalnych i lotniczego skanowania laserowego.....	15
4.3. Czy temperatura korony mierzona z poziomu lotniczego może być wskaźnikiem zdrowia drzew w środowisku miejskim?	16
5. Wnioski	18
Literatura	19
Streszczenie.....	22
Summary	24

Załączniki:

Kopie publikacji wchodzących w skład rozprawy doktorskiej

Oświadczenia współautorów publikacji wchodzących w skład rozprawy doktorskiej

Źródła finansowania

Badania w niniejszej pracy doktorskiej prowadzone były w ramach projektów:



Unia Europejska
Europejski Fundusz Społeczny



"InterDOC-START – Interdyscyplinarne Studia Doktoranckie na Wydziale BiOŚ UŁ” – Program Operacyjny Wiedza Edukacja Rozwój 2014-2020, Oś priorytetowa III. Szkolnictwo wyższe dla gospodarki i rozwoju, Działanie 3.2 Studia doktoranckie. Nr projektu: POWR.03.02.00-IP.08-00-DOK/16. Realizowany w latach 2018-2022. Kierownik – prof. dr hab. Agnieszka Marczak.



Rzeczpospolita
Polska

Unia Europejska
Fundusz Spójności



MIERZ WYSOKO

MGGPAERO 

Program Operacyjny Infrastruktura i Środowisko działanie 2.4.4d ocena stanu zasobów przyrodniczych w parkach narodowych przy wykorzystaniu nowoczesnych technologii teledetekcyjnych. Projekt pn: Inwentaryzacja i ocena stanu zasobów przyrodniczych w Wielkopolskim Parku Narodowym przy wykorzystaniu nowoczesnych technologii teledetekcyjnych.

Program Operacyjny Infrastruktura i Środowisko działanie 2.4.4d ocena stanu zasobów przyrodniczych w parkach narodowych przy wykorzystaniu nowoczesnych technologii teledetekcyjnych. Projekt pn: Pozyskanie wieloźródłowych danych teledetekcyjnych oraz ich analiza dla obszaru Wigierskiego Parku Narodowego z częścią zlewni jeziora Wigry i rzeki Czarnej Hańczy.

Dorobek naukowy

Niniejsza rozprawa doktorska oparta jest na trzech artykułach oryginalnych:

1. **Zakrzewska, A.**, Kopec, D., Krajewski, K., Charyton, J., 2022. Canopy temperatures of selected tree species growing in the forest and outside the forest using aerial thermal infrared (3.6–4.9 μm) data. *European Journal of Remote Sensing*, 55(1), 313-325.
IF₂₀₂₁ = 3,168; MEiN = 70 pkt.
2. **Zakrzewska, A.**, Kopec, D., 2022. Remote sensing of bark beetle damage in Norway spruce individual tree canopies using thermal infrared and airborne laser scanning data fusion. *Forest Ecosystems*, 9, 100068.
IF₂₀₂₁ = 4,274; MEiN = 140 pkt.
3. **Zakrzewska, A.**, Kopec, D., Ochtyra, A., Potůčková, M., 2023. Can canopy temperature acquired from an airborne level be a tree health indicator in an urban environment? *Urban Forestry & Urban Greening*, 79, 127807.
IF₂₀₂₁ = 5,766; MEiN = 100 pkt.

Sumaryczny współczynnik oddziaływania (*ang.* Impact Factor, IF) publikacji wchodzących w skład rozprawy doktorskiej wynosi **13,208**. Całkowita liczba punktów za publikacje stanowiące rozprawę doktorską, według listy czasopism punktowanych MEiN wynosi **310**.

Pozostały dorobek naukowy

A) Publikacje

1. Kopec, D., **Zakrzewska, A.**, Halladin-Dąbrowska, A., Wylazłowska, J., Kania, A., Niedzielko, J., 2019. Using Airborne Hyperspectral Imaging Spectroscopy to Accurately Monitor Invasive and Expansive Herb Plants: Limitations and Requirements of the Method. *Sensors* 19(13), 2871.
IF₂₀₂₀ = 3,576; MEiN = 100 pkt.

A) Komunikaty zjazdowe

1. **Zakrzewska, A.**, Kopec, D., Jarocińska, A., Kycko, M., Sabat-Tomala, A., Niedzielko, J., Niedzielko, M., Sławik, Ł. Review of non-forest Natura 2000 habitats mapping methods using remote sensing data. Conference: Sixth International Conference on Remote Sensing and Geoinformation of the Environment, 26-29 marca 2018, Paphos, Cypr.
2. Kopec, D., Michalska-Hejduk, D., Radecka, A., Wylazłowska, J., Halladin-Dąbrowska, A., Kuświk, K., **Zakrzewska, A.**, Górski, K., Osińska-Skotak, K. Expansion Of Trees And Shrubs To Natura 2000 Habitats - Monitoring Using Remote Sensing Methods. Conference: Sixth International Conference on Remote Sensing and Geoinformation of the Environment, 26-29 marca 2018, Paphos, Cypr.

3. Kopeć, D., Szporak-Wasilewska, S., Wylazłowska, J., Halladin-Dąbrowska, A., Kuc, G., Jarocińska, A., Sabat-Tomala, A., Borzuchowski, J., Sławik, Ł., **Zakrzewska, A.**, Piórkowski, H., Bzdęga, K., Tokarska-Guzik, B. Comparing the efficiency of selected invasive plant species mapping using airborne remote sensing methods. Conference: NEOBIOOTA 2018 10th International Conference on Biological Invasions New Directions in Invasion Biology, 3-7 września 2018, Dún Laoghaire, Dublin, Irlandia.
4. **Zakrzewska, A.**, Będkowski, K. Zastosowanie teledetekcji w badaniach pojemności żerowej obwodów łowieckich na przykładzie zwierząt z rodziny jeleniowatych. Konferencja: XXIII Ogólnopolska Konferencja Fotointerpretacji i Teledetekcji „Współczesna teledetekcja w badaniach geograficznych”, 24-25 września 2018, Łódź, Polska.
5. **Zakrzewska, A.**, Kopeć, D. Wykorzystanie lotniczych danych termalnych do rejestracji temperatury koron drzew rosnących na obszarach leśnych i rolniczych. Konferencja: XXIV Ogólnopolska Konferencja Fotointerpretacji i Teledetekcji, 27-28 września 2021, Poznań, Polska.
6. **Zakrzewska, A.**, Kopeć, D., Ochtyra, A. Canopy Temperature Acquired from Daytime and Nighttime Aerial Data as an Indicator of Trees' Health Status. Konferencja: Urban Heat Island Adaptation Strategies, 19-20 lipca 2022, Helsinki, Finlandia.
7. Ochtyra, A., Sławik, Ł., Kopeć, D., Marcinkowska-Ochtyra, A., Jarocińska, A., Gryguc, K., **Zakrzewska, A.** Teledetekcja w praktyce – stan koron drzew w Warszawie. Konferencja: Warszawa w świetle badań naukowych, 29-30 września 2022, Warszawa, Polska.
8. Wietecha, M., Kopeć, D., Wylazłowska, J., **Zakrzewska, A.** Analiza przesuszenia torfowisk w Borach Tucholskich z wykorzystaniem wielosensorowych danych lotniczych. Konferencja: XXV Ogólnopolska Konferencja Fotointerpretacji i Teledetekcji, 28-30 listopada 2022, Warszawa, Polska.

C) Staże naukowe

1. Staż zagraniczny finansowany w ramach Projektu InterDOC-START – Interdyscyplinarne Studia Doktoranckie na Wydziale BiOŚ UŁ w Department of Applied Geoinformatics and Cartography, Faculty of Science, Uniwersytet Karola, Praga, Czechy (1.12.2021 - 28.02.2022).

1. Wstęp

1.1. Ocena stanu zdrowotnego drzew

Monitoring stanu zdrowotnego drzew jest jednym z zadań realizowanych w ramach zarządzania obszarami chronionymi, kontroli zieleni miejskiej czy ochrony lasu. Drzewa o osłabionej kondycji lub zamierające nie dostarczają (lub dostarczają w sposób ograniczony) usług ekosystemowych (Dale i in., 2016). Mogą natomiast stanowić realne zagrożenie dla ludzi i infrastruktury (Ball, 2011). Dodatkowo drzewa o osłabionej kondycji zdrowotnej obniżają wartości estetyczne miasta (Roy i in., 2012). Takie osobniki muszą być szybko zidentyfikowane, aby je usunąć lub przeprowadzić prace pielęgnacyjne (Roman, 2013). Drzewa należy monitorować również w lasach gospodarczych, gdzie jednym z zagrożeń jest np. kornik drukarz (*Ips typographus* L.; Grodzki i in., 2004; Gutowski, 2004). Z powodu specyficznego cyklu życia kornika, konieczna jest szybka identyfikacja miejsc jego występowania, w celu ograniczenia jego gradacji.

Jedną z metod określania stanu zdrowotnego drzew jest ich wizualna ocena (*Visual Tree Assessment*). Inspekcja wykonywana jest w terenie przez wyznaczone służby i specjalistów (Mattheck i Breloer, 1994; Witkoś-Gnach i Krynicki, 2021). Metoda ta, ze względu na czasochłonność jej przeprowadzenia, nie jest możliwa do zastosowania w sposób regularny dla wszystkich drzew na dużych obszarach. W tym celu opracowuje się metody selekcyjne, które ze zbioru wszystkich drzew pozwalają wskazać te, które w pierwszej kolejności powinny być objęte szczegółową oceną (Degerickx i in., 2018).

Szybka identyfikacja drzew o osłabionej kondycji jest możliwa z wykorzystaniem technik teledetekcyjnych, które pozwalają na zdalne pozyskanie informacji na dużych obszarach. Popularne w tym celu jest użycie danych multispektralnych (Filchev, 2012; Long i Lawrence, 2016) i hiperspektralnych (Degerickx i in., 2018; Jarocińska i in., 2018), jak również lotniczego skanowania laserowego (Stereńczak i in., 2019; Wang i in., 2022). Jednym z typów danych coraz częściej wykorzystywanych do badania kondycji drzew są dane termalne. Przez lata stosowano różne nośniki kamer termalnych, tj. satelity, samoloty, helikoptery i drony (Spronken-Smith i Oke, 1998; Quattrochi i Ridd, 1998; Gluch i in., 2006; Santesteban i in., 2017; De Faria Peres i in., 2018). Jednak najpopularniejszym źródłem informacji o temperaturze obiektów są darmowe dane satelitarne (Malakar i in., 2018). Z powodu jednak ich niskich rozdzielczości przestrzennych (wymiar terenowy pojedynczego piksela to 100x100 metrów dla danych satelity Landsat 8), nie pozwalają one na analizę pojedynczych drzew. Natomiast inne nośniki kamer, czyli bezzałogowe statki

powietrzne mają ograniczony zasięg pozyskiwania danych do niewielkich obszarów i nie mogą być skutecznie zastosowane na terenie całego parku narodowego, nadleśnictwa czy miasta. Dane termalne uzyskane z samolotu są alternatywą w tym zakresie, pozwalają zarówno na rejestrację temperatury pojedynczych drzew (wymiar terenowy piksela to 1x1 metr), równocześnie pozyskując dane dla dużych obszarów w czasie jednego lotu.

1.2. Wykorzystanie teledetekcyjnych danych termalnych do szacowania stanu zdrowotnego drzew

W badaniach stanu zdrowotnego drzew za pomocą zobrazowań termalnych wykorzystano zależność między temperaturą korony a stanem drzew, który przejawia się, np. przebarwieniami liści. Zdrowe drzewa prawidłowo przeprowadzają proces ewapotranspiracji, przez co skutecznie ochładzają powierzchnię liści (Kimball i Bernacchi, 2006). Natomiast drzewa o przebarwionych liściach, mają zaburzony proces ewapotranspiracji, co powoduje, że szybciej się nagrzewają pod wpływem wysokich temperatur i promieniowania słonecznego (Leuzinger i Körner, 2007). Dzięki temu możliwa jest identyfikacja i rozróżnienie stanów kondycji zdrowotnej drzew na danych termalnych. Zależność ta jest szeroko wykorzystywana w sadownictwie (Maes i Steppe, 2012; Ishimwe i in., 2014; Egea i in., 2017; Khanal i in., 2017; Zhou i in., 2021). Z przeprowadzonych w ostatnich latach badań (Möller i in., 2007; Wang i in., 2010; Kim i in., 2018) wynika, że zobrazowania termalne mają bardzo duży potencjał aplikacyjny i mogą być wykorzystywane w monitoringu drzew w różnych środowiskach.

W leśnictwie jednym z dynamicznie rozwijających się nurtów badań jest wykrywanie, z wykorzystaniem teledetekcji, miejsc żerowania szkodników, w tym kornika drukarza. Badania z wykorzystaniem satelitarnych zobrazowań termalnych wykazały, że temperatura koron drzew pozwala na bardziej precyzyjną identyfikację zmian fizjologicznych wywołanych przez kornika drukarza niż spektralne wskaźniki roślinności (Abdullah i in., 2019). Temperatura koron drzew okazuje się kluczową cechą w wykrywaniu zaatakowanych drzewostanów. W badaniu Haisa i Kucery (2008) przy wykorzystaniu danych satelitarnych zaobserwowano, że temperatura powierzchni obumarłych lasów świerkowych jest średnio o 3,5°C wyższa niż zdrowych drzewostanów. Badania te prowadzono jednak nie na pojedynczych drzewach, ale na całych płatach zbiorowisk leśnych. Późniejsze badania (Junttila i in., 2016) skupiały się na wpływie stanu zdrowotnego drzew i struktury lasu na zarejestrowaną temperaturę wykorzystując lotnicze dane termalne i skanowanie laserowe. Wysoka rozdzielczość przestrzenna danych (wymiar terenowy

pojedynczego piksela to 1x1 metr) umożliwiła analizę temperatury koron indywidualnych drzew. W badaniach Junttilli i in. (2016) stwierdzono statystycznie istotną różnicę w temperaturze koron drzew żywych i martwych, jednak identyfikacja drzew o osłabionej kondycji z powodu wczesnego etapu ataku kornika drukarza pozostało wyzwaniem.

W środowisku miejskim prowadzono badania koncentrujące się na pojedynczych drzewach i zależności temperatury ich koron od gatunku (Leuzinger i in., 2010). Autorzy ustalili, że temperatury koron drzew są specyficzne dla gatunku i zależą od lokalizacji drzewa w mieście, wielkości jego liści, przewodnictwa szparkowego i architektury korony. Meier i Scherer (2012) i Zheng i in. (2018) badali również temperatury pojedynczych koron różnych gatunków drzew w ujęciu przestrzennym i czasowym oraz ustalili związek między temperaturą korony a temperaturą powietrza. Autorzy wskazali, że różnice temperatur między koronami wynikają z przynależności gatunkowej, obecności nieprzepuszczalnych powierzchni pod koroną oraz lokalizacji drzew w terenie. Wykorzystanie lotniczych danych termalnych do identyfikacji stanu zdrowotnego drzew w mieście nie było jednak badane.

Dotychczas lotnicze dane termalne pozyskiwano głównie z wykorzystaniem sensorów rejestrujących temperaturę w zakresie spektralnym 7–15 μm , określanym jako zakres długiej podczerwieni (*Long Wave Infrared*). W badaniach stanowiących moją dysertację po raz pierwszy wykorzystano dane termalne z zakresu średniej podczerwieni 3,6–4,9 μm (*Middle Wave Infrared*), który nie był wcześniej użyty w teledetekcyjnych badaniach roślinności. Według Gerbera i in. (2011) i Ullah i in. (2012) okno atmosferyczne w przedziale 3–5 μm jest dedykowane badaniu zawartości wody w roślinności. Można więc przyjąć, że zakres ten jest odpowiedni do wykrywania drzew w złym stanie zdrowotnym i martwych.

2. Cel pracy

Celem pracy było sprawdzenie, czy dane termalne z zakresu średniej podczerwieni (3,6–4,9 μm) pozyskane z pułapu lotniczego, mogą być wykorzystane do badań kondycji zdrowotnej drzew.

Cel ten został zrealizowany w wyniku przeprowadzenia trzech niezależnych analiz na trzech obszarach badawczych. W Wielkopolskim Parku Narodowym (sekcja 4.1.) zbadano, czy temperatura koron drzew jest cechą specyficzną dla gatunku i jak zmienia się ona w ciągu dnia (lotnicze dane termalne pozyskiwano od godz. 8:10 do 14:00). Sprawdzono również, czy położenie drzewa w terenie jest czynnikiem różnicującym temperaturę koron.

Badania w Wigierskim Parku Narodowym (sekcja 4.2.) skupiały się na identyfikacji osobników osłabionych i martwych świerka pospolitego (*Picea abies* (L.) H. Karst) w środowisku naturalnym. Badaniom towarzyszyła idea wykonania automatycznego schematu postępowania w detekcji takich drzew z wykorzystaniem fuzji danych: termalnych i skanowania laserowego. Kolejne badania przeprowadzono w centrum Warszawy (sekcja 4.3.). Ich celem było sprawdzenie, czy temperatura koron różnych gatunków może służyć jako wskaźnik zdrowotny drzew w mieście. W czasie tych badań sprawdzono i porównano przydatność lotniczych danych termalnych pozyskanych w dniu i w nocy w określaniu kondycji drzew.

3. Materiały i metody

3.1. Opis terenów badań i gatunków

Na trzech różnych obszarach prowadzono badania łącznie na 11 gatunkach drzew. Pierwsze badania przeprowadzono na podstawie danych pozyskanych w roku 2019 dla obszaru Wielkopolskiego Parku Narodowego (sekcja 4.1.). Teren badań obejmował 102,33 km² i został podzielony na cztery bloki, które odpowiadają różnym godzinom pozyskania lotniczych danych termalnych. Badaniami objęto trzy rodzime gatunki: olsza czarna (*Alnus glutinosa* (L.) Gaertn.), sosna zwyczajna (*Pinus sylvestris* L.) i dąb bezszypułkowy (*Quercus petraea* (Matt.) Liebl.) oraz dwa obce, inwazyjne gatunki we florze Polski: dąb czerwony (*Quercus rubra* L.) i robinia akacjowa (*Robinia pseudoacacia* L.).

Drugie badania były prowadzone w roku 2020 na terenie Wigierskiego Parku Narodowego (sekcja 4.2.). Wybrano obszar badawczy o powierzchni 9 km², gdzie głównym zbiorowiskiem roślinnym jest subborealny bór mieszany (*Serratulo-Pinetum*) z dominacją świerka pospolitego (*Picea abies* (L.) H. Karst). Obszar badań znajdował się na terenie ochrony ścisłej. Badanym gatunkiem był świerk pospolity w różnych stanach kondycji zdrowotnej.

Ostatnie badania prowadzono w roku 2020 w centrum Warszawy na obszarze 50 km² (sekcja 4.3.). Analizowany obszar charakteryzuje się szerokim spektrum zróżnicowania pokrycia terenu: zabudowa jednorodzinna i wielorodzinna, jednostki przemysłowe, handlowe, publiczne, wojskowe, zielone obszary miejskie, wody i otwarte przestrzenie z niską roślinnością (Urban Atlas, 2018). Wybrany obszar był reprezentatywną częścią miasta pod względem zróżnicowania powierzchni i różnorodności dendroflory. Na obszarze

badania znajdowały się gatunki rodzime dla flory Polski, obce i obce inwazyjne oraz gatunki w odmianach hodowlanych (Sikorska et al., 2019). Badaniami objęto pięć gatunków uważanych za najbardziej narażone na zamieranie na badanym terenie: klon zwyczajny (*Acer platanoides* L.), klon jawor (*Acer pseudoplatanus* L.), kasztanowiec zwyczajny (*Aesculus hippocastanum* L.), lipa drobnolistna (*Tilia cordata* Mill.) i lipa krymska (*Tilia×euchlora* K. Koch). Wybrane gatunki charakteryzowały się zróżnicowanym stanem zdrowia.

3.2. Zbiór i przetwarzanie danych teledetekcyjnych

Dane teledetekcyjne pozyskano w sezonach wegetacyjnych 2019–2020. Na wszystkich trzech obszarach, dane termalne rejestrowano z wykorzystaniem jednego modelu kamery (Tab. 1). Poza danymi termalnymi na poszczególnych obszarach pozyskiwano różne typy danych: chmurę punktów uzyskaną ze skanowania laserowego, zdjęcia hiperspektralne, obrazy RGB (*Red-Green-Blue*) i CIR (*Color-Infrared*), które były wykorzystane pomocniczo w procesach przetwarzania danych i w analizach statystycznych. Dla wszystkich obszarów pozyskano dane termalne o rozdzielczości przestrzennej równej 1 m (Tab. 1).

Tabela 1. Parametry sensorów i lotów przeprowadzonych podczas badań.

Typ danych	Model sensora	Parametry danych	Data lotu	Godziny lotu	Obszar badań
Dane termalne	ImageIR 9400	Wymiar piksela 1 [metr]	9 czerwca 2019	8:10–14:00	Wielkopolski Park Narodowy
			26 czerwca 2020	14:07–14:28	Wigierski Park Narodowy
			3 sierpnia 2020 (noc) i 15 sierpnia 2020 (dzień)	00:25–01:10 (noc) i 12:21–13:06 (dzień)	Warszawa
Skanowanie laserowe	Riegl VQ-780i	Gęstość 18 [pkt/m ²]	9 czerwca 2019	8:10–14:00	Wielkopolski Park Narodowy
		Gęstość 7,6 [pkt/m ²]	17 sierpnia 2019	9:18–9:45	Wigierski Park Narodowy
		Gęstość 4 [pkt/m ²]	15 sierpnia 2020	12:21–13:06	Warszawa

Dane hiperspektralne	HySpex VNIR-1800 0,4–0,9 μm	Wymiar piksela 1 [metr]	9 czerwca 2019	8:10–14:00	Wielkopolski Park Narodowy
	HySpex SWIR-384 0,9–2,5 μm	Wymiar piksela 1 [metr]	9 czerwca 2019	8:10–14:00	
Zobrazowania RGB/CIR	Intergraph DMCII	Wymiar piksela 0,1 [metra]	17 sierpnia 2019	9:18–9:45	Wigierski Park Narodowy
	PhaseOne IXM-100	Wymiar piksela 0,13 [metra]	15 sierpnia 2020	12:21–13:06	Warszawa

Dokładne opisy przetworzenia danych termalnych, skanowania laserowego, danych hiperspektralnych oraz RGB i CIR, w tym użyte programy i metody, znajdują się w publikacjach stanowiących niniejszą rozprawę.

3.3. Pozyskanie naziemnych danych referencyjnych

Dane referencyjne to zbiór pomiarów lokalizacji drzew powstały w wyniku badań terenowych. W przedstawionych analizach pojedynczym obiektem referencyjnym była korona drzewa. Dane terenowe na każdym z obszarów zbierano do siedmiu dni po pozyskaniu lotniczych danych termalnych. Zbieżność pozyskania danych teledetekcyjnych i naziemnych była konieczna w celu wyeliminowania możliwej zmiany stanu zdrowotnego drzew pomiędzy temperaturą korony zarejestrowaną z kamery termalnej a stanem ocenianym w czasie badań terenowych. Współrzędne indywidualnych drzew były rejestrowane z dokładnością do 1 metra przy użyciu odbiornika Trimble Catalyst GNSS i podłączoną do niego aplikacją pomiarową MapIT (Mapit GIS LTD, Wishaw, UK). Pomiarzy zostały rozmieszczone możliwie równomiernie w obszarze badań, biorąc pod uwagę rzeczywiste występowanie badanych gatunków. Przy wyborze badanych drzew tylko te o gęstych i zwartych koronach były wskazywane jako referencyjne. Zapewniało to, że zarejestrowana temperatura jest temperaturą korony drzewa, a nie powierzchni pod nią. Mapy rozmieszczenia drzew referencyjnych na badanych obszarach znajdują się w publikacjach stanowiących niniejszą rozprawę. W terenie dla każdego drzewa referencyjnego zapisywano takie informacje jak: przynależność gatunkowa, współrzędne geograficzne i wynik wizualnej oceny stopnia przebarwienia korony (w procentach [%]).

W badaniach prowadzonych w Wielkopolskim Parku Narodowym (sekcja 4.1.) w każdym bloku pozyskania danych zostało wybranych po 20 drzew dla każdego badanego

gatunku (10 w lesie i 10 poza lasem). Łącznie wytypowano 400 drzew referencyjnych. Wszystkie drzewa charakteryzowały się brakiem wizualnych oznak obniżenia kondycji zdrowotnej.

W badaniach prowadzonych w Wigierskim Parku Narodowym (sekcja 4.2.) wytypowano 340 drzew referencyjnych dla *Picea abies* w różnym stanie kondycji zdrowotnej (Tab. 2). Każde drzewo zostało przypisane do jednej z trzech klas kondycji ('zdrowe', 'osłabiona kondycja', 'martwe'). Drzewa wybrane jako osłabione i martwe posiadały ślady żerowania kornika drukarza.

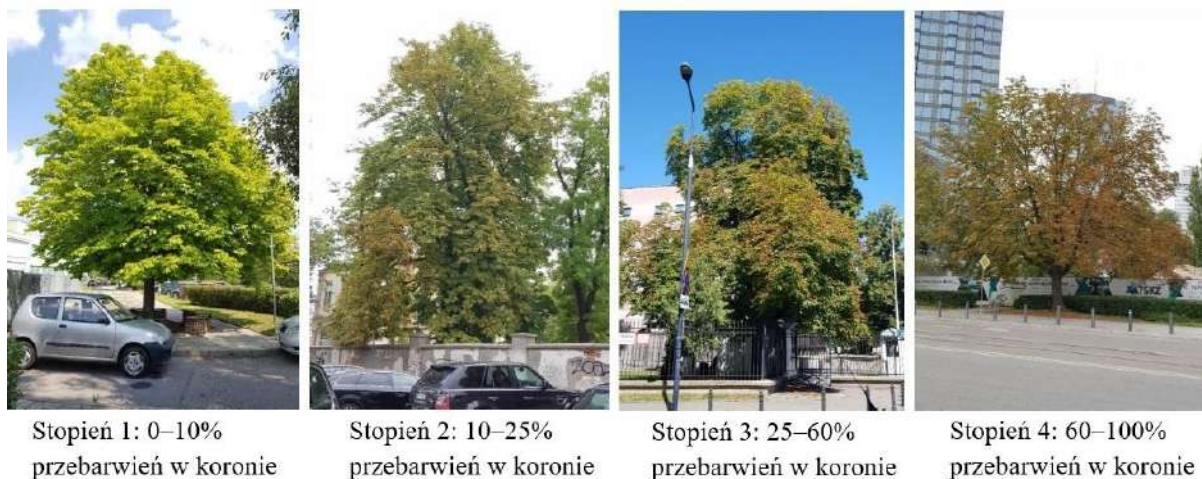
Tabela 2. Charakterystyka klas kondycji zdrowotnej drzew stosowana w badaniach przeprowadzonych w Wigierskim Parku Narodowym.

Nr	Klasa kondycji	Opis klasy
1	zdrowe	brak oznak pogorszenia stanu zdrowia, brak przebarwienia igieł, brak śladów żerowania kornika drukarza
2	osłabiona kondycja	widoczne pogorszenie kondycji zdrowotnej, przebarwienia igieł ponad 20% w koronie, potwierdzone żerowanie kornika drukarza
3	martwe	martwe drzewa, brak igieł lub wszystkie igły przebarwione, potwierdzone żerowanie kornika drukarza

W badaniach prowadzonych w Warszawie (sekcja 4.3.) wytypowano 617 drzew referencyjnych dla pięciu gatunków. Drzewa zostały podzielone na cztery klasy kondycji zdrowotnej według Tabeli 3. Ocena przebarwień korony drzew została przeprowadzona w terenie na podstawie metody Hanischa i Kliza (1990; Tab. 3). Przebarwienie liści zostało uznane za wizualny znak stanu zdrowia, gdzie im wyższy procent przebarwień liści w koronie drzewa, tym gorsza jego kondycja (Ryc. 1).

Tabela 3. Klasy uszkodzeń stosowane w szacowaniu przebarwień liści w badaniach przeprowadzonych w Warszawie.

Nr	Stopień przebarwienia korony	Klasa kondycji	Udział procentowy przebarwienia korony
1	brak	zdrowe	0–10%
2	niewielki	nieznacznie osłabiona kondycja	10–25%
3	średni	osłabiona kondycja	25–60%
4	znacznym	drzewo zamierające lub martwe	60–100%



Rycina 1. Wizualizacja procentowego stopnia przebarwienia korony drzewa – na przykładzie danych referencyjnych z Warszawy (fot. A. Zakrzewska).

3.4. Wyznaczanie temperatur koron drzew

Przedmiotem badań w niniejszej rozprawie była temperatura poszczególnych koron drzew. Temperaturę wyznaczono jako wartość statystyczną z pikseli danych termalnych znajdujących się w całości w obrębie korony. Pierwszym etapem procesu przetwarzania danych było wyznaczenie w postaci poligonu zasięgu koron drzew w rzucie pionowym. Poligony wykonano metodą fotointerpretacji modelu wysokości pokrywy roślinnej (*Canopy Height Model*) lub za pomocą automatycznej segmentacji (w badaniach w Wigierskim Parku Narodowym).

Drugim etapem procesu było wyłączenie z analizy pikseli danych termalnych, które mogły uwzględnić temperaturę gruntu lub sąsiadujących koron drzew. Piksele te zostały wyłączone z analiz poprzez zmniejszenie powierzchni poligonu stosując bufor do wewnątrz i eliminację pikseli o niskim stopniu zawartości pokrywy roślinności oszacowanym na podstawie danych skanowania laserowego. W ten sposób zminimalizowano wpływ podłoża na wynik obliczenia średniej temperatury całej korony.

Kolejnym etapem przetwarzania danych było obliczenie miar statystycznych: średnia i odchylenie standardowe (z danych termalnych) dla zasięgu koron wyznaczonych w etapie pierwszym. Wyznaczenie poligonów koron i obliczenie miar statystycznych wykonano w programie ArcGIS 10.6 firmy ESRI.

3.5. Analizy statystyczne

W Wielkopolskim Parku Narodowym, za pomocą testu t-Studenta dla prób niezależnych, sprawdzono różnicę między temperaturami koron drzew w lesie i poza lasem, osobno dla każdego bloku pozyskania. Zbadano również międzygatunkową zmienność

temperatur koron w zależności od pory dnia i lokalizacji, a istotność wyników sprawdzono za pomocą analizy wariancji (ANOVA). Do analizy normalności rozkładu badanych prób wykorzystano test Shapiro-Wilka. Za próg istotności statystycznej przyjęto $p < 0,05$. Porównując różnicę między gatunkami wykorzystano test post-hoc Tukey'a dla grup równolicznych.

W Wigierskim Parku Narodowym, drzewa referencyjne podzielono według klas kondycji za pomocą losowania warstwowego (*stratified random sampling*; Acharya i in., 2013) na dwa zbiory: testowy i walidacyjny. Zbiór testowy posłużył do wyznaczenia średnich temperatur koron drzew znajdujących się w trzech klasach zdrowotnych wykorzystując algorytm centroidów (metoda *K-mean clustering*; Zhang i in., 2018). Zbiór walidacyjny posłużył do sprawdzenia uzyskanych wyników za pomocą powszechnie stosowanych w teledetekcji miar dokładności: dokładność ogólna (*overall accuracy*), dokładność producenta (*producer's accuracy*) i dokładność użytkownika (*user's accuracy*).

W Warszawie dla indywidualnych koron drzew obliczono statystyki takie jak: średnia, odchylenie standardowe, wartości minimalną i maksymalną w poligonie oraz 5-ty i 95-ty percentyl. Istotność różnicy temperatur między klasami kondycji sprawdzono, za pomocą testu ANOVA (do analizy normalności rozkładu badanych prób wykorzystano test Shapiro-Wilka, a za próg istotności statystycznej przyjęto $p < 0,05$) i testu post-hoc Tukey'a dla grup różnolicznych.

Analizy statystyczne przeprowadzono w programie Statistica 13 firmy TIBCO Software.

4. Omówienie wyników prac wchodzących w skład rozprawy doktorskiej

4.1. Zmienność temperatury koron wybranych gatunków drzew rosnących w lesie i poza lasem z wykorzystaniem lotniczych danych termalnych (3,6–4,9 μm)

Badania prowadzone w Wielkopolskim Parku Narodowym skupiały się na analizie zmian temperatury koron drzew między godziną 8:10 a 14:00 dla pięciu gatunków z uwzględnieniem położenia drzewa w terenie. Wyniki wskazują, że najbliższe otoczenie jest ważnym czynnikiem wpływającym na temperaturę korony. Wykazano istotną różnicę między temperaturami koron drzew poza lasem i w lesie, niezależnie od godziny pozyskania danych termalnych. Najmniejszą różnicę między temperaturami koron w lesie i poza lasem zanotowano w godzinach porannych (tj. 8:10–9:45) i wynosiła 0,41°C. Największą różnicę zaobserwowano w południe (tj. 12:00–13:00), kiedy drzewa znajdujące się poza lasem były

o 0,70°C cieplejsze od drzew rosnących w lesie. Dodatkowo o tej godzinie wszystkie gatunki różnią się od siebie pod względem temperatur koron niezależnie od położenia drzewa w terenie.

Porównanie temperatury poszczególnych gatunków wskazuje, że *Quercus rubra* i *Quercus petraea* to gatunki o najbardziej zbliżonej do siebie temperaturze koron w trakcie trwania badań. Równocześnie są to gatunki o najniższych temperaturach w porównaniu do innych badanych gatunków, np. w godzinach 8:10–9:45 *Quercus rubra* w lesie charakteryzowały się temperaturą koron 14,63°C, a *Quercus petraea* 15,44°C. *Pinus sylvestris* charakteryzuje się najwyższą w porównaniu do innych gatunków temperaturą korony, niezależnie od położenia względem innych drzew i czasu pozyskania danych. Dla drzew położonych w lesie korony tego gatunku mają najwyższą temperaturę sięgającą 21,54°C w godzinach 13:00–14:00. *Robinia pseudoacacia* i *Alnus glutinosa* nie wyróżniały się skrajnymi wartościami temperatur w trakcie trwania badania. Dla *Robinia pseudoacacia* najniższe temperatury koron zanotowano w godzinach porannych i wyniosła 15,28°C, a najwyższe w godzinach popołudniowych i osiągnęła 20,75°C. *Alnus glutinosa* charakteryzuje się niską, w porównaniu do innych gatunków temperaturą korony. Dla tego gatunku najniższą wartość temperatury zanotowano w godzinach 8:10–9:45 (średnio 14,93°C), a najwyższą w godzinach 13:00–14:00 (20,51°C).

Na podstawie porównania całego okresu objętego analizą (od godziny 8:10 do 14:00) można stwierdzić, że *Quercus rubra*, *Quercus petraea* i *Alnus glutinosa* to gatunki o niskich temperaturach koron drzew, a gatunkiem o stosunkowo wysokiej temperaturze jest *Pinus sylvestris*.

4.2. Oszacowanie uszkodzeń w indywidualnych koronach drzew świerka pospolitego spowodowane przez kornika drukarza przy użyciu fuzji danych termalnych i lotniczego skanowania laserowego

W badaniach prowadzonych w Wigierskim Parku Narodowym sprawdzono, czy dane termalne można wykorzystać do identyfikacji drzew *Picea abies* o osłabionej kondycji i martwych z powodu gradacji kornika drukarza. Uzyskane zakresy średnich temperatur dla poszczególnych klas kondycyjnych zestawiono w Tabeli 4. Wyniki analizy statystycznej pozwalają stwierdzić, że poszczególne klasy kondycji zdrowotnej świerka istotnie różniły się między sobą temperaturą korony. Drzewa martwe były średnio o 1,60°C cieplejsze od tych w osłabionej kondycji, a osłabione były o 0,87°C cieplejsze od drzew zdrowych.

Tabela 4. Zakresy wartości temperatur koron drzew dla klas kondycyjnych.

Klasa kondycji	Średnia temperatura koron [°C]	Zakres zmienności (minimalna - maksymalna) średniej temperatury koron [°C]
zdrowe	27,70	26,81–28,13
osłabiona kondycja	28,57	28,14–29,27
martwe	30,17	29,28–32,50

W drugim etapie badań opracowano i przetestowano skuteczność identyfikacji drzew martwych i w osłabionej kondycji z uwzględnieniem automatycznej segmentacji koron drzew na danych z chmury punktów a uzyskane wyniki porównano z tymi uzyskanymi w oparciu o metodę manualnego wyznaczania zasięgu koron. Uzyskane wyniki metod opartych na fotointerpretacji i segmentacji porównano na zbiorze 170 drzew walidacyjnych. Interpretacja i wyniki miar dokładności zostały przedstawione w rozdziałach 2.6 *Accuracy metrics* i 3.2 *Result comparison of validation set created with two tree canopy delineated methods*. Wykorzystując w analizie klasyfikacji manualnie wyznaczone zasięgi koron wynika, że ze 100 drzew zdrowych, 67 było prawidłowo sklasyfikowanych, z 20 drzew o osłabionej kondycji, 19 przypisano prawidłowo do tej klasy, a z 50 drzew martwych tylko 16 znalazło się w tej klasie. Wykorzystując w analizie klasyfikacji automatyczne segmenty koron uzyskano prawidłowe przypisanie 64 drzew ze 100 do klasy 'zdrowe'. Tylko 5 z 50 drzew przypisano do klasy 'martwe'. 45 martwych drzew przypisano do klasy 'osłabiona kondycja'. Wszystkie drzewa o 'osłabionej kondycji' zostały prawidłowo sklasyfikowane. Uzyskano dokładność ogólną na poziomie 0,60 dla metody manualnej i 0,52 dla segmentacji. Porównanie efektywności dwóch metod identyfikacji stanu zdrowotnego drzew pokazało, że automatyczna segmentacja zmniejsza precyzję detekcji martwych drzew o 8 punktów procentowych w porównaniu do metody manualnej.

4.3. Czy temperatura korony mierzona z poziomu lotniczego może być wskaźnikiem zdrowia drzew w środowisku miejskim?

Celem badań prowadzonych w Warszawie było sprawdzenie, czy temperatura korony może być wskaźnikiem kondycji zdrowotnej drzew rosnących w mieście. Analizując dane termalne pozyskane w nocy stwierdzono, że średnia temperatura koron drzew między skrajnymi klasami kondycji różni się zaledwie o 1,06°C (Tab. 5). Zauważalna jest również zależność, że im większe przebarwienie liści, tym wyższe wartości odchylenia

standardowego temperatury wewnątrz korony (Tab. 5). Wyniki analiz statystycznych wykazały, że jedynie klasa drzew 'zdrowych' tworzyła odrębną, istotnie wyróżniającą się grupę pod względem temperatury. Natomiast klasy grupujące drzewa w nieznacznie osłabionej kondycji, osłabionej kondycji i drzewa zamierające nie różniły się istotnie.

Tabela 5. Charakterystyka temperatur koron drzew dla danych dziennych i nocnych w podziale na klasę kondycji.

		Dla danych pozyskanych w nocy		Dla danych pozyskanych w dzień	
Klasa kondycji (liczba oszacowanych drzew)	Średnia liczba pikseli w koronie drzewa	Średnia temperatura korony drzewa [°C]	Średnie odchylenie standardowe korony drzewa [°C]	Średnia temperatura korony drzewa [°C]	Średnie odchylenie standardowe korony drzewa [°C]
zdrowe (311)	33	14,49	0,21	25,31	1,32
nieznacznie osłabiona kondycja (139)	30	15,10	0,25	26,40	1,46
osłabiona kondycja (89)	26	15,41	0,34	27,03	1,54
drzewo zamierające lub martwe (78)	27	15,55	0,47	28,59	1,93

Opierając się na wnioskach uzyskanych z poprzednich badań (sekcja 4.1.) dane termalne z nalogu dziennego pozyskano w południe, w godzinach 12:00–12:30. Na danych pozyskanych w ciągu dnia zaobserwowano taką samą zależność jak na danych nocnych, że im wyższy procent przebarwienia liści, tym wyższa średnia temperatura korony (Tab. 5). Różnica pomiędzy średnią temperaturą koron drzew w skrajnych stanach kondycji wynosiła aż 3,28°C. Tak samo jak na danych nocnych, zróżnicowanie temperatury wewnątrz korony drzewa wzrasta wraz z procentowym udziałem przebarwionych liści w koronie i wynosi dla drzew zamierających 1,93°C. Analiza wariancji potwierdziła istotne statystycznie różnice w temperaturze koron w ciągu dnia między grupami drzew z różnych klas kondycji.

Podsumowując można stwierdzić, że korony drzew zdrowych były chłodniejsze, niż korony drzew zamierających. Różnica w temperaturze między drzewami zdrowymi a umierającymi wynosiła 3,28°C na danych pozyskanych w ciągu dnia i 1,06°C na danych

pozyskanych w nocy. Tylko na danych termalnych pozyskanych w ciągu dnia możliwe było rozróżnienie czterech stanów kondycyjnych drzew.

5. Wnioski

1. Temperatura korony jest cechą specyficzną dla gatunku i zależy od położenia drzewa w terenie. Drzewa znajdujące się poza lasem są cieplejsze od tych znajdujących się w lesie.
2. Wskazano, że *Alnus glutinosa*, *Quercus rubra* i *Quercus petraea* mają niskie średnie temperatury koron względem innych badanych gatunków, natomiast *Pinus sylvestris* ma najwyższe temperatury koron spośród badanych gatunków niezależnie od godziny pozyskania danych.
3. Dane termalne z zakresu średniej podczerwieni mogą być wykorzystane do identyfikacji *Picea abies* o osłabionej kondycji i martwych w wyniku gradacji kornika drukarza. Wyniki wskazują, że fuzja danych termalnych i skanowania laserowego pozwala na stworzenie schematu postępowania, dzięki któremu można wyznaczać indywidualne korony drzew i identyfikować ich stan zdrowotny o dokładności ogólnej 0,52. Ograniczeniem opracowanej metody jest brak możliwości rozdzielenia od siebie drzew martwych od tych w osłabionej kondycji.
4. Badając w centrum Warszawy pięć pospolicie występujących gatunków wykazano, że grupy drzew różniące się stopniem przebarwienia liści różnią się jednocześnie temperaturą korony zarejestrowanej z pułapu lotniczego. Analiza temperatur koron zarejestrowanych w ciągu dnia pozwala na identyfikację czterech klas kondycji zdrowotnej, podczas gdy temperatur zarejestrowana w nocy tylko dwóch klas.

Podsumowując moje badania można stwierdzić, że dane termalne z zakresu średniej podczerwieni (3,6–4,9 μm) pozyskane z pułapu lotniczego mogą być wskaźnikiem kondycji zdrowotnej wybranych gatunków drzew. Zmienność temperatur koron może być wskaźnikiem stanu zdrowotnego drzew rosnących zarówno w środowisku naturalnym jak i miejskim.

Literatura

1. Abdullah, H., Darvishzadeh, R., Skidmore, A.K., Heurich, M., 2019. Sensitivity of Landsat-8 OLI and TIRS data to foliar properties of early stage bark beetle (*Ips typographus* L.) infestation. *Remote sensing*, 11 (4), 398. <https://doi.org/10.3390/rs11040398>
2. Acharya, A. S., Prakash, A., Saxena, P., Nigam, A. 2013. Sampling: Why and how of it. *Indian Journal of Medical Specialties*, 4 (2), 330-333.
3. Ball, D., 2011. Common sense risk management of trees: guidance on trees and public safety in the UK for owners, managers and advisers. Forestry Commission, Edinburgh.
4. Dale, A. G., Youngsteadt, E., Frank, S. D., 2016. Forecasting the effects of heat and pests on urban trees: impervious surface thresholds and the ‘pace-to-plant’ technique. *Arboriculture & Urban Forestry*, 42 (3), 181-191. https://ecoipm.org/wp-content/uploads/Dale_2016_Arb.pdf
5. Degerickx, J., Roberts, D. A., McFadden, J. P., Hermy, M., Somers, B., 2018. Urban tree health assessment using airborne hyperspectral and LiDAR imagery. *International journal of applied earth observation and geoinformation*. 73, 26-38. <https://doi.org/10.1016/j.jag.2018.05.021>
6. de Faria Peres, L., de Lucena, A. J., Rotunno Filho, O. C., de Almeida França, J. R., 2018. The urban heat Island in Rio de Janeiro, Brazil, in the last 30 years using remote sensing data. *International Journal of Applied Earth Observation and Geoinformation*, 64, 104–116. <https://doi.org/10.1016/j.jag.2017.08.012>
7. Egea, G., Padilla-Díaz, C.M., Martinez-Guanter, J., Fernandez, J.E., Perez-Ruiz, M., 2017. Assessing a crop water stress index derived from aerial thermal imaging and infrared thermometry in super-high density olive orchards. *Agricultural Water Management*, 187, 210–221. <https://doi.org/10.1016/j.agwat.2017.03.030>
8. Filchev, L., 2012. An assessment of European spruce bark beetle infestation using Worldview-2 satellite data. In: European SCGIS Conference “Best Practices: Application of GIS Technologies for Conservation of Natural and Cultural Heritage Sites.” Sofia, Bulgaria. <https://doi.org/10.13140/2.1.3005.2647>
9. Gerber, F., Marion, R., Olioso, A., Jacquemoud, S., Da Luz, B. R., Fabre, S., 2011. Modeling directional–hemispherical reflectance and transmittance of fresh and dry leaves from 0.4 μm to 5.7 μm with the PROSPECT-VISIR model. *Remote sensing of environment*, 115 (2), 404-414. <https://doi.org/10.1016/j.rse.2010.09.011>
10. Gluch, R., Quattrochi, D. A., Luvall, J. C., 2006. A multi-scale approach to urban thermal analysis. *Remote Sensing of Environment*, 104 (2), 123–132. <https://doi.org/10.1016/j.rse.2006.01.025>
11. Grodzki, W., McManus, M., Knížek, M., Meshkova, V., Mihalciuc, V., Novotny, J., Turcani, M., Slobodyan, Y., 2004. Occurrence of spruce bark beetles in forest stands at different levels of air pollution stress. *Environmental Pollution*, 130 (1), 73–83. <https://doi.org/10.1016/j.envpol.2003.10.022>
12. Gutowski, J. M., 2004. Kornik drukarz–gatunek kluczowy. *Parki Narodowe*, 1, 13–15.
13. Hais, M., Kučera, T., 2008. Surface temperature change of spruce forest as a result of bark beetle attack: remote sensing and GIS approach. *European Journal of Forest Research*, 127 (4), 327-336. <https://doi.org/10.1007/s10342-008-0208-8>
14. Hanisch, B., Kilz, E., 1990. Monitoring of forest damage: spruce and pine. Verlag Eugen Ulmer, Stuttgart.

15. Ishimwe, R., Abutaleb, K., Ahmed, F., 2014. Applications of thermal imaging in agriculture—A review. *Advances in Remote Sensing*, 3 (3), 128. <http://dx.doi.org/10.4236/ars.2014.33011>
16. Jarocińska, A., Białczak, M., Sławik, Ł., 2018. Application of aerial hyperspectral images in monitoring tree biophysical parameters in urban areas. *Miscellanea Geographica*, 22 (1), 56–62. <https://doi.org/10.1515/mgrsd-2017-0034>
17. Junntila, S., Vastaranta, M., Hämäläinen, J., Latva-Käyrä, P., Holopainen, M., Hernández Clemente, R., Hyypä, H., Navarro-Cerrillo, R. M., 2016. Effect of forest structure and health on the relative surface temperature captured by airborne thermal imagery – Case study in Norway Spruce-dominated stands in Southern Finland. *Scandinavian Journal of Forest Research*, 32 (2), 154-165. <https://doi.org/10.1080/02827581.2016.1207800>
18. Khanal, S., Fulton, J., Shearer, S., 2017. An overview of current and potential applications of thermal remote sensing in precision agriculture. *Computers and Electronics in Agriculture*, 139, 22-32. <https://doi.org/10.1016/j.compag.2017.05.001>
19. Kim, Y., Still, C. J., Roberts, D. A., Goulden, M. L., 2018. Thermal infrared imaging of conifer leaf temperatures: Comparison to thermocouple measurements and assessment of environmental influences. *Agricultural and Forest Meteorology*, 248, 361-371. <https://doi.org/10.1016/j.agrformet.2017.10.010>
20. Kimball, B. A., Bernacchi, C. J., 2006. Evapotranspiration, canopy temperature, and plant water relations. *Managed ecosystems and CO2*, Springer-Verlag, Berlin. 311-324. https://doi.org/10.1007/3-540-31237-4_17
21. Leuzinger, S., Körner, C., 2007. Tree species diversity affects canopy leaf temperatures in a mature temperate forest. *Agricultural and Forest Meteorology*, 146 (1-2), 29-37. <https://doi.org/10.1016/j.agrformet.2007.05.007>
22. Leuzinger, S., Vogt, R., Körner, C., 2010. Tree surface temperature in an urban environment. *Agricultural and Forest Meteorology*, 150 (1), 56-62. <https://doi.org/10.1016/j.agrformet.2009.08.006>
23. Long, J.A., Lawrence, R.L., 2016. Mapping percent tree mortality due to mountain pine beetle damage. *Forest Science*, 62 (4), 392–402. <https://doi.org/10.5849/forsci.15-046>
24. Maes, W. H., Steppe, K., 2012. Estimating evapotranspiration and drought stress with ground-based thermal remote sensing in agriculture: a review. *Journal of experimental botany*, 63 (13), 4671-4712. <https://doi.org/10.1093/jxb/ers165>
25. Malakar, N. K., Hulley, G. C., Hook, S. J., Laraby, K., Cook, M., Schott, J. R., 2018. An operational land surface temperature product for Landsat thermal data: Methodology and validation. *IEEE Transactions on Geoscience and Remote Sensing*, 56 (10), 5717–5735. <https://doi.org/10.1109/TGRS.2018.2824828>
26. Mattheck, C., Breloer, H., 1994. Field guide for visual tree assessment (VTA). *Arboricultural Journal*, 18 (1), 1-23. <https://doi.org/10.1080/03071375.1994.9746995>
27. Meier, F., Scherer, D., 2012. Spatial and temporal variability of urban tree canopy temperature during summer 2010 in Berlin, Germany. *Theoretical and Applied Climatology*, 110 (3), 373–384. <https://doi.org/10.1007/s00704-012-0631-0>
28. Möller, M., Alchanatis, V., Cohen, Y., Meron, M., Tsipris, J., Naor, A., Ostrovsky, V., Sprintsin, M., Cohen, S., 2007. Use of thermal and visible imagery for estimating crop water status of irrigated grapevine. *Journal of experimental botany*, 58(4), 827-838. <https://doi.org/10.1093/jxb/erl115>
29. Quattrochi, D. A., Ridd, M. K., 1998. Analysis of vegetation within a semi-arid urban environment using high spatial resolution airborne thermal infrared remote sensing data. *Atmospheric Environment*, 32 (1), 19–33. [https://doi.org/10.1016/S1352-2310\(97\)00179-9](https://doi.org/10.1016/S1352-2310(97)00179-9)

30. Roman, L. A., 2013. Urban tree mortality. University of California, Berkeley.
31. Roy, S., Byrne, J., Pickering, C., 2012. A systematic quantitative review of urban tree benefits, costs, and assessment methods across cities in different climatic zones. *Urban forestry & urban greening*, 11 (4), 351-363. <https://doi.org/10.1016/j.ufug.2012.06.006>
32. Santesteban, L. G., Di Gennaro, S. F., Herrero-Langreo, A., Miranda, C., Royo, J. B., Matese, A., 2017. High-resolution UAV-based thermal imaging to estimate the instantaneous and seasonal variability of plant water status within a vineyard. *Agricultural Water Management*, 183, 49–59. <https://doi.org/10.1016/j.agwat.2016.08.026>
33. Sikorska, D., Sikorski, P., Archiciński, P., Chormański, J., Hopkins, R. J., 2019. You can't see the woods for the trees: Invasive *Acer negundo* L. in urban riparian forests harms biodiversity and limits recreation activity. *Sustainability*, 11 (20), 5838. <https://doi.org/10.3390/su11205838>
34. Spronken-Smith, R. A., Oke, T. R., 1998. The thermal regime of urban parks in two cities with different summer climates. *International journal of remote sensing*, 19 (11), 2085-2104. <https://doi.org/10.1080/014311698214884>
35. Stereńczak, K., Mielcarek, M., Modzelewska, A., Kraszewski, B., Fassnacht, F.E., Hilszczański, J., 2019. Intra-annual *Ips typographus* outbreak monitoring using a multi-temporal GIS analysis based on hyperspectral and ALS data in the Białowieża Forests. *Forest Ecology and Management*, 442, 105–116. <https://doi.org/10.1016/j.foreco.2019.03.064>
36. Ullah, S., Schlerf, M., Skidmore, A. K., Hecker, C., 2012. Identifying plant species using mid-wave infrared (2.5–6 μm) and thermal infrared (8–14 μm) emissivity spectra. *Remote Sensing of Environment*, 118, 95–102. <https://doi.org/10.1016/j.rse.2011.11.008>
37. Urban Atlas, 2018. <https://land.copernicus.eu/local/urban-atlas/urban-atlas-2018> (dostęp: 4 marca 2022).
38. Wang, X., Yang, W., Wheaton, A., Cooley, N., Moran, B., 2010. Automated canopy temperature estimation via infrared thermography: a first step towards automated plant water stress monitoring. *Computers and Electronics in Agriculture*, 73 (1), 74-83. <https://doi.org/10.1016/j.compag.2010.04.007>
39. Wang, J., Meng, S., Lin, Q., Liu, Y., Huang, H., 2022. Detection of Yunnan pine shoot beetle stress using UAV-based thermal imagery and LiDAR. *Applied Sciences*, 12 (9), 4372. <https://doi.org/10.3390/app12094372>
40. Witkoś-Gnach K., M. Krynicki M. 2021. Standard inspekcji i diagnostyki drzew. Fundacja EkoRozwoju, Wrocław.
41. Zhang, Y., Liu, N., Wang, S., 2018. A differential privacy protecting K-means clustering algorithm based on contour coefficients. *PLoS One* 13 (11). <https://doi.org/10.1371/journal.pone.0206832>
42. Zheng, S., Guldmann, J. M., Liu, Z., Zhao, L., 2018. Influence of trees on the outdoor thermal environment in subtropical areas: An experimental study in Guangzhou, China. *Sustainable Cities and Society*, 42, 482–497. <https://doi.org/10.1016/j.scs.2018.07.025>
43. Zhou, Z., Majeed, Y., Naranjo, G. D., Gambacorta, E. M., 2021. Assessment for crop water stress with infrared thermal imagery in precision agriculture: A review and future prospects for deep learning applications. *Computers and Electronics in Agriculture*, 182, 106019. <https://doi.org/10.1016/j.compag.2021.106019>

Streszczenie

Monitoring stanu zdrowotnego drzew jest jednym z zadań realizowanych w ramach zarządzania obszarami chronionymi, kontroli zieleni miejskiej czy ochrony lasu. Prowadzone są szeroko zakrojone badania nad opracowaniem szybkiej i precyzyjnej metody identyfikacji osłabionych i martwych osobników rosnących w różnych środowiskach.

Celem pracy było sprawdzenie, czy dane termalne z zakresu średniej podczerwieni (3,6–4,9 μm) pozyskane z pułapu lotniczego mogą być wykorzystane do badań kondycji zdrowotnej drzew. W tym celu przeprowadzono trzy analizy na niezależnych zbiorach danych w różnych środowiskach.

Badania wykonane na danych termalnych pozyskanych w ciągu dnia wykazały, że temperatura korony jest cechą specyficzną dla gatunku i zależy od położenia drzewa w terenie. Drzewa znajdujące się wewnątrz lasu miały niższą temperaturę koron do 0,70°C niż te rosnące poza lasem. Gatunkiem o najwyższej temperaturze, niezależnie od godziny pozyskania danych lotniczych, był *Pinus sylvestris*. Niskimi temperaturami charakteryzowały się *Alnus glutinosa*, *Quercus rubra* i *Quercus petraea*.

Badania nad identyfikacją miejsc żerowania kornika drukarza wykazały, że fuzja danych termalnych i skanowania laserowego umożliwiły wyznaczenie temperatury koron pojedynczych drzew *Picea abies* i sklasyfikowanie ich do trzech klas zdrowotnych (drzewa 'zdrowe' o średniej temperaturze 27,70°C; 'o osłabionej kondycji' 28,57°C i 'martwe' 30,17°C). Opracowany został schemat postępowania wykorzystujący automatyczną segmentację i uczenie maszynowe do identyfikacji drzew 'o osłabionej kondycji' i 'martwych'. Jednak, nie było możliwe rozdzielenie tych dwóch klas kondycyjnych wzorując się jedynie na danych termalnych, ponieważ większość drzew martwych była przypisywana do klasy 'osłabiona kondycja'. Wynik można interpretować jako wyodrębnienie klasy przejściowej, w której identyfikowane są ogólnie drzewa zaatakowane przez kornika drukarza.

Badania przeprowadzone w środowisku miejskim wykazały statystycznie istotne różnice między klasami kondycji zdrowotnej drzew zarówno na danych pozyskanych w dzień jak i w nocy. Korony drzew zdrowych były chłodniejsze w porównaniu do koron drzew zamierających. Średnia wartość różnicy wynosiła 3,28°C w ciągu dnia oraz 1,06°C w nocy.

Podsumowując, lotnicze dane termalne z zakresu średniej podczerwieni mogą być wykorzystane do badań kondycji zdrowotnej wybranych gatunków drzew. Zmienność

temperatur koron jest cechą zależną od gatunku i może być wskaźnikiem stanu zdrowotnego w środowisku naturalnym i miejskim. Dalsze badania są wymagane w zakresie zwiększenia precyzji określania stanu zdrowotnego drzew, szczególnie dla drzew uszkodzonych z powodu żerowania kornika drukarza. Zwiększenie dokładności identyfikacji drzew o osłabionej kondycji i martwych pozwoliłoby na skuteczniejsze zarządzanie obszarami leśnymi. Do rozwinięcia i ulepszenia przedstawionej metody można zastosować fuzję z innymi typami danych (np. zobrażenia hiperspektralne), lub posłużyć się danymi z innych nośników rejestrujących (np. bezzałogowe statki powietrzne).

Summary

Trees' health condition monitoring is one of the tasks carried out as part of the protected areas management, urban greenery control, and forest protection. Extensive research is underway to develop a quick and precise method of identifying dead trees and trees in poor condition growing in different environments.

This study aimed to check whether airborne thermal data from the middle-wave infrared range (3.6–4.9 μm) can be used to study the health condition of trees. For this purpose, three analyses were performed on independent data sets in different environments.

Studies performed on thermal data obtained during the day showed that canopy temperature is a species-specific feature and depends on a tree's location in the study area. Trees growing in the forest had a lower canopy temperature of up to 0.7°C than those growing outside. Species with the highest canopy temperatures, despite the time of airborne data acquisition, was *Pinus sylvestris*. Low canopy temperatures were found for *Alnus glutinosa*, *Quercus rubra*, and *Quercus petraea*.

Research on the identification of bark beetle feeding sites showed that the fusion of thermal data and laser scanning made it possible to determine the temperature of the individual tree crowns of *Picea abies* and classify them into three health classes ('healthy' trees with an average temperature of 27.70°C; 'in poor condition' 28, 57°C and 'dead' 30.17°C). A workflow was constructed using automatic segmentation and machine learning to identify trees in 'poor condition' and 'dead'. However, it was impossible to separate these two condition classes based on thermal data alone, as most of the dead trees were assigned to the 'poor condition' class. The result can be interpreted as the separation of a transition class in which trees attacked by the bark beetle are identified.

Studies conducted in an urban environment showed statistically significant differences between trees' health condition classes on data obtained during the day and at night. The canopies of healthy trees were cooler than those of dying trees. The mean difference between healthy and dying trees was 3.28°C during the day and 1.06°C at night.

In conclusion, middle-wave infrared thermal data acquired from an airborne level can be used to study health conditions of selected trees. The variability of canopy temperatures is a species-specific feature and can be a health status indicator in a natural and urban environment. Further research is required to increase the precision of determining the trees' health status, especially for trees damaged due to bark beetle feeding. Increasing the accuracy of identifying trees in poor condition and dead would allow for more effective

management of forest areas. To develop and improve the presented method, fusion with other types of data (i.e. hyperspectral imagery) can be used, or data from other sensor carriers (i.e. unmanned aerial vehicles).

Kopie publikacji wchodzących w skład rozprawy doktorskiej

Canopy temperatures of selected tree species growing in the forest and outside the forest using aerial thermal infrared (3.6–4.9 μm) data

Agata Zakrzewska ^a, Dominik Kopeć ^{a,b}, Karol Krajewski ^b and Jakub Charyton ^b

^aDepartment of Biogeography, Paleoecology and Nature Conservation, Faculty of Biology and Environmental Protection, University of Lodz, Łódź, Poland; ^bDepartment of Remote Sensing, Mggp Aero Sp. Z O.O, Tarnów, Poland

ABSTRACT

Studies conducted in recent years have demonstrated high application potential of thermal remote sensing data in environmental analyses. The main goal of our studies was to determine the variability of tree canopy temperatures using a new sensor which acquires data in the still rarely used thermal spectral range (3.6–4.9 μm). This study was conducted on five selected tree species growing in the forest and outside the forest: *Alnus glutinosa*, *Pinus sylvestris*, *Quercus petraea*, *Quercus rubra* and *Robinia pseudoacacia*. Thermal data were acquired on 9 June 2019, between 8:10 and 14:00 (CET). The findings were as follows: i) Trees growing in the forest are on average 0.4–0.7°C cooler than trees outside the forest; ii) The canopy temperatures of species under study differ statistically irrespective of data acquisition time. *Alnus glutinosa*, *Quercus rubra* and *Quercus petraea* are species with the lowest canopy temperatures, and *Pinus sylvestris* has the highest canopy temperature. The studies showed that the biggest variation between species in the canopy temperature occurs at noon (12:00–13:00); iii) A thermal spectral range of 3.6–4.9 μm registers the canopy temperature of tree species with a high accuracy, which supports its usage in remote sensing vegetation studies.

ARTICLE HISTORY

Received 27 October 2021
Revised 28 March 2022
Accepted 30 March 2022

KEYWORDS



Infrared thermography; thermal imagery; middle wave infrared; tree species; invasive species; land surface temperature*


Introduction

Acquisition of thermal infrared data (TIR) using remote sensing techniques is an increasingly popular method to obtain information about the temperature of objects. A variety of carriers of thermal cameras have been used throughout the years, such as satellites (De Faria Peres et al., 2018; Gluch et al., 2006), aeroplanes (Quattrochi & Ridd, 1998), helicopters (Spronken-Smith & Oke, 1998), Unmanned Aerial Vehicles (UAV; Santesteban et al., 2017), truck-cranes (Möller et al., 2007), tripods (Cohen et al., 2005) and flux towers (Still et al., 2021). The most commonly used source of land surface temperature (LST) is satellite data. Despite their numerous advantages, such as the ability to capture huge areas at a single scene (e.g. Landsat-8 satellite scene size is 185 km \times 180 km), satellite data have limitations as well. Their first limitation is data resolution (Ground Sample Distance (GSD) of 100 m), which precludes analysis of the temperature of individual tree-type objects. The second limitation is the acquisition time. Satellite data are acquired from a sun-synchronous orbit, meaning that for a given location the data are always sourced at the same time of day or night. For instance, data for study areas in central Poland are always acquired around 10:00 a.m. (<https://earthexplorer.usgs.gov>). This is not the best time to study

many environmental phenomena such as the urban surface heat Island (Majkowska et al., 2017). The most popular source of TIR data are Landsat satellites, which TIR spectral bands are Long Wave Infrared (LWIR) from 10.4 to 12.5 μm (Malakar et al., 2018). Most of the research, which use satellite data are conducted in this atmospheric transmission window.

Aerial data are an alternative to satellite data but they are far less popular. However, sensors determining thermal properties of objects have been significantly developed in recent years. Precision and resolution of sensors have increased, as well as their use in UAV (Gallardo-Saavedra et al., 2018), which results in lower prices and higher availability of cameras of this type. It is also possible to obtain a temperature of a single object, and analyze changes of these objects (e.g. temperature variations in tree crowns). It is easier to plan accurate airborne data acquisition during a day or a night by setting a specific time, which depends on the study goal. It is particularly important, because an object's temperature changes during the day. According to Zheng et al. (2018) the highest temperature of leaves takes place at different times for various tree species. Environmental remote sensing studies conducted from the airborne level have used cameras with a range of 7.5–14 μm (e.g.: Leuzinger & Körner, 2007; Marešová et al., 2020; Richter et al., 2021) and from the satellite level with

CONTACT Dominik Kopeć  dominik.kopec@biol.uni.lodz.pl  Department of Biogeography, Paleoecology and Nature Conservation, Department of Remote Sensing, University of Lodz, Łódź 90-237, Poland

 Supplemental data for this article can be accessed online at <https://doi.org/10.1080/22797254.2022.2062055>

© 2022 The Author(s). Published by Informa UK Limited, trading as Taylor & Francis Group.

This is an Open Access article distributed under the terms of the Creative Commons Attribution License (<http://creativecommons.org/licenses/by/4.0/>), which permits unrestricted use, distribution, and reproduction in any medium, provided the original work is properly cited.

a range 10.4–12.5 μm . In our studies, we used a different spectral range, namely 3.6–4.9 μm , which had not been used in remote sensing vegetation studies before. The use of this range ensures greater dynamics of imaging and the ability to capture smaller temperature differences due to the emissivity curve, which is essential in the case of small temperature differences between species or individuals (Livache, 2019). The 4.25 μm center-wavelength of the MWIR sensor used in our study falls on the steep rising edge of the emissivity curve, which translates to larger sensor response to small temperature differences of observed surfaces. According to Z.-L. Li et al. (2013a); Z. L. Li et al. (2013b) in the MWIR the direct solar irradiation reflected by the surface is on the same order of magnitude as the radiance directly emitted by the surface, if the surface albedo is about 0.1, the introduction of the MWIR channels in LST greatly improves the accuracy of the estimated LST.

LST is one of the indicators of the environment condition, it can be easily interpreted and used in various studies. These data are used, for example, to identify the presence of an urban heat Island (Price, 1979; Tran et al., 2006), the influence of city parks on reducing its effect (Dimoudi & Nikolopoulou, 2003), and to identify crop hydration and health status of crops and fruit trees (Egea et al., 2017; Khanal et al., 2017). In macroscale, TIR data can be also used to study peatlands (Ciężkowski et al., 2020; Kopeć et al., 2016), and in microscale to determine the temperature of individual leaves of deciduous trees (Jiménez-Bello et al., 2011) and coniferous trees (Kim et al., 2018). The studies carried out in recent years demonstrate that TIR data have a very high application potential and can be used to determine the canopy temperature (CT) of trees in most types of environments. CT is the temperature of the outer layer of the tree crown recorded from the top, most of which are leaves. It is widely known that trees affect air quality, successfully lowering air temperature (Dimoudi & Nikolopoulou, 2003; Fahmy & Sharples, 2009; Morakinyo et al., 2017). Only few authors to date have reported data on how the environment affects CT. The temperatures of trees in a forest (Leuzinger & Körner, 2007) or in an urban environment were investigated (Meier & Scherer, 2012; Rahman et al., 2017; Spronken-Smith & Oke, 1998), but the difference of CT of trees in the forest and outside the forest for the same species at the same time has hardly been studied. Research in this area would improve understanding of the environment's influence on CT. Most of the research, which focus on tree crown temperatures were carried out in the forest (Junttila et al., 2017), or in orchards (Sobrino et al., 1990).

The influence of an environment on trees outside the forest is barely known, especially in the case of its detection by remote sensing methods (Wani et al., 2020). Not only knowledge about the influence of the environment on CT is important, but also knowledge of the variance of the crown temperature of individual species. This is an essential aspect in order to correctly interpret the results of a different CT for one species.

The main goal of our studies was to determine the variability of CT using a new sensor with a spectral range 3.6–4.9 μm . Detailed research questions were as follows: (i) What is the difference between trees in the forest and trees outside the forest as regards their CT? (ii) Does CT differentiate tree species? (iii) Is TIR data acquired from ImageIR 9400 camera in the 3.6–4.9 μm spectral range accurate enough to be used in CT analyses?

Materials and methods

Study area

The studies were conducted in the area of the National Park of Wielkopolska (NPW) located in Poland (52° 16' N, 16°47' E). The study area is in the humid continental climate zone (Peel et al., 2007). The average annual temperature is 8.3°C, and the average rainfall is 475 mm/yr. The study area spans 102.33 km². The NPW was established in 1957 to preserve the landforms of the postglacial landscape (Journal of Laws of 1957 No. 24, Item 114). Today, the NPW is mainly covered by human-modified forests dominated by Scots pine (*Pinus sylvestris*), sessile oak (*Quercus petraea*) and common oak (*Quercus robur*). Despite the fact that the study area was a national park, large part of the tree populations were invasive and non-native species, e.g. *Robinia pseudoacacia* and *Quercus rubra*. A large part of the NPW consists of agricultural areas and single-family housing, which is the main reason behind the presence of non-native and invasive species in this area.

Study species

The study covered three native tree species which are considered forest-forming species for the NPW and are widespread in the North European Plain, namely *Alnus glutinosa*, *Pinus sylvestris* and *Quercus petraea*, and two species non-native in the Polish flora: *Quercus rubra* and *Robinia pseudoacacia*.

Alnus glutinosa (L.) Gaertn.

Black alder grows up to 30 m in height and has a slender trunk with a wide, elongated crown. Its leaves are 4–10 cm long, green on both sides,

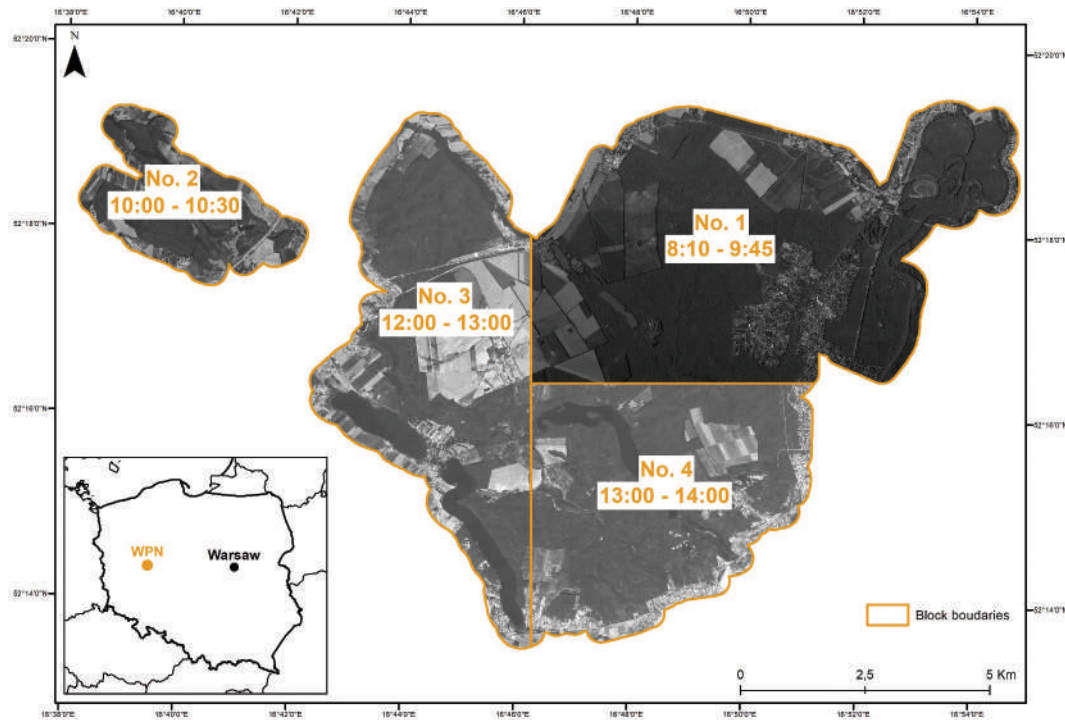


Figure 1. Division of the study area (National Park of Wielkopolska – NPW) into blocks with information about airborne data acquisition time. The base for the map consists of thermal images acquired on 9 June 2019. Solar noon on the date of data acquisition – 12:00 (11:00 UTC).

with a glossy upper surface. Black alder is a forest-forming species for the alder carr and riparian forests, i.e. peatland forests with high groundwater levels (McVean, 1953). The tree stands are evenly distributed in the NPW, and are most numerous in the immediate vicinity of lakes in the valleys of smaller rivers.

Pinus sylvestris L.

Scots pine is a coniferous tree which grows up to 30–40 m in height. The needles are stiff and hard, glaucous grey-green, 4–7 cm in length, occurring in fascicles of two on the tip of shoots (Mátyás et al., 2004). In nature, the species is found on poor, sandy soils but it used to be planted on fertile sites as well. The Scots pine is the most common species in the NPW.

Quercus petraea (Matt.) Liebl.

Sessile oak grows up to 20–30 m in height with a dense crown. The leaves are evenly lobed, 5–14 cm long. It grows best in sandy loam soils, forming dense oak forests or mixed forests with a large share of pine trees (Rutkowski, 1998). It is evenly distributed in the territory of the NPW.

Quercus rubra L.

Northern red oak grows up to 20–25 m in height with a dense, wide crown. The leaves are up to 22 cm long, sharply toothed, dark green on the upper surface and light green on the underside. The species is considered

invasive in Poland (Woziwoda et al., 2014), growing quickly and forming mixed forests (Sander, 1990). In the NPW it is found within forest complexes.

Robinia pseudoacacia L.

Black locust is up to 25 m high. The leaves are odd-pinnate with small, ovate leaflets with rounded tips. They are light green on the upper surface and grey-green underneath. The species is considered invasive in Poland (Dyderski & Jagodziński, 2019). It is widespread in urban habitats, along the roads and rivers, as well as in open areas and semi-natural forests (Cierjacks et al., 2013). In the NPW it is found both in built-up areas and within forest complexes.

Airborne data acquisition

At the peak of the 2019 growing season, three types of airborne data were acquired using a fusion of instruments: TIR data with a spatial resolution of GSD = 0.5 m, Airborne Laser Scanner (ALS) with a density of 18 points/m² and Hyperspectral (HS) data with a spatial resolution of GSD = 1 m. For the purpose of data acquisition, the study area was divided into four blocks (Figure 1). All flights were performed with an aircraft Vulcanair P-68 Observer 2 (Table 2).

A separate flight plan was prepared for each of the blocks. On 9 June 2019, data were acquired consecutively for all of the four blocks at times shown in Figure 1. Data were acquired between 8:10 and 14:00 CET (7:10 and 13:00 UTC). During the flight, the air temperature was between 21.9 and 24.3°C, there was

Table 1. Weather conditions during data acquisition for individual blocks on 9 June 2019.

Block number	Acquisition time	Air temperature [°C]	Humidity [%]	Wind speed [m s ⁻¹]	Wind direction	Solar radiation [w/m ²]
1	8:10–9:45	21.9	29.0	0.66	SW	493.52
2	10:00–10:30	22.6	26.1	1.29	S	392.36
3	12:00–13:00	23.7	24.1	2.03	SW	425.10
4	13:00–14:00	24.3	23.2	1.83	SW	590.78

a total lack of cloud cover, and the wind speed did not significantly exceed 2 m s⁻¹ (Table 1). Wind speed of up to 2 m s⁻¹ is an important requirement in the case of studies using a TIR camera as strong gusts of wind cool the surface of the leaves. For instance, wind speed of 2 m s⁻¹ can lower the temperature of the leaves. In order to register the correct temperature of the canopy in full sunlight, the measurement should be performed at the maximum 2 m s⁻¹ wind speed threshold (Ansari & Loomis, 1959; Grace, 1988).

All detailed flight and data parameters are listed in Table 2. TIR data were acquired using ImageIR 9400 camera by InfraTec GmbH (Dresden, Germany). The spectral range of the images was 3.6–4.9 µm, which is determined as Middle Wave Infrared (MWIR). Declared absolute accuracy of the camera is in range ±1°C (±1%), however a certificate of radiometric calibration in the ranges of -10°C to 100°C showed differences lower than 0.2°C. IRBIS Professional v.3.1 software was used to process and correct raw thermal images. Atmospheric correction was made, which was calculated individually for each of the acquisition blocks, and took into account the atmospheric transmittance model using ambient temperature, relative humidity and flight altitude (Table 1; Minkina & Dudzik, 2009). The average emissivity of plant objects in the MWIR range was determined at $\epsilon = 0.95$ based on the literature reports (Ullah et al., 2012). Using one emissivity value was caused by the size of the study area. This study is also focused only on tree canopy temperatures, which emissivity is similar. Geometric correction of thermal photos was performed with a typical photogrammetric process. Thermal photos were processed as aerial photos to create a thermal orthomosaic. The first step of this process included lens distortion correction. The thermal images were aerotriangulated using the Inpho Match AT (Trimble Inc., Sunnyvale, CA, USA) based on GCP (Ground Point Controls), where the final RMSE of the match was 85 cm. Next, orthorectification on the newest and

high-resolution DEM (Digital Elevation Model) was performed in Inpho OrthoMaster (Trimble Inc., Sunnyvale, CA, USA) software. Last stage involved fit control based on 45 control points transferred from RGB. Data were georeferenced and mosaicked in the Inpho OrthoVista program (Trimble Inc., Sunnyvale, CA, USA). Finally, the TIR data were downscaled to a resolution of 1 m to ensure compatibility with the ALS and HS data. The data were then corrected geometrically and radiometrically. The geometric corrections to the data involved a typical photogrammetry processing steps, applicable to any aerial survey, and included geometric correction of lens distortion (Interior Orientation), based on geometric calibration certificate, aerotriangulation of image coordinate space to world coordinates with ground control points (obtained from high-resolution RGB orthomosaic) and orthorectification of images on the triangulated ground model of the LiDAR-derived Digital Terrain Model (DTM). Radiometric correction involved resolving of light fall-off due to radiation travel path differences through the lens. The resulting thermal orthomosaic, divided into blocks, was used to determine the temperature of the tree canopies.

The ALS and HS data were used in the postprocessing of ground reference data. Laser scanning was acquired using a Riegl VQ-780 sensor with a point density of 18 points/m². The obtained point cloud was classified to basic ASPRS specification and used to create a Canopy Height Model (CHM) with a resolution of 1 m. To extract the ground, Axelsson algorithm implemented in commercial software TerraScan (Terrasolid Ltd., Espoo, Finland) was used (Axelsson, 2000). Other classes, according to ASPRS specification were obtained using TerraScan customized classification rules. LAStools (rapidlasso GmbH, Gilching, Germany), a lasheight tool with a buffering parameter was used to normalize height values in the collected point cloud. ALS data were used to create single canopy range polygons. HS data were

Table 2. Parameters of flight and sensors used. Abbreviations: TIR – Thermal InfraRed; HS – Hyperspectral; ALS – Aerial Laser Scanning; VNIR – Visible-Near Infrared; SWIR – Short Wave Infrared; GSD – Ground Sampling Distance.

Data Type	Sensor Type	Data Parameters	Swath Width [m]	Aircrafts	Flight Level [m] and Airspeed [m/s]	Date of Flight	Hour of Flight
TIR	ImageIR 9400	GSD 0.5 [m]	30	Vulcanair P-68	1300 above ground level, 61.8	9 June 2019	8:10 (6:10 UTC) –14:00 (12:00 UTC)
ALS point cloud	Riegl VQ-780i	Density 18 [pts./m ²]	60	Observer 2			
HS images	HySpex VNIR-1800	GSD 1 [m]	60				
	0.4–0.9 µm						
HS images	HySpex SWIR-384	GSD 1 [m]	60				
	0.9–2.5 µm						

acquired using the HySpex sensor (Norwegian Norsk Elektro Optikk company) made of two sensors: VINR-1800 with a spectral range of 0.4–0.9 μm and SWIR-384 with a spectral range of 0.9–2.5 μm . The acquired data were georeferenced and mosaicked. HS data were used to prepare an illumination map.

Ground reference data

At the peak of the 2019 growing season, 400 ground reference data for five tree species (Sec. 2.2) were collected. The measurements were made using a Trimble Catalyst GNSS receiver: a Trimble DA1 antenna (measurement accuracy of about 1 m) and the MapIT application (Mapit GIS LTD, Wishaw, UK) connected to it. The data were saved as points in GeoJSON format. For each reference point, the taxonomic information, location in the area (in the forest or outside the forest) and the coordinates of the canopy center were recorded in the study area. All individuals were healthy and had a dense, compact crown, which ensured that the temperature recorded was the temperature of the tree canopy, and not the ground temperature. In each block, 20 individual trees for each study species were acquired (10 individuals in the forest and 10 outside the forest). All individuals were distributed as evenly as possible, taking into account their actual occurrence both in the entire study area, and in each block separately (Figure 2). The reference data collected in this way were then postprocessed.

Delineating the range of a tree's crown

The analyses of the ground and TIR data were carried out in stages.

The first step involved photointerpretation of the range of individual tree canopies. For each of the 400 trees, points from ground reference data were transformed into polygons covering its entire canopy. Polygons were created based on the photointerpretation of the CHM data (Figure 3). Only the pixels that were entirely within the drawn canopy were counted for each polygon. Extreme canopy pixels, i.e. those that could include the temperature of tree canopy and the ground were excluded from the analysis by using a 0.1 m buffer inside the range to minimize the effect of the ground on the final temperature of the entire canopy.

Next, pixels covering a tree's shaded part were eliminated from its canopy range based on HS data which were used to create the illumination map. This map was prepared in the ATCOR-4 program using the *at_shadowdetect* tool. Pixels in the illumination map range from 0.1 for full shadow to 1 for full sun. Pixels whose value was 0.1 were excluded from further analyses (Supplementary Materials). An original, whole tree canopy range, created based on CHM model (called Range 1) was reduced to Range 2. After using an illumination map, pixels in full shadow were eliminated in Range 2 (Figure 3).

The illumination map helped to exclude the pixels located in the shadow of the tree from the canopy range, as they could ultimately lower the overall

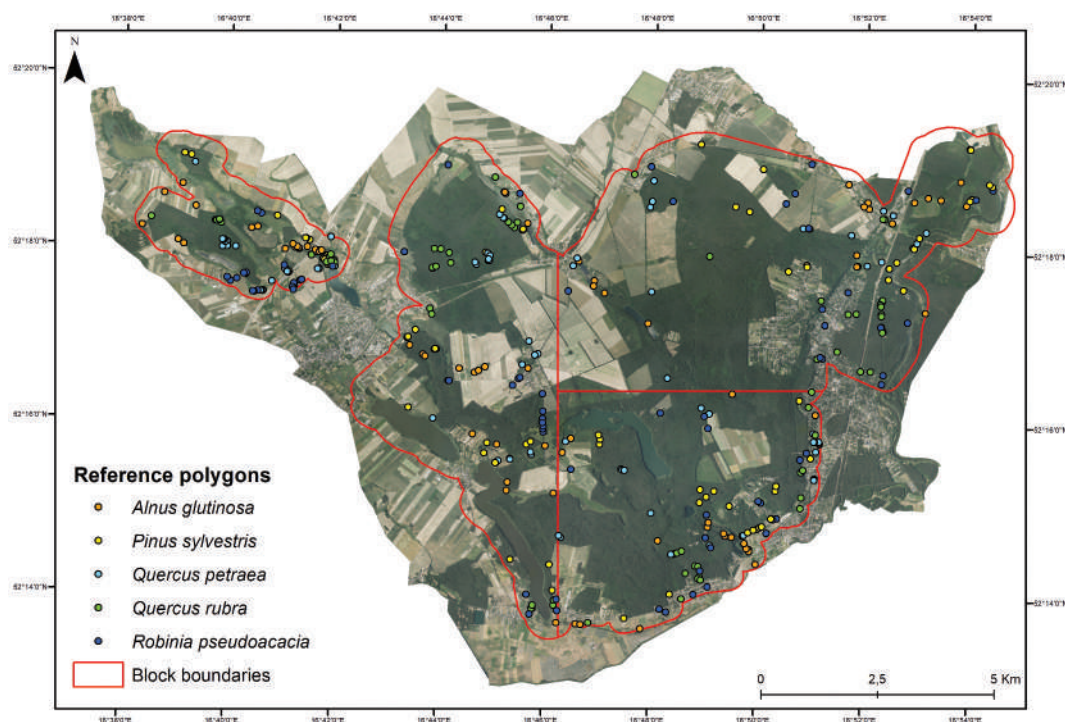


Figure 2. Distribution of reference polygons by species and by study area divided into blocks of airborne data acquisition. The number of measurements for each species is given in brackets. Base: orthophoto mosaic in real colors.

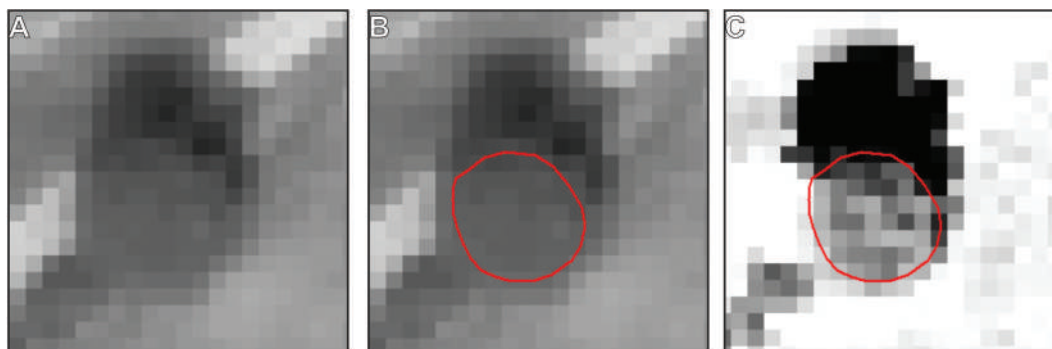


Figure 3. Sample process of creating a tree canopy range polygon. A – thermal image, B – thermal image with a tree canopy range (Range 1), C – illumination map based on hyperspectral data with a tree canopy range (Range 2); black pixels were eliminated from the analysis at further stages of the studies as their insolation value = 0.1.

temperature of the canopy. Then, for a polygon covering only the sunlit part of the canopy, the mean of the pixel values was calculated.

Statistical analysis

The data set prepared in this way was analyzed to answer the research questions. In the first analysis, the significance of differences in CT between two groups of trees (trees growing in the forest or outside the forest) was checked using the Student's t-test for independent samples, separately for each block. Secondly, the interspecies variability of CT in individual time blocks was analyzed (Figure 1). The purpose of this analysis was to determine the interspecies variability of tree temperature at different times of the day and different locations. The ANOVA test was the basis for determining the significance of differences in temperature between species in the consecutive time blocks. All statistical calculations were performed in ArcGIS 10.6 by ESRI and Statistica 13 by TIBCO Software.

Results

Canopy Temperatures in the forest and outside the forest

The results indicate that the immediate surroundings are an important factor that affects the temperature of individual trees (Figure 4). If trees grow in the forest, their average temperature is about 0.4–0.7°C lower than that of trees growing outside the forest. This correlation was observed throughout the time period under analysis (Figure 4). The smallest difference in CT was observed between 8:10 and 9:45 and amounted to 0.41°C. The biggest difference was observed in block no. 3, i.e. between 12:00 and 13:00 and amounted to 0.71°C (Figure 5). A statistically significant difference was obtained in all blocks, but block no. 3 differed the most significantly as regards CT ($p < 0.001$). Due to this variance, the next step of the research was conducted with the trees divided into two groups: in the forest and outside the forest.

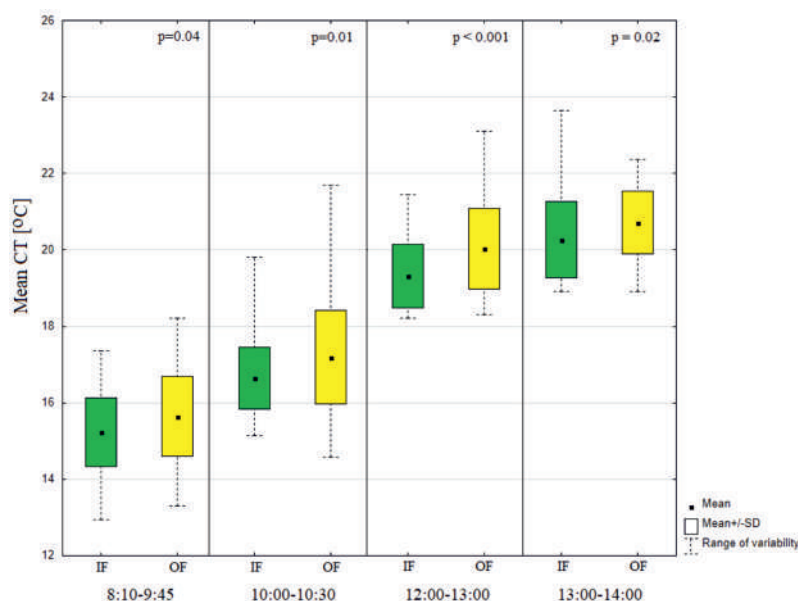


Figure 4. Comparison of average temperatures of tree canopies in terms of their location in the study area. Calculated using the Student's t-test for independent samples. IF – in the forest, OF – outside the forest.

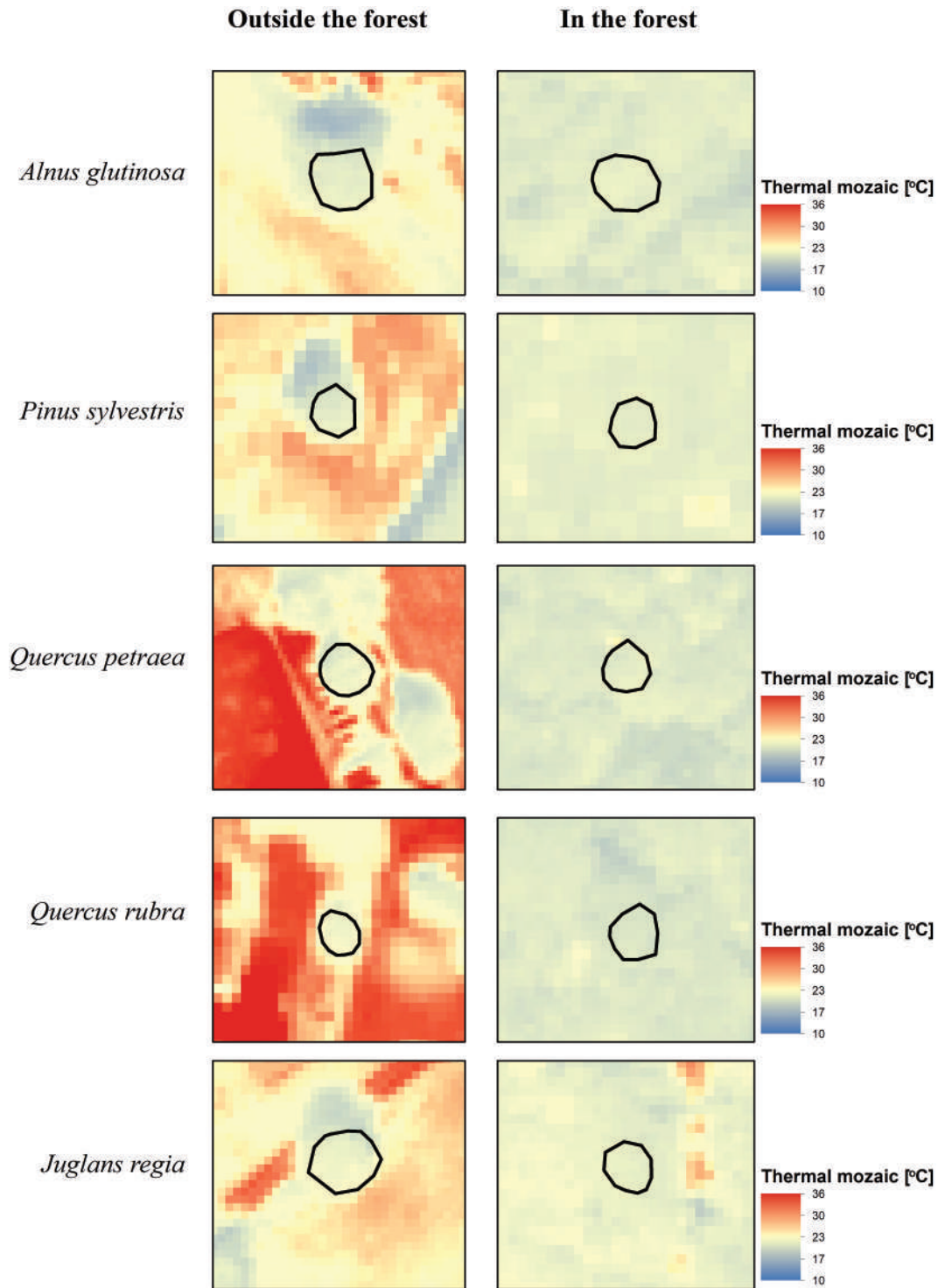


Figure 5. Differences in canopy temperature of all species in the forest and outside the forest of block no. 3 (12:00–13:00).

Canopy Temperatures of studied species

Comparative analysis of CT at a block time indicates that the temperature difference of individual trees, regardless of their taxonomic separation, ranges from 1.91°C for trees in the forest at 12:00–13:00 (min. CT for *Quercus rubra* – 18.21°C, max. CT for *Pinus sylvestris* – 22.47°C) to 3.61°C for trees outside the forest at 10:00–10:30 (min. CT for *Quercus petraea* – 14.59°C, max. CT for *Pinus sylvestris* – 21.69°C).

The analysis of the interspecies variation in CT in the blocks indicates that the studied species differ statistically significantly in all cases, except between 13:00 and 14:00 for trees outside the forest (Figure 7). In block no. 1, i.e. between 8:10 and 9:45, the biggest difference in CT between trees in different locations of the same species was observed for *Alnus glutinosa* (1.10°C). For trees in the forest, *Quercus rubra* was the species with the lowest temperature (14.63°C), while *Pinus sylvestris* had the highest temperature

(15.90°C). In this block, trees outside the forest with high CT involve especially *Alnus glutinosa* (16.03°C), and *Robinia pseudoacacia* (15.99°C).

In block no. 2, i.e. 10:00–10:30, for trees in the forest, *Alnus glutinosa* had the lowest CT (16.12°C), and again *Pinus sylvestris* had the highest CT (17.24°C). The lowest temperature for trees outside the forest was determined for *Alnus glutinosa* outside the forest (16.19°C). In this block, species are divided into three groups of similarity, for both trees in the forest and outside the forest, but the temperature difference between them increases significantly, especially for trees outside the forest ($p = 0.001$).

The biggest variance differences in CT between species are noted between 12:00 and 13:00. In block no. 3, the greatest difference in location is observed between *Quercus rubra* (difference of 1.32°C) and *Robinia pseudoacacia* (1.20°C). In this block, the temperature difference between *Pinus sylvestris* trees in the forest and outside the forest is the smallest (0.05°C). Despite that, *Pinus sylvestris* in both locations has the highest CT. The lowest temperature for trees in the forest was determined for *Quercus rubra* (18.80°C), and for trees outside the forest it was for *Alnus glutinosa* (19.27°C). Species are still divided into three groups of similarity for trees in the forest.

In block no. 4 of data acquisition, i.e. 13:00–14:00, for trees in the forest, the lowest CT is noted for *Quercus petraea* (19.73°C), and the highest for *Pinus sylvestris* (21.54°C). They differ by 1.81°C. Despite the small difference between these species, in this block the species were divided into two groups of similarity for trees in the forest. CT of trees outside the forest did not differentiate the species.

Based on the comparison of the entire period covered by the analysis (from 8:00 to 14:00), the species with the lowest CT in the course of data collection were *Quercus rubra*, *Quercus petraea* and *Alnus glutinosa*, and the species with the highest temperatures was *Pinus sylvestris*.

Discussion

Influence of the environment on Canopy Temperature

Tree temperature is significantly affected by canopy architecture, but it is also largely influenced by the immediate surroundings of the tree. Our studies have shown a significant difference between CT of trees outside the forest and trees in the forest, especially at noon (Figure 4). Trees growing in the forest

are 0.7°C cooler than trees growing outside the forest. In the morning and in the afternoon, the difference of CT, regardless of tree location, is 0.4°C but it is still statistically significant. The data indicate that the position in relation to other trees is an important factor that influences CT. This conclusion is in agreement with the results of previous studies (Leuzinger et al., 2010). The differences in canopy temperature of trees growing in parks and along the roads were investigated and a difference of about 1°C was shown regardless of species. The groups of trees can create a local microclimate, by their cooling abilities, by a combination of shadow cast and evapotranspiration process (Spronken-Smith & Oke, 1998), which explains a lower canopy temperatures of trees inside the forest.

The influence of the environment on CT was also demonstrated by the authors of the study in which CT of subtropical species were determined (Zheng et al., 2018). The studies demonstrated that the cooling properties of each individual tree canopy depend on the species and the ground. Also, the presence of other trees or the vicinity of buildings (in the case of urban studies) may significantly affect the cooling properties of a tree and the CT. Similar conclusions were also drawn by scientists studying the urban heat Island effect (Melaas et al., 2016), who emphasize that the form of land cover and the size of the vegetation patches have a key influence on the surface temperature. There is a high probability that the difference in temperature values of species may result from a different environment.

Canopy temperature of tree species

The use of high-resolution TIR data as source data for remote sensing analyses is still rare. One of the reasons behind their low popularity is that it is difficult to obtain thermally stable data with accurate radiometric and geometric fit (Prakash, 2000). The TIR data collected by a camera with a new spectral range (3.6–4.9 μm) was used, for the first time, to analyze CT on such a large scale (area over 40 km^2 for block no. 1) and with such high resolution (GSD = 1 m).

The acquisition time and data resolution in our studies made it possible to analyze the temperature of individual tree canopies (Figure 3). The results of our studies (Figure 5; Figure 6) indicate at the same time that the studied species differ as regards CT in the time interval between 8:00 and 14:00. *Quercus rubra* and *Quercus petraea* were shown to be the species with the lowest CT, while *Pinus sylvestris* has the highest CT. The difference in CT between these groups of species is about 1.1°C for trees in the forest and 0.9°C for trees outside the forest. These differences

may arise primarily from the size and architecture of a given tree canopy and its immediate surroundings as discussed in Sec. 4.1. Also, new information about canopy temperature of non-native species like *Quercus rubra* and *Robinia pseudoacacia* might be used in the further research. Especially if the aim of the studies are detecting invasive species by remote sensing techniques. TIR data are used in vegetation monitoring (Sagan et al., 2019) and tree assessment (Catena & Catena, 2008), which can be developed into species detection.

One of the earlier studies, which included the analysis of CT of individual tree species, was carried out in NW Switzerland (Leuzinger et al., 2010). These results cannot be directly compared, because there are too many variables that make the conditions and parameters of obtaining both collections different. The key differences are flight altitude and spectral range (7.5–14 μm). According to Gerber et al. (2011), 3–5 μm atmospheric window is more dedicated to study vegetation water content, and 8–14 μm wavelength range is more relevant to differentiating plant species. Nevertheless, Ullah et al. (2012) also confirm that both atmospheric windows contained significantly different vegetation, making them regions suitable for discriminating between vegetation species.

Potential applications of new thermal spectral range in tree species studies

HS and ALS imaging is now widely and successfully used to identify tree species (Dalponte et al., 2012; Liu et al., 2017) and to determine their health status (Degerickx et al., 2018; Sampson et al., 2003). The application potential of very high-resolution TIR data is not fully exploited. This is primarily due to processing difficulties which on the one hand result from high dynamics of object temperature changes during the day, and on the other hand, from the problems with their geometric correction. Various thermal spectral ranges are dedicated to different types of research, such as its species classification or assessment of tree health condition (Gerber et al., 2011). The studies proved that the time of TIR data acquisition should be matched with the objectives of a given study. If the goal is to analyze water stress in plants, it is best to make measurements of each species separately, because CT of healthy trees differentiates them significantly (Figure 6; Figure 7). It is also important to always include tree location and its environment in calculations (Figure 4). At solar noon, CT in healthy individuals differs from each other, in terms of their taxonomic separation and location in the study area (Figure 5; Figure 6), and it is at these times when the

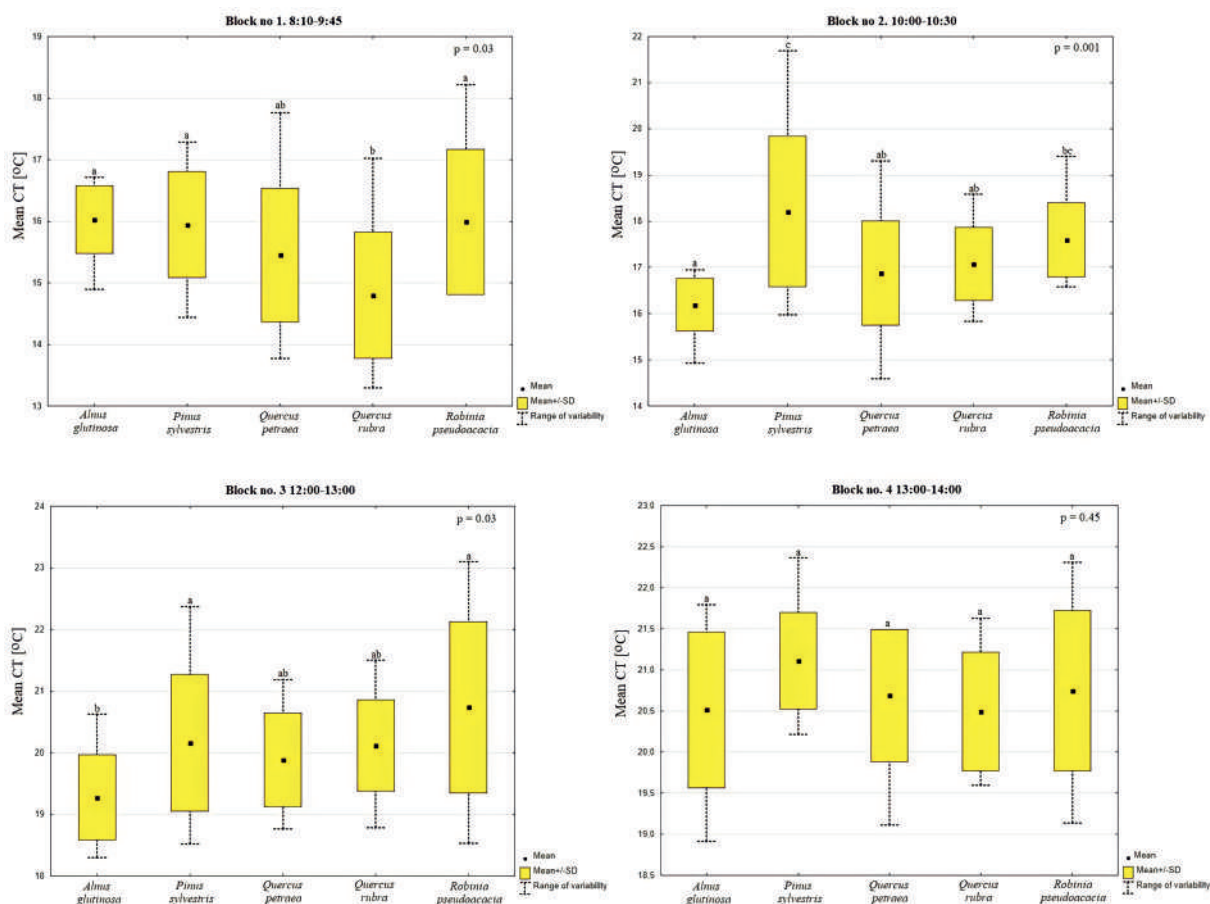


Figure 6. Temperature of tree canopy for the studied species in the forest, divided by the time of thermal data acquisition. The p-value was determined on the basis of the ANOVA test. a,b,c values represent belonging to a group according to the post-hoc Tukey test. a,b,c values represent belonging to a group according to the post-hoc Tukey test.

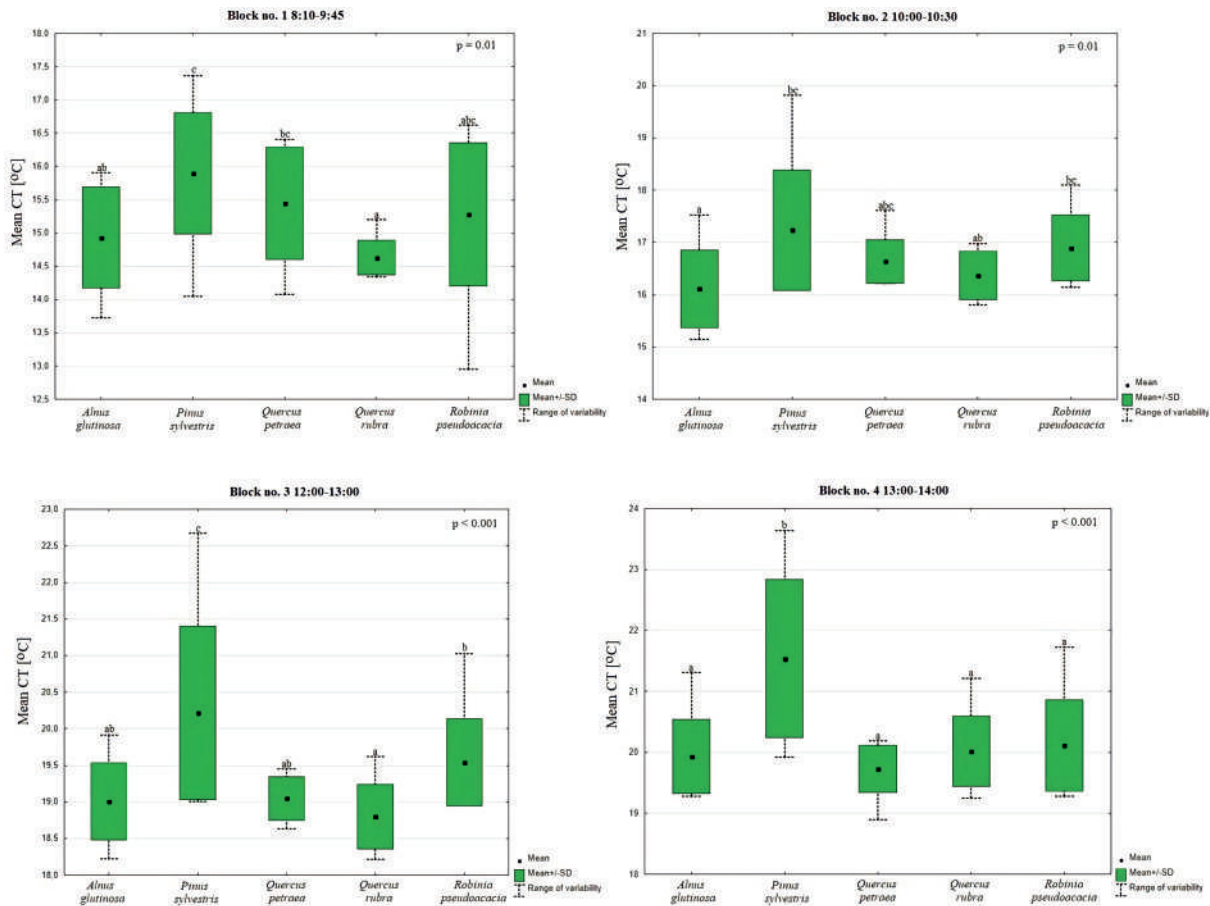


Figure 7. Temperature of tree canopy for the studied species outside the forest, divided by the time of thermal data acquisition. The p-value was determined on the basis of the ANOVA test. a,b,c values represent belonging to a group according to the post-hoc Tukey test. a,b,c values represent belonging to a group according to the post-hoc Tukey test.

differences in health condition can be best shown. Solar noon additionally reduces the shadow effect inside the canopy, which can effectively lower the temperature of the entire tree.

New spectral range (3.6–4.9 μm) was chosen for this study, because of its very high sensitivity in detection, which was compared with other camera models and spectral ranges (Aldave et al., 2013). The 3–5 μm window is found to be most suitable and is one of the important atmospheric transmission window used in thermal imaging (Awasthi et al., 2014, 2012; Bhatt et al., 2010). It is hard to show disadvantages of using this wavelength, because of the lack of enough research and information about it, and it is hard to compare to other research results, which are typically made in LWIR (8–14 μm).

Studies show that the CT is a variable that differentiates individual species (Figure 6; Figure 7). Thus, an assumption can be made that the use of these data in the process of species classification with the use of machine learning algorithms may improve the accuracy of the identification result. That is why these data should be further tested as supplementary to the HS in the classification of trees, especially when it is technically possible to collect them during one flight by instrument fusion (Table 2). Further studies in this area with the use of TIR data are planned.

Conclusions

The results of our studies confirm that TIR data acquired from the airborne level may be used to analyze CT during the day. The primary conclusion from our studies is that CT is a species-specific feature and depends on a tree's location. At noon CT of trees growing in the forest is on average 0.7°C lower than that of trees growing outside the forest. It was also shown that the similarity of individual species in terms of temperature changes throughout the day. Moreover, *Alnus glutinosa*, *Quercus rubra* and *Quercus petraea* are the species with the lowest CT. *Pinus sylvestris* has the highest CT, irrespective of the time of measurement. Additionally, at about noon, i.e. at 12.00–13.00, the CTs of all tree species are stable and differ from each other, regardless of the trees' location in the study area. Identification of this time may be crucial when TIR data are planned to be used to determine differences in CT between trees in good health condition, and those with a worse health status. Statistically the highest differences in tree temperatures between species are observed at noon. The new TIR spectral range (3.6–4.9 μm) registers CT with high accuracy and makes it possible to use this value to differentiate tree species.

Acknowledgments

The authors thank Agnieszka Janczak for the helpful comments and English proofreading.

Disclosure statement

No potential conflict of interest was reported by the authors.

Funding

Publication's printing cost and research were supported by the European Union from the European Social Fund under the "InterDOC-START" project POWR.03.02.00-00-I033/16-00 and from the Operational Programme Infrastructure and Environment under the program 2.4.4d – assessment of the state of natural resources in national parks using modern remote sensing technologies, "Inventory and assessment of the state of natural resources of the National Park of Wielkopolska using modern remote sensing technologies" project.

ORCID

Agata Zakrzewska  <http://orcid.org/0000-0003-2718-2855>
 Dominik Kopec  <http://orcid.org/0000-0003-0831-2992>
 Karol Krajewski  <http://orcid.org/0000-0003-1434-2709>
 Jakub Charyton  <http://orcid.org/0000-0003-2052-9051>

References

- Aldave, I. J., Bosom, P. V., González, L. V., De Santiago, I. L., Vollheim, B., Krausz, L., & Georges, M. (2013). Review of thermal imaging systems in composite defect detection. *Infrared Physics & Technology*, 61, 167–175. <http://dx.doi.org/10.1016/j.infrared.2013.07.009>
- Ansari, A. Q., & Loomis, W. E. (1959). Leaf temperatures. *American Journal of Botany*, 46(10), 713–717. <https://doi.org/10.1002/j.1537-2197.1959.tb07076.x>
- Awasthi, S., Nautiyal, B. B., & Bandyopadhyay, P. K. (2014). Marine environment compatible antireflection coating with nanotop layer on silicon optics. *Infrared Physics & Technology*, 65, 113–116. <http://dx.doi.org/10.1016/j.infrared.2014.04.001>
- Awasthi, S., Nautiyal, B. B., Kumar, R., & Bandyopadhyay, P. K. (2012). Multi-spectral antireflection coating on zinc sulphide simultaneously effective in visible, eye safe laser wave length and MWIR region. *Infrared Physics & Technology*, 55(5), 395–398. <http://dx.doi.org/10.1016/j.infrared.2012.06.003>
- Axelsson, P. E. (2000). DEM generation from laser scanner data using adaptive TIN models. *International Archives of the Photogrammetry and Remote Sensing*, 33, 110–117.
- Bhatt, M., Nautiyal, B. B., & Bandyopadhyay, P. K. (2010). High efficiency antireflection coating in MWIR region (3.6–4.9 μm) simultaneously effective for germanium and silicon optics. *Infrared Physics & Technology*, 53(1), 33–36. <https://doi.org/10.1016/j.infrared.2009.08.006>
- Catena, A., & Catena, G. (2008). Overview of thermal imaging for tree assessment. *Arboricultural Journal*, 30(4), 259–270. <https://doi.org/10.1080/03071375.2008.9747505>
- Cierjacks, A., Kowarik, I., Joshi, J., Hempel, S., Ristow, M., von der Lippe, M., & Weber, E. (2013). Biological flora of the British Isles: *Robinia pseudoacacia*. *Journal of Ecology*, 101(6), 1623–1640. <https://doi.org/10.1111/1365-2745.12162>
- Ciężkowski, W., Szporak-Wasilewska, S., Kleniewska, M., Józwiak, J., Gnatowski, T., Dąbrowski, P., Góraj, M., Szatyłowicz, J., Ignar, S., & Chormański, J. (2020). Remotely sensed land surface temperature-based water stress index for wetland habitats. *Remote Sensing*, 12(4), 631. <https://doi.org/10.3390/rs12040631>
- Cohen, Y., Alchanatis, V., Meron, M., Saranga, Y., & Tsipris, J. (2005). Estimation of leaf water potential by thermal imagery and spatial analysis. *Journal of Experimental Botany*, 56(417), 1843–1852. <https://doi.org/10.1093/jxb/eri174>
- Dalponde, M., Ørka, H. O., Gobakken, T., Gianelle, D., & Næsset, E. (2012). Tree species classification in boreal forests with hyperspectral data. *IEEE Transactions on Geoscience and Remote Sensing*, 51(5), 2632–2645 <http://doi.org/10.1109/TGRS.2012.2216272>.
- de Faria Peres, L., de Lucena, A. J., Rotunno Filho, O. C., & de Almeida França, J. R. (2018). The urban heat Island in Rio de Janeiro, Brazil, in the last 30 years using remote sensing data. *International Journal of Applied Earth Observation and Geoinformation*, 64, 104–116. <https://doi.org/10.1016/j.jag.2017.08.012>
- Degerickx, J., Roberts, D. A., McFadden, J. P., Hermy, M., & Somers, B. (2018). Urban tree health assessment using airborne hyperspectral and LiDAR imagery. *International Journal of Applied Earth Observation and Geoinformation*, 73, 26–38. <https://doi.org/10.1016/j.jag.2018.05.021>
- Dimoudi, A., & Nikolopoulou, M. (2003). Vegetation in the urban environment: Microclimatic analysis and benefits. *Energy and Buildings*, 35(1), 69–76. [https://doi.org/10.1016/S0378-7788\(02\)00081-6](https://doi.org/10.1016/S0378-7788(02)00081-6)
- Dyderski, M. K., & Jagodziński, A. M. (2019). Seedling survival of *Prunus serotina* Ehrh, *Quercus rubra* L. and *Robinia pseudoacacia* L. in temperate forests of Western Poland. *Forest Ecology and Management*, 450, 117498. <https://doi.org/10.1016/j.foreco.2019.117498>
- Egea, G., Padilla-Díaz, C. M., Martínez-Guanter, J., Fernández, J. E., & Pérez-Ruiz, M. (2017). Assessing a crop water stress index derived from aerial thermal imaging and infrared thermometry in super-high density olive orchards. *Agricultural Water Management*, 187, 210–221. <https://doi.org/10.1016/j.agwat.2017.03.030>
- Fahmy, M., & Sharples, S. (2009). On the development of an urban passive thermal comfort system in Cairo, Egypt. *Building and Environment*, 44(9), 1907–1916. <https://doi.org/10.1016/j.buildenv.2009.01.010>
- Gallardo-Saavedra, S., Hernández-Callejo, L., & Duque-Perez, O. (2018). Technological review of the instrumentation used in aerial thermographic inspection of photovoltaic plants. *Renewable and Sustainable Energy Reviews*, 93, 566–579. <https://doi.org/10.1016/j.rser.2018.05.027>
- Gerber, F., Marion, R., Oliosio, A., Jacquemoud, S., Da Luz, B. R., & Fabre, S. (2011). Modeling directional-hemispherical reflectance and transmittance of fresh and dry leaves from 0.4 μm to 5.7 μm with the PROSPECT-VISIR model. *Remote Sensing of Environment*, 115(2), 404–414. <https://doi.org/10.1016/j.rse.2010.09.011>
- Gluch, R., Quattrochi, D. A., & Luvall, J. C. (2006). A multi-scale approach to urban thermal analysis. *Remote Sensing of Environment*, 104(2), 123–132. <https://doi.org/10.1016/j.rse.2006.01.025>

- Grace, J. (1988). 3 Plant response to wind. *Agriculture, Ecosystems & Environment*, 22, 71–88. [https://doi.org/10.1016/0167-8809\(88\)90008-4](https://doi.org/10.1016/0167-8809(88)90008-4)
- Granier, A., Loustau, D., & Bréda, N. (2000). A generic model of forest canopy conductance dependent on climate, soil water availability and leaf area index. *Annals of Forest Science*, 57(8), 755–765. <https://doi.org/10.1051/forest:2000158>
- Jiménez-Bello, M. A., Ballester, C., Castel, J. R., & Intrigliolo, D. S. (2011). Development and validation of an automatic thermal imaging process for assessing plant water status. *Agricultural Water Management*, 98(10), 1497–1504. <https://doi.org/10.1016/j.agwat.2011.05.002>
- Junttila, S., Vastaranta, M., Hämäläinen, J., Latva-Käyrä, P., Holopainen, M., Hernández Clemente, R., Hyypä, H., & Navarro-Cerrillo, R. M. (2017). Effect of forest structure and health on the relative surface temperature captured by airborne thermal imagery—case study in Norway spruce-dominated stands in Southern Finland. *Scandinavian Journal of Forest Research*, 32(2), 154–165. <https://doi.org/10.1080/02827581.2016.1207800>
- Khanal, S., Fulton, J., & Shearer, S. (2017). An overview of current and potential applications of thermal remote sensing in precision agriculture. *Computers and Electronics in Agriculture*, 139, 22–32. <https://doi.org/10.1016/j.compag.2017.05.001>
- Kim, Y., Still, C. J., Roberts, D. A., & Goulden, M. L. (2018). Thermal infrared imaging of conifer leaf temperatures: Comparison to thermocouple measurements and assessment of environmental influences. *Agricultural and Forest Meteorology*, 248, 361–371. <https://doi.org/10.1016/j.agrformet.2017.10.010>
- Kopeć, D., Michalska-Hejduk, D., Ślawik, Ł., Berezowski, T., Borowski, M., Rosadziński, S., & Chormański, J. (2016). Application of multisensoral remote sensing data in the mapping of alkaline fens Natura 2000 habitat. *Ecological Indicators*, 70, 196–208. <https://doi.org/10.1016/j.ecolind.2016.06.001>
- Leuzinger, S., & Körner, C. (2007). Tree species diversity affects canopy leaf temperatures in a mature temperate forest. *Agricultural and Forest Meteorology*, 146(1–2), 29–37. <https://doi.org/10.1016/j.agrformet.2007.05.007>
- Leuzinger, S., Vogt, R., & Körner, C. (2010). Tree surface temperature in an urban environment. *Agricultural and Forest Meteorology*, 150(1), 56–62. <https://doi.org/10.1016/j.agrformet.2009.08.006>
- Li, Z. L., Tang, B. H., Wu, H., Ren, H., Yan, G., Wan, Z., Trigo, I., & Sobrino, J. A. (2013b). Satellite-derived land surface temperature: Current status and perspectives. *Remote Sensing of Environment*, 131, 14–37. [doi:https://doi.org/10.1016/j.rse.2012.12.008](https://doi.org/10.1016/j.rse.2012.12.008)
- Li, Z.-L., Wu, H., Wang, N., Qiu, S., Sobrino, J. A., Wan, Z., Tang, B.-H., & Yan, G. (2013a). Land surface emissivity retrieval from satellite data. *International Journal of Remote Sensing*, 34(9–10), 3084–3127. <https://doi.org/10.1080/01431161.2012.716540>
- Liu, L., Coops, N. C., Aven, N. W., & Pang, Y. (2017). Mapping urban tree species using integrated airborne hyperspectral and LiDAR remote sensing data. *Remote Sensing of Environment*, 200, 170–182. <https://doi.org/10.1016/j.rse.2017.08.010>
- Livache, C. (2019). *Quantum-confined nanocrystals for infrared optoelectronics: Carrier dynamics and intraband transitions* [Doctoral dissertation]. Sorbonne Université.
- Majkowska, A., Kolendowicz, L., Pórolniczak, M., Hauke, J., & Czernecki, B. (2017). The urban heat Island in the city of Poznań as derived from Landsat 5 TM. *Theoretical and Applied Climatology*, 128(3–4), 769–783. <https://doi.org/10.1007/s00704-016-1737-6>
- Malakar, N. K., Hulley, G. C., Hook, S. J., Laraby, K., Cook, M., & Schott, J. R. (2018). An operational land surface temperature product for Landsat thermal data: Methodology and validation. *IEEE Transactions on Geoscience and Remote Sensing*, 56(10), 5717–5735. <https://doi.org/10.1109/TGRS.2018.2824828>
- Marešová, J., Majdák, A., Jakuš, R., Hradecký, J., Kalinová, B., & Blaženec, M. (2020). The short-term effect of sudden gap creation on tree temperature and volatile composition profiles in a Norway spruce stand. *Trees*, 34(6), 1397–1409. <https://doi.org/10.1007/s00468-020-02010-w>
- Mátyás, C., Ackzell, L., & Samuel, C. J. A. (2004). EUFORGEN technical guidelines for genetic conservation and use for Scots pine (*Pinus sylvestris*) EUFORGEN. In *Bioversity International*. Rome, Italy: International Plant Genetic Resources Institute 6.
- McVean, D. N. (1953). *Alnus glutinosa* (L.) Gaertn. *Journal of Ecology*, 41(2), 447–466.
- Meier, F., & Scherer, D. (2012). Spatial and temporal variability of urban tree canopy temperature during summer 2010 in Berlin, Germany. *Theoretical and Applied Climatology*, 110(3), 373–384. <https://doi.org/10.1007/s00704-012-0631-0>
- Melaas, E. K., Wang, J. A., Miller, D. L., & Friedl, M. A. (2016). Interactions between urban vegetation and surface urban heat Islands: A case study in the Boston metropolitan region. *Environmental Research Letters*, 11(5), 054020. <https://doi.org/10.1088/1748-9326/11/5/054020>
- Minkina, W., & Dudzik, S. (2009). *Infrared thermography: Errors and uncertainties*. John Wiley & Sons. <https://doi.org/10.1002/9780470682234.fmatter>
- Möller, M., Alchanatis, V., Cohen, Y., Meron, M., Tsipris, J., Naor, A., Ostrovsky, V., Sprintsin, M., & Cohen, S. (2007). Use of thermal and visible imagery for estimating crop water status of irrigated grapevine. *Journal of Experimental Botany*, 58(4), 827–838. <https://doi.org/10.1093/jxb/erl115>
- Morakinyo, T. E., Kong, L., Lau, K. K. L., Yuan, C., & Ng, E. (2017). A study on the impact of shadow-cast and tree species on in-canyon and neighborhood's thermal comfort. *Building and Environment*, 115, 1–17. <https://doi.org/10.1016/j.buildenv.2017.01.005>
- Peel, M. C., Finlayson, B. L., & McMahon, T. A. (2007). Updated world map of the Köppen-Geiger climate classification. *Hydrology and Earth System Sciences*, 11(5), 1633–1644. <https://doi.org/10.5194/hess-11-1633-2007>
- Prakash, A. (2000). Thermal remote sensing: Concepts, issues and applications. *International Archives of Photogrammetry and Remote Sensing*, 33(B1; PART 1), 239–243.
- Price, J. C. (1979). Assessment of the urban heat Island effect through the use of satellite data. *Monthly Weather Review*, 107(11), 1554–1557. [https://doi.org/10.1175/1520-0493\(1979\)107<1554:AOTUHI>2.0.CO;2](https://doi.org/10.1175/1520-0493(1979)107<1554:AOTUHI>2.0.CO;2)
- Quattrochi, D. A., & Ridd, M. K. (1998). Analysis of vegetation within a semi-arid urban environment using high spatial resolution airborne thermal infrared remote sensing data. *Atmospheric Environment*, 32(1), 19–33. [https://doi.org/10.1016/S1352-2310\(97\)00179-9](https://doi.org/10.1016/S1352-2310(97)00179-9)
- Rahman, M. A., Moser, A., Rötzer, T., & Pauleit, S. (2017). Within canopy temperature differences and cooling ability of *Tilia cordata* trees grown in urban conditions. *Building and Environment*, 114, 118–128. <https://doi.org/10.1016/j.buildenv.2016.12.013>
- The regulation of the Council of Ministers of April 16, 1957 considering the creation of the National Park of Wielkopolska (Journal of Laws of 1957 No. 24, Item 114).
- Richter, R., Hutengs, C., Wirth, C., Bannehr, L., & Vohland, M. (2021). Detecting tree species effects on forest canopy temperatures with thermal remote sensing: The role of spatial resolution. *Remote Sensing*, 13(1), 135. <https://doi.org/10.3390/rs13010135>

- Rutkowski, L. (1998). *Klucz do oznaczania roślin naczyniowych Polski niżowej 2*, Warsaw, Poland: Wydawnictwo Naukowe PWN. 816.
- Sagan, V., Maimaitijiang, M., Sidike, P., Eblimit, K., Peterson, K. T., Hartling, S., Esposito, F., Khanal, K., Newcomb, M., Pauli, D., Ward, R., Fritschi, F., Shakoob, N., & Mockler, T. (2019). UAV-based high resolution thermal imaging for vegetation monitoring, and plant phenotyping using ICI 8640 P, FLIR Vue Pro R 640, and thermomap cameras. *Remote Sensing*, 11(3), 330. <https://doi.org/10.3390/rs11030330>
- Sampson, P. H., Zarco-Tejada, P. J., Mohammed, G. H., Miller, J. R., & Noland, T. L. (2003). Hyperspectral remote sensing of forest condition: Estimating chlorophyll content in tolerant hardwoods. *Forest Science*, 49(3), 381–391. <https://doi.org/10.1093/forestscience/49.3.381>
- Sander, I. L. (1990). *Quercus rubra* L. Northern red oak. *Silvics of North America*, 2, 727–733.
- Santesteban, L. G., Di Gennaro, S. F., Herrero-Langreo, A., Miranda, C., Royo, J. B., & Matese, A. (2017). High-resolution UAV-based thermal imaging to estimate the instantaneous and seasonal variability of plant water status within a vineyard. *Agricultural Water Management*, 183, 49–59. <https://doi.org/10.1016/j.agwat.2016.08.026>
- Sobrino, J. A., Caselles, V., & Becker, F. (1990). Significance of the remotely sensed thermal infrared measurements obtained over a citrus orchard. *ISPRS Journal of Photogrammetry and Remote Sensing*, 44(6), 343–354. [https://doi.org/10.1016/0924-2716\(90\)90077-O](https://doi.org/10.1016/0924-2716(90)90077-O)
- Spronken-Smith, R. A., & Oke, T. R. (1998). The thermal regime of urban parks in two cities with different summer climates. *International Journal of Remote Sensing*, 19(11), 2085–2104. <https://doi.org/10.1080/014311698214884>
- Still, C. J., Rastogi, B., Page, G. F., Griffith, D. M., Sibley, A., Schulze, M., Hawkins, L., Pau, S., Detto, M., & Helliker, B. R. (2021). Imaging canopy temperature: Shedding (thermal) light on ecosystem processes. *New Phytologist*, 230(5), 1746–1753. <https://doi.org/10.1111/nph.17321>
- Tran, H., Uchihama, D., Ochi, S., & Yasuoka, Y. (2006). Assessment with satellite data of the urban heat Island effects in Asian mega cities. *International Journal of Applied Earth Observation and Geoinformation*, 8(1), 34–48. <https://doi.org/10.1016/j.jag.2005.05.003>
- Ullah, S., Schlerf, M., Skidmore, A. K., & Hecker, C. (2012). Identifying plant species using mid-wave infrared (2.5–6 µm) and thermal infrared (8–14 µm) emissivity spectra. *Remote Sensing of Environment*, 118, 95–102. <https://doi.org/10.1016/j.rse.2011.11.008>
- Wani, A. A., Mehraj, B., Masoodi, T. H., Gattoo, A. A., & Mugloo, J. A. (2020). Assessment of Trees Outside Forests (TOF) with Emphasis on Agroforestry Systems Dagar, Jagdish Chander, Gupta, Sharda Rani, Teketay, Demel. In *Agroforestry for Degraded Landscapes* (pp. 87–107). Springer. https://doi.org/10.1007/978-981-15-6807-7_4
- Wozniwoda, B., Kopec, D., & Witkowski, J. (2014). The negative impact of intentionally introduced *Quercus rubra* L. on a forest community. *Acta societatis botanicorum Poloniae*, 83(1), 39–49. <https://doi.org/10.5586/asbp.2013.035>
- Zheng, S., Guldmann, J. M., Liu, Z., & Zhao, L. (2018). Influence of trees on the outdoor thermal environment in subtropical areas: An experimental study in Guangzhou, China. *Sustainable Cities and Society*, 42, 482–497. <https://doi.org/10.1016/j.scs.2018.07.025>

Supplementary Materials

**Canopy temperatures of selected tree species growing in the forest and
outside the forest using aerial thermal infrared (3.6–4.9 μm) data**

Agata Zakrzewska^a, Dominik Kopec^{a,b}, Karol Krajewski^b and Jakub Charyton^b

*^aDepartment of Biogeography, Paleoecology and Nature Conservation, Faculty of Biology
and Environmental Protection, University of Łódź, Łódź, Poland;*

^bDepartment of Remote Sensing, Mggp Aero Sp. Z O.O, Tarnów, Poland

Table S1. List of tree species with the assigned number of pixels used for calculations before and after using the illumination map.

Tree species	Number of individual tree canopies	Sum of tree canopies surface [m²]	Number of pixels in tree canopies before using the illumination map (Range 1)	Number of pixels in tree canopies after using the illumination map (Range 2)	Pixel difference (Range 1 – Range 2)	Pixel difference as a percentage [%]
<i>Alnus glutinosa</i>	80	4444.06	4441	3923	518	12
<i>Pinus sylvestris</i>	80	2039.14	2042	1753	289	14
<i>Quercus petraea</i>	80	4720.55	4734	4277	457	10
<i>Quercus rubra</i>	80	3938.23	3968	3277	691	17
<i>Robinia pseudoacacia</i>	80	5070.25	5075	4605	470	9



Remote sensing of bark beetle damage in Norway spruce individual tree canopies using thermal infrared and airborne laser scanning data fusion

Agata Zakrzewska^a, Dominik Kopeć^{a,b,*}

^a Department of Biogeography, Paleocology and Nature Protection, Faculty of Biology and Environmental Protection, University of Lodz, Łódź, Poland

^b MGGP Aero Sp. z o.o., Tarnów, Poland

ARTICLE INFO

Keywords:

Infrared thermography
Picea abies
Ips typographus
 Middle wave infrared
 Forest invasion
 Forest health
 K-mean clustering

ABSTRACT

Background: Increasing threat to Central Europe's forests from the growing population of the European spruce bark beetle *Ips typographus* (L.) calls for developing highly effective methods of detection of the infestation spots. The main goal of this study was to establish an automatic workflow for detection of dead trees and trees in poor condition of *Picea abies* using Middle Wave Infrared spectral range obtained from the aircraft.

Methods: The studies were conducted in Wigry National Park (Poland) in 2020. A fusion of aircraft thermal data and laser scanning was used. Synchronous with thermal data acquisition ground reference data were obtained for *P. abies* in different health conditions. Determination of the range of canopy temperatures characteristic of the three condition states ('healthy', 'poor condition', 'dead') was performed using K-mean clustering. The accuracy of the method was evaluated on two validation sets: (1) individual tree canopies determined by photointerpretation, and (2) automatic segmentation of laser scanning data.

Results: The results showed that the average temperature of 'healthy' trees was 27.70 °C, trees in 'poor condition' 28.57 °C, and 'dead' trees 30.17 °C. High temperature differences between 'healthy' and 'dead' *P. abies* made it possible to distinguish these two condition classes with high accuracy. Lower accuracies were obtained for the class of 'poor condition', which was found to be confusing with both 'healthy' and 'dead' trees. According to results from the first validation set, a high overall accuracy of 0.60 was obtained. For the second validation set, the overall accuracy was reduced by 11%.

Conclusions: This study indicates that canopy temperature recorded from the airborne level is a variable that differentiates 'healthy' spruces from those in 'poor condition' and the 'dead' trees. The results confirmed that thermal and airborne laser scanning data fusion allows for creating a quick and simple workflow, which can successfully separate individual tree canopies and identify *P. abies* attacked by *I. typographus*. Further research is needed to identify trees in the early stages of invasion.

1. Introduction

Increasing threat to forests from the European spruce bark beetle (*Ips typographus* L.) has severe economic consequences (Christiansen and Bakke, 1988). Due to its detrimental effect on wood production, there is a need to develop a method for rapid and precise detection of trees infested by *I. typographus*. One of the current strategies for suppression relies on early detection of infested trees, followed by cutting and removal (Hedgren and Schroeder, 2004). The most impacted trees in North and

Central Europe are the Norway spruce (*Picea abies* [L.] H. Karst), and less frequently the Scots pine (*Pinus sylvestris* L.), the European silver fir (*Abies alba* Mill.), and the European larch (*Larix decidua* Mill.) (Grodzki, 2013). The bark beetle more frequently attacks trees that have been weakened or stressed by environmental pollution, droughts and storms caused by climate change (Hlásny et al., 2011). Older, 80 to 100-year-old trees are also more susceptible to infestation. Healthy trees deter the bark beetle for example by formation of resin ducts and by local changes in metabolism (Rohde et al., 1996).

Abbreviations: UAV, Unmanned Aerial Vehicles; ALS, Airborne Laser Scanning; CHM, Canopy Height Model; TIR, Thermal Infrared; LWIR, Long Wave Infrared; MWIR, Middle Wave Infrared; WNP, Wigry National Park; CIR, Color-Infrared; GSD, Ground Sampling Distance; NDVI, Normalized Difference Vegetation Index; ITC, Individual Tree Canopy; GIS, Geographic Information System.

* Corresponding author. Department of Biogeography, Paleocology and Nature Protection, Faculty of Biology and Environmental Protection, University of Lodz, Łódź, Poland.

E-mail address: dominik.kopec@biol.uni.lodz.pl (D. Kopeć).

<https://doi.org/10.1016/j.fecs.2022.100068>

Received 23 May 2022; Received in revised form 3 October 2022; Accepted 3 October 2022

2197-5620/© 2022 The Authors. Publishing services by Elsevier B.V. on behalf of KeAi Communications Co. Ltd. This is an open access article under the CC BY license (<http://creativecommons.org/licenses/by/4.0/>).

Both adult beetles and larvae of *I. typographus* feed on the live tissues of trees. In the first stage, adult forms penetrate into live tissues and create tunnels for mating and laying eggs. The larvae that feed inside the tree then create side tunnels from the main corridor. As the larvae grow, the corridors get wider and longer, causing significant damage to the tree. In the eclosion phase, another stage of supplementary feeding takes place, after which the adult forms leave the corridor to colonize another tree (Wermelinger, 2004). All stages of the development in the bark beetle can lead to the dying of the tree. The presence of the spruce bark beetle in an attacked tree is manifested by discoloration and defoliation of leaves. The development of one generation in Polish weather conditions takes about two months. Two or three generations of bark beetle may be produced annually (Jönsson et al., 2011). Also, climatic conditions such as mild winters or warm and dry summers facilitate the process. Such weather conditions have been observed in recent years in Poland where weather anomalies are increasingly shifting towards mild and warm winters (Wypych et al., 2017).

I. typographus infestation is particularly severe in wood production forests, such as spruce monoculture (Gutowski, 2004). However, it can also be present in protected forests (Rachwald et al., 2022). For instance, Wigry National Park was established in areas that previously were wood production forests. The attacked trees are not removed due to the strict protection regulations and the bark beetle is listed here as keystone species (Müller et al., 2008). Significant increases in the population and activity of *I. typographus* have been observed in the Polish national parks due to the aging of forest stands and the fact that human interference in natural processes is prohibited or restricted in their territory (Gutowski and Krzysztofia, 2005). In northeastern Poland, and also in Wigry National Park territory, *I. typographus* outbreaks tend to occur more frequently (Gutowski, 2002).

Due to the large-scale beetle population attacks as well as its rapid growth and specific life cycle, it is necessary to develop a method for quick and effective detection of both spots of infestation and individual dead trees. Large populations of *I. typographus* can result in the reduction of significant forest areas in Eurasia (Grodzki et al., 2004). Using remote sensing data to identify infestation spots is entirely justifiable considering not only the speed of data acquisition for a large study area but also the progressing accuracy of data recording instruments. It seems necessary to create an automatic workflow for data acquisition and processing. Quick and regular identification of weakened *P. abies*, followed by their removal, can be effective in controlling the *I. typographus* spread. Although *I. typographus* is one of the causes of dying of coniferous species, e.g., *Pinus sylvestris* (Jaime et al., 2019), most of the remote sensing studies have focused on the detection of damaged and dead *P. abies*. The study of other coniferous species is only an addition to the main studies of *P. abies* (Näsi et al., 2018), or concern other species, i.e., Ips bark beetle *Ips acuminatus* (Kuchma et al., 2021) or the Mountain pine beetle *Dendroctonus ponderosae* (Coops et al., 2010; Sprintsin et al., 2011).

Review of literature confirms that it is possible to effectively map bark beetle invasions using remote sensing techniques through analysis of multispectral (Long and Lawrence, 2016), hyperspectral (Fassnacht et al., 2012, 2014), and thermal (Hais, 2003) image data. To date, detecting trees that are dead or in the advanced stage of decay (called red and gray attacks) have proven particularly efficient. Satellite data, due to its spatial resolutions, has been used to identify the regions with dead trees and trees susceptible to *I. typographus* infestation (Filchev, 2012; Latifi et al., 2014). Alternative methods of detecting areas infested by the bark beetle are based on the data fusion. Studies using RapidEye data and TerraSAR-X data showed a relatively low classification accuracy for detection of the bark beetle infestation spots (Cohen's Kappa Coefficient (kappa) of 0.23 for TerraSAR-X data and 0.51 for RapidEye). Only the combination of both these data types yielded a high detection rate at the level of kappa = 0.74 (Ortiz et al., 2013). This allowed the researchers to classify a large study area with varying density of dead trees.

Hyperspectral airborne data were previously used to estimate tree health condition, where 673–724 nm region exhibited maximum

sensitivity to initial damage (Campbell et al., 2004). The correlation between spectral indices and biophysical parameters varied from –0.61 to 0.88. Lausch et al. (2013) found that although *I. typographus* infestations were best visible within the spectral range of 450–890 nm relating to prominent chlorophyll absorption, 64% accuracy was still insufficient in informing the forest management intervention. Data obtained from UAVs (Unmanned Aerial Vehicles) provide better results in the early detection of lesions in trees, especially when combined with airborne laser scanning (ALS) data, as shown in assessment of pine shoot beetle (*Tomicus* spp.) (Lin et al., 2019, 2021).

In the green attack stage of the European spruce bark beetle invasion, tree needles remain green. Detection of *I. typographus*-induced tree mortality was successfully achieved by fusion of high-resolution airborne hyperspectral data and ALS (Stereńczak et al., 2019). Incorporating ALS helped delineate single tree canopies based on Canopy Height Model (CHM). ALS data was used in the process of delineating tree crowns and assessment of their reflectance values, thus a very high accuracy of separating healthy and dead trees was obtained (kappa = 0.95). However, acquisition of hyperspectral and ALS data annually for one area and then processing them can be laborious and costly (Lu et al., 2020). Therefore, trees attacked by *I. typographus* may potentially be identified by alternative approach such as recording their canopy temperature.

Thermal Infrared (TIR) cameras are increasingly used in remote sensing, mainly to determine the temperature of individual objects or Land Surface Temperature mapping (Trigo et al., 2008; Jiang and Tian, 2010). The tree crowns with healthy and green leaves contain a high level of chlorophyll content and maintain normal evapotranspiration process for effectively cooling the leaf surface (Kimball and Bernacchi, 2006). The presence of the bark beetle causes damage to trees, including discoloration and defoliation. Consequently, chlorophyll content in leaves is reduced, and the evapotranspiration process is impaired or blocked, which may in turn increase canopy temperature (Leuzinger and Körner, 2007). Therefore, it is possible to identify and distinguish different condition states on the thermal data mosaic.

Vegetation temperature has been used to monitor the early responses of plants to different stressors (Hernández-Clemente et al., 2019), and there are studies on determination of tree canopy temperature in agricultural crops (Wang et al., 2010) as well as in the natural environment for assessment of growth conditions (Kim et al., 2018). Object temperature is one of the indicators of environment condition and has numerous applications. For instance, by identifying the thermal properties of each species, the environmental and growth conditions of orchards can be estimated by monitoring the canopy temperature (Möller et al., 2007; Egea et al., 2017). However, acquisition of TIR data requires determination of meteorological conditions as well as the time of a day and season for the suitable signals to be used (Prakash, 2000). With better understanding of these aspects, the present state of knowledge can be extended and data can be used to study damaged and dead trees in various environments.

Studies using TIR satellite data (Landsat-8 satellite) showed that the canopy temperature identifies bark beetle-induced physiological changes in trees more efficiently than spectral vegetation indices alone (Abdullah et al., 2019). Tree canopy temperature proves to be the key feature in detecting infested forest areas when combined with other spectral indices. Abdullah et al. (2019) suggest that higher efficiency may be achieved if data of higher resolution than satellite and a combination of TIR and hyperspectral data are used. It is impossible to assess individual tree canopy temperatures, because spatial resolution of thermal data obtained from Landsat-8 is 100 m (or resampled 30 m). In the study of Hais and Kučera (2008), where TIR satellite data was used, temperature of dead or decaying spruce forest is on average 3.5 °C higher than healthy forest areas. However, these studies were conducted not on individual trees but the entire patches of forest. It was suggested that the higher temperature may result from higher reflectance in the case of single dead trees and the different evapotranspiration in the two forest communities in different health conditions (Hais and Kučera, 2008). Another study

that drew on the previous suggestions was Junttila et al. (2016), where the impact of the health condition of trees and forest structure on the obtained Land Surface Temperature was studied using aerial TIR and ALS data. A 1-m spatial resolution made it possible to analyze each single tree canopy temperature. Junttila et al. (2016) obtained high detectability of dead and damaged trees on the thermal data mosaic, but detecting the green attack using TIR data remains a challenge. It was suggested that similar studies should be performed in warmer weather conditions than those that were carried out during the tests (air temperature above 2.5 °C; Junttila et al., 2016).

Other studies (e.g., Hais and Kučera, 2008; Junttila et al., 2016; Abdullah et al., 2019) on the detection of the *P. abies* attacked by *I. typographus*, were carried out in 8–14 µm Long Wave Infrared (LWIR), probably due to the availability of cameras in this spectral range. In our current research, we proposed the use of temperature registered in the Middle Wave Infrared (MWIR) range. This wavelength was successfully used to differentiate canopy temperatures of tree species in the natural environment (Zakrzewska et al., 2022). There are no remote sensing studies that would use the MWIR range to assess *P. abies* health status. However, the range of 3.6–4.9 µm enabled greater dynamics of imaging and consequently smaller temperature differences to be recorded (Livache, 2019). This is particularly important in vegetation studies where temperature differences between species, or individuals in different condition states may be small. It is also important that changes in chlorophyll content and water deficit occur in *P. abies* attacked by *I. typographus* (Cheng et al., 2010; Ali et al., 2021). According to Gerber et al. (2011), 3–5 µm TIR atmospheric window is more dedicated to study vegetation water content, which may explain the high detection efficiency of trees in poor health condition and dead in MWIR spectral range.

Fast and inexpensive detection of dead and dying trees as a result of an attack by the spruce bark beetle is crucial in forest management. Taking into account the results and comments of previous researchers, new studies were performed. The aims of this study were to determine: (1) can the airborne TIR data registered in spectral range of 3.6–4.9 µm be used to detect *P. abies* that are in poor condition or dead due to *I. typographus* infestation, and (2) is it possible to create an automatic workflow of detection of dead *P. abies* trees and trees in poor condition using airborne TIR and ALS data fusion?

We used the middle wave infrared spectral range (3.6–4.9 µm) for the first time to study the health status of trees infected by *I. typographus*. Moreover, middle wave infrared data were obtained for the first time from airplane level to study this issue for a vast study area, much greater than standard UAV study areas. We aim to establish a functional, automatic segmentation method based on ALS and TIR data fusion, that could be a new method of fast and automatic assessment of tree health status. Our assumption is that it is possible to differentiate healthy trees from dead trees and those in poor condition only by comparing needle discoloration with canopy temperatures obtained from an aircraft level.

2. Materials and methods

2.1. Study area

The study area was located in Wigry National Park (WNP) situated in northeastern Poland (Fig. 1). The analyzed area spanned 9 km² in the eastern part of WNP, where mixed coniferous forest is the dominant vegetation type with podzolic soil (The Forest Data Bank, <https://www.bdl.lasy.gov.pl/portal>). The landform of the study area is postglacial landscape and elevation fluctuation is about 140–156 m above sea level. The main forest species found in WNP include Scots pine (*Pinus sylvestris*) and Norway spruce (*Picea abies*). Other common species are the Common oak (*Quercus robur* L.), the Silver birch (*Betula pendula* Roth), and the Black alder (*Alnus glutinosa* [L.] Gaertn.). Vegetation under tree canopies with a coverage of up to 50%–80%, consists of young trees, herbaceous species, and others such as buckthorn, fir, juniper, rowan and also hazel (Kliczkowska, 2004). The age of *P. abies* in the study area varies from 33 to 161 years (The Forest Data Bank, <https://www.bdl.lasy.gov.pl/portal>). The study area was located within the strictly protected area of WNP covered by the regulation on total and permanent abandonment of direct human interference in the course of natural processes, condition of ecosystems and formations and elements of nature (Journal of Laws of Journal of Laws of 1988 No. 25, Item 173). Since logging and removal of timber is prohibited, there is a large number of wood clusters and single damaged or dead trees in the area. The study area was located in a humid continental climate zone but significantly influenced by the Baltic Sea and the eastern continental block. Summer begins in the middle of June

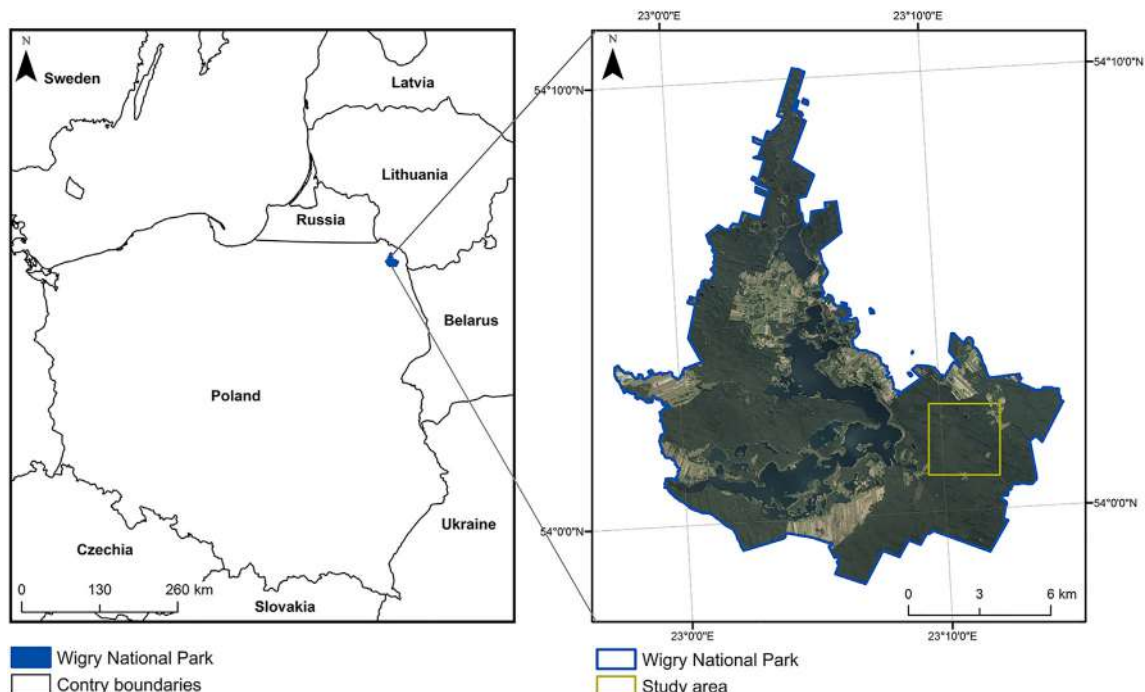


Fig. 1. Location of the study area.

and lasts until the end of August, with an average temperature of 16–18 °C (Łuczak, 2019) and the highest rainfall of approximately 80 mm. The wind speed in WNP is moderate (up to 5 m·s⁻¹) and the growing season is approximately 190 d (Krzyštofiak and Olszewski, 1999).

2.2. Airborne data acquisition

Three types of airborne data were acquired in order to conduct research using Vulcanair P-68 Observer 2 aircraft (Table 1). The airborne laser scanning data and color-infrared image were collected on August 17, 2019. Measurements with both of these sensors were carried out synchronously on the same aircraft (Table 1). TIR was the main data of this research and was used to calculate tree canopy temperatures. ALS and color-infrared (CIR) was used as additional data in processing and statistical analysis.

TIR data were acquired on June 26, 2020 between 14:07 and 14:28 UTC using ImageIR 9400 infrared camera by InfraTec GmbH (Dresden, Germany). The spectral range of the camera was 3.6–4.9 µm, which is described as Middle Wave Infrared (MWIR). ALS and CIR images were acquired for the study area on August 17, 2019.

2.2.1. Thermal infrared data processing

Weather conditions are crucial during TIR data acquisition. During the flight, air temperature was 29 °C, relative humidity was 37%, the average wind speed was 4 m·s⁻¹, and there was an absence of cloud cover. IRBIS Professional v.3.1 software was used to process and correct thermal images. Atmospheric correction was applied by the atmospheric transmittance model using ambient temperature, relative humidity recorded during data acquisition, and flight altitude taken into account (method performed by Minkina and Dudzik, 2009). The average emissivity of *P. abies* range was determined at $\epsilon = 0.90$ based on the literature reports (Kraniotis et al., 2016). Since it is the only tree species studied, there was no need to estimate emissivity to other objects. During the TIR data acquisition, 30 reference field measurements of surface temperatures were recorded in the study area using Fluke 64 MAX pyrometer (Fig. 2). At the ground level, various surfaces were measured in the test area (cobblestones at 7 points, asphalt 8 points, herbs 5 points, gravel 4 points, concrete slabs 3 points, sand 2 points, and farmland 1 point). The location coordinates of each pyrometer point were recorded using a Trimble Catalyst GNSS receiver with a Trimble DA1 antenna. Additionally, temperature for each point was measured five times and these measurements were averaged for data calibration. The temperatures recorded from the points were used for radiometric correction, in order to remove radiometric errors and adjust the values obtained from the aerial level (Osińska-Skotak, 2007). After radiometric correction, the mean difference between the airborne TIR and the pyrometer data calculated from 30 reference points was 0.49 °C. The resulting thermal mosaic with Ground Sample Distance (GSD) resolution = 1 m was used to determine the canopy temperature.

2.2.2. Airborne laser scanning and color-infrared image processing

CIR image was obtained using DMCI camera with a spectral range of 0.7 µm. The source CIR images have been processed in INPHO OrthoVista software package (Trimble Inc., Sunnyvale, CA, USA). The photos were taken with a 70% forward overlap and a 30% lateral overlap. The

orthophotomap was made in digital technology. The orthorectification of all photos was performed with the Inpho OrthoMaster software (Trimble Inc., Sunnyvale, CA, USA). The geometrical accuracy of the orthophotomap was 0.1 m. GSD of CIR orthophotomap was 0.1 m. These images were used to calculate NDVI (Normalized Difference Vegetation Index) values (necessary in automatic tree crown segmentation) and as base-maps to figures. NDVI allows the determination of the developmental state and the condition of vegetation (Gandhi et al., 2015).

ALS data were acquired using Riegl VQ-780 with a density of 7.6 pt·m⁻². Point cloud from ALS was classified in TerraScan software in TerraSolid package (TerraSolid Ltd., Espoo, Finland). CHM with a resolution of 0.5 m was generated based on the obtained point cloud. The CHM was then used to manually delineate tree canopy polygons recorded in the field and to create an automatic individual tree crown segmentation. Additionally, ALS data were used for mapping of Gap Fraction (Maltamo et al., 2014). Gap Fraction indicates the rate of laser ray penetration through the canopy in relation to a spatial unit. The pixels in the Gap Fraction have values from 0 for complete branching (light ray absorbed by the canopy) to 1 in open areas (light ray reaches the ground) (Danson et al., 2007).

Because of the earlier acquisition of ALS and CIR data (2019) relative to TIR data (2020), the timeliness of ALS and CIR data was verified during field measurements. Ground reference points of *P. abies* were compared with airborne data from 2019. Only those trees whose health status was visible on the CIR image and crown shape did not change between 2019 and 2020 were selected as reference trees (as a last resort, 340 trees were selected as shown in Section 2.3).

TIR, ALS and CIR images were used in the data fusion analysis. Center projection of TIR images may be a problem in the process of segment creation. It is especially important for tall objects, e.g. tree crowns. That's why it is necessary to reduce geometric distortion. The error from geometric distortion between ALS and TIR has been significantly reduced by the same points cloud in the orthorectification process of TIR data and by creating the CHM model of tree crowns. Additionally, the offset positions error was minimized at the stage of assigning TIR data pixel values to segments. Only pixels that were fully inside the segment were assigned to the given canopy segment.

2.3. Ground reference data

For the purpose of the analyses, 340 ground reference points of *P. abies* in various health condition states were collected in the study area synchronously with the TIR data acquisition. The location coordinates of individual trees were recorded with an accuracy of 1 m using a Trimble Catalyst GNSS receiver with a Trimble DA1 antenna and MapIT application connected to it (MapIT GIS LTD, Wishaw, UK). Data in the field were recorded in the form of a point layer in GeoJSON format. Measurements were distributed evenly across the study area (Fig. 3). Each tree was assigned to one of the three condition classes based on examination in the field and detection of *I. typographus* (Fig. 4). The trees were divided into three classes ('healthy', 'poor condition' and 'dead') following visual assessment of the discoloration of needles according to the method proposed by Hanisch and Kilz (1990) (Table 2). The threshold level of discoloration for 'poor condition' was 20%, which is considered to be visually noticeable (Eichhorn et al., 2004). Three health

Table 1
Parameters of flight and sensors used. GSD: Ground Sampling Distance.

Data type	Sensor type	Data parameters	Date of flight	Hour of flight	Flight level and airspeed	Aircraft
TIR	ImageIR 9400	GSD = 1 m	June 26, 2020	14:07–14:28 UTC	Flight level = 1270 m above ground level, Airspeed = 120 m·s ⁻¹	Vulcanair P-68 Observer 2
ALS point cloud	Riegl VQ-780i	Density = 7.6 pt·m ⁻²	August 17, 2019	9:18–9:45 UTC		
CIR images	Intergraph DMCI	GSD = 0.1 m				

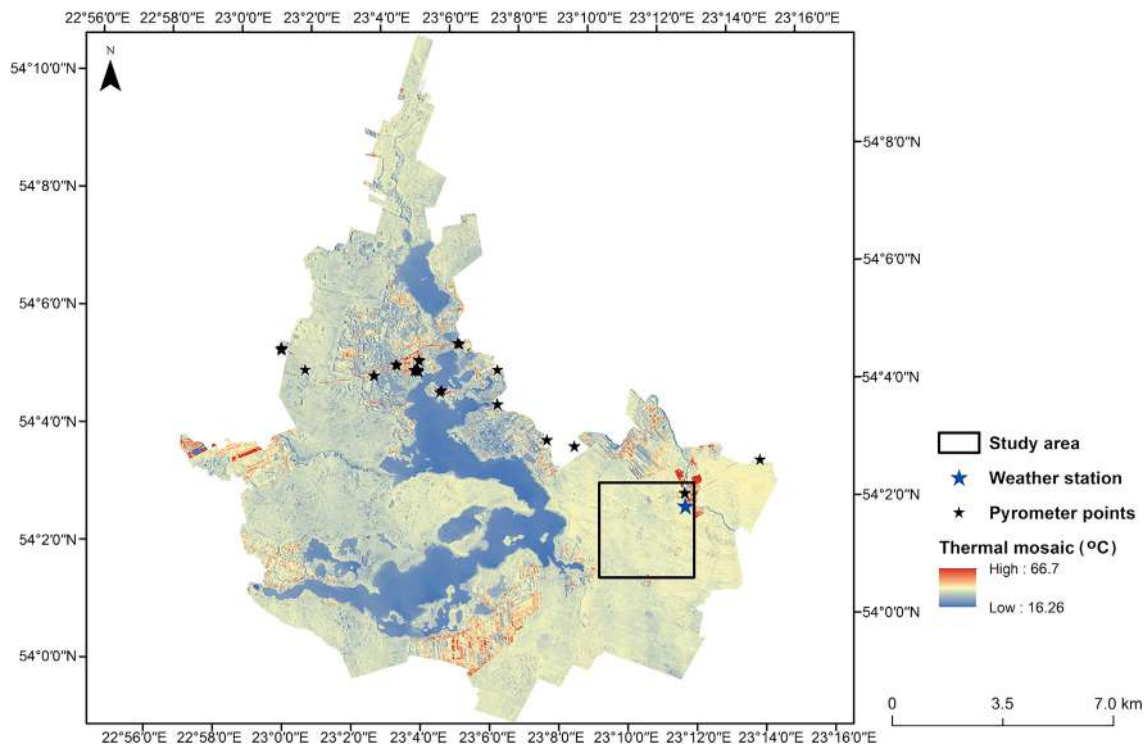


Fig. 2. Locations of the weather stations and pyrometer points for Thermal Infrared data calibration. Basemap: Thermal Infrared (TIR) mosaic.

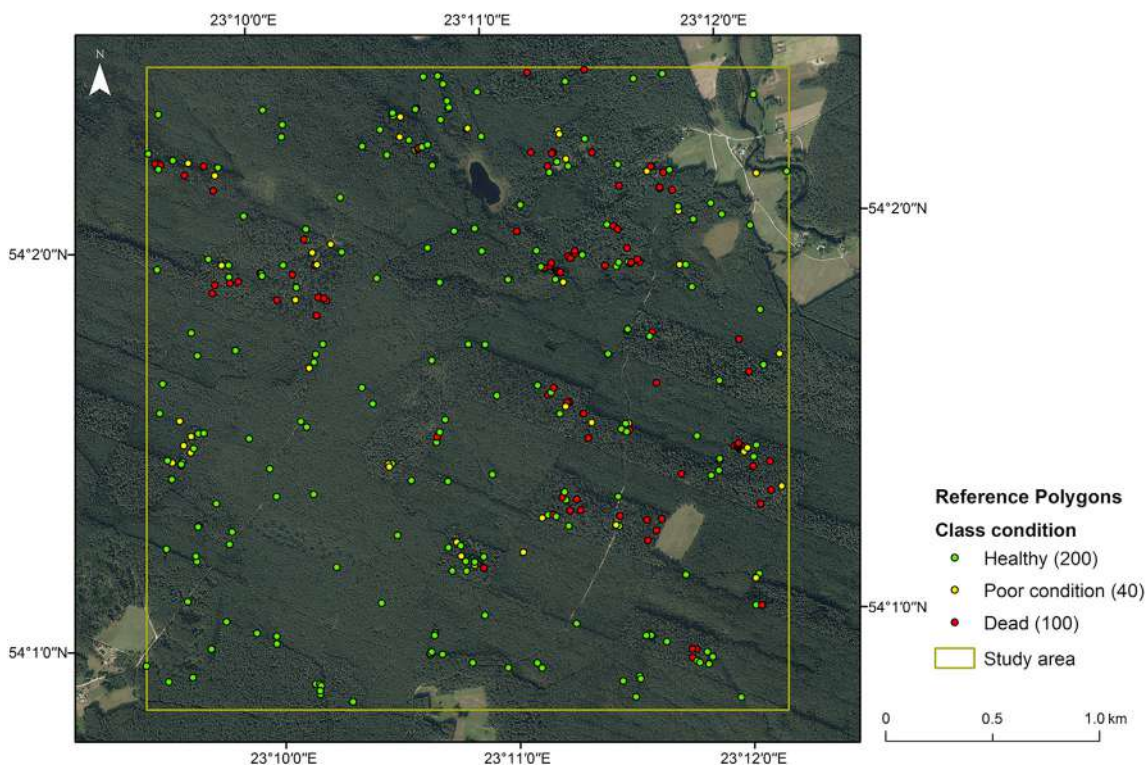


Fig. 3. Distribution of reference trees of *Picea abies* divided by health status. In brackets, the number of collected individuals was given. Basemap: orthophotomap in real colors. (For interpretation of the references to color in this figure legend, the reader is referred to the Web version of this article.)

classes were distinguished, and their numbers reflect the actual proportions in the studied area. These three classes can be visually separated during ground reference collection without the need for additional parameters, which is necessary because of the speed and ease of usage and repetition of this method. The acquired field data were then subjected to

lab processing.

2.4. Segmentation of individual tree canopy using canopy height model

The purpose of data processing was to assign the information of the

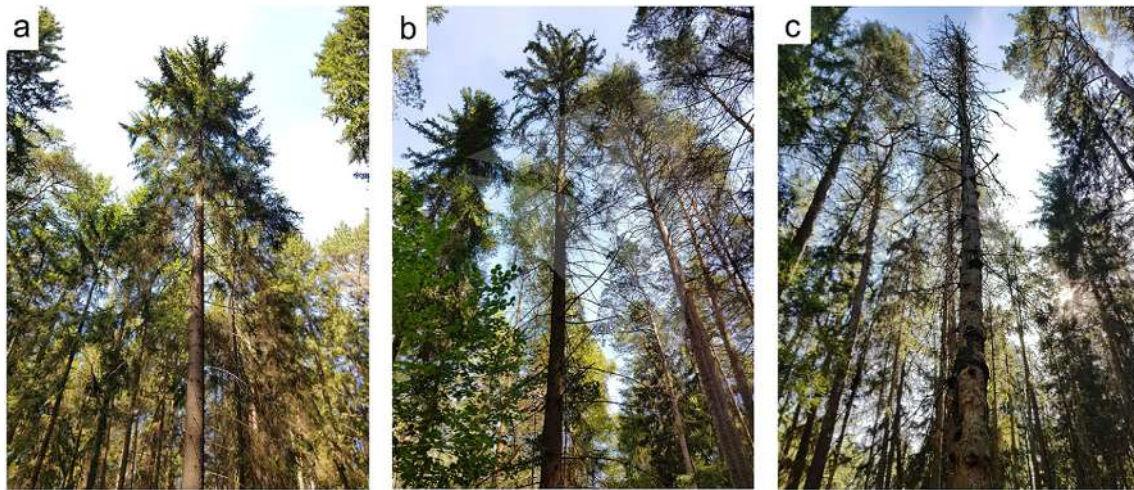


Fig. 4. Representation of three health condition classes of *Picea abies* (a: 'healthy', b: 'poor condition', c: 'dead').

Table 2
Division of ground reference data into condition classes.

Condition class	Number of trees	Class description
Healthy	200	No signs of deterioration of health condition, no discoloration of needles, no signs of <i>Ips typographus</i> feeding
Poor condition	40	Visible deterioration of health condition, discoloration of needles over 20% of the canopy, confirmed feeding of <i>Ips typographus</i>
Dead	100	Dead standing trees, no needles, confirmed feeding of <i>Ips typographus</i>

canopy temperature to individual trees. For 340 points of *P. abies* identified in the study area, Individual Tree Canopies (ITC) were delineated using two independent methods: manual/photointerpretation (ITC#1) and automatic segmentation of the CHM data (ITC#2) (Fig. 5). The purpose of using two methods of identifying single canopies was to carry out the analysis of TIR data without the influence of the quality of automatic segments (method ITC#1) and to check the usage of TIR data obtained from segments in application workflow, which could be used in the forest management in the future (method ITC#2).

ITC#1 was created from ground reference data points (Fig. 5), by photointerpretation of CHM data and polygon delineation of entire tree

canopies. Subsequently, a 1-m buffer was formed inside each ITC#1 for reducing the tree canopy range. Thereby, extreme pixels, which might have potentially included ground or adjacent canopies, were eliminated from further analyses. At the final stage, gap fraction correction was applied. All pixels with a gap fraction value higher than 0.2 were excluded from further analyses to eliminate the influence of the ground on the canopy temperatures.

Segmentation was focused on detection of single tree canopies with a minimum peak height of 3 m. Tree segmentation was performed by determining the boundaries of individual trees using detected vertices. Tree detection and segmentation were performed using the R programming language. First stage of ITC#2 was detection of individual trees using variable size windows (Popescu and Wynne, 2004). Using detected treetops as seed, watershed algorithm was used to determine the extents of single crowns. At this stage, it was necessary to determine the minimum height of the canopy of a single tree (2.5 m) that will enter its range. Also, NDVI obtained from the CIR images was used. Segments with maximum NDVI pixel values less than 0.2 were eliminated. ITC#2 were also reduced by a 1-m buffer and gap fraction high values, reducing the tree canopy range, the same way as in ITC#1 processing (Fig. 6).

The final preparatory stage comprised calculating zonal statistics. Mean and standard deviation of the temperature values from the TIR data were calculated for ITC#1 and ITC#2. Statistical calculations were made using ESRI's ArcGIS 10.6 and TIBCO Software's Statistica 13. The dataset prepared in this way was analyzed to answer the research questions.

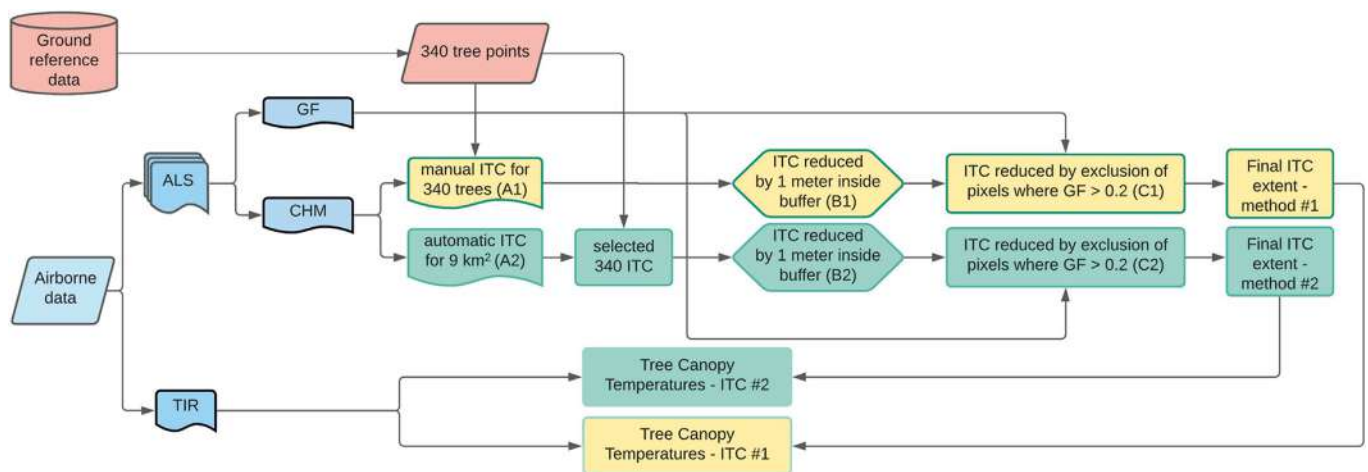


Fig. 5. Workflow of data processing and creating tree canopy ranges. TIR: Thermal Infrared; ALS: Airborne Laser Scanning; GF: Gap Fraction; CHM: Canopy Height Model; ITC: Individual Tree Canopy; Shortcuts in brackets are represented in Fig. 6: a1, b1, c1 for manual polygons; a2, b2, c2 for segments.

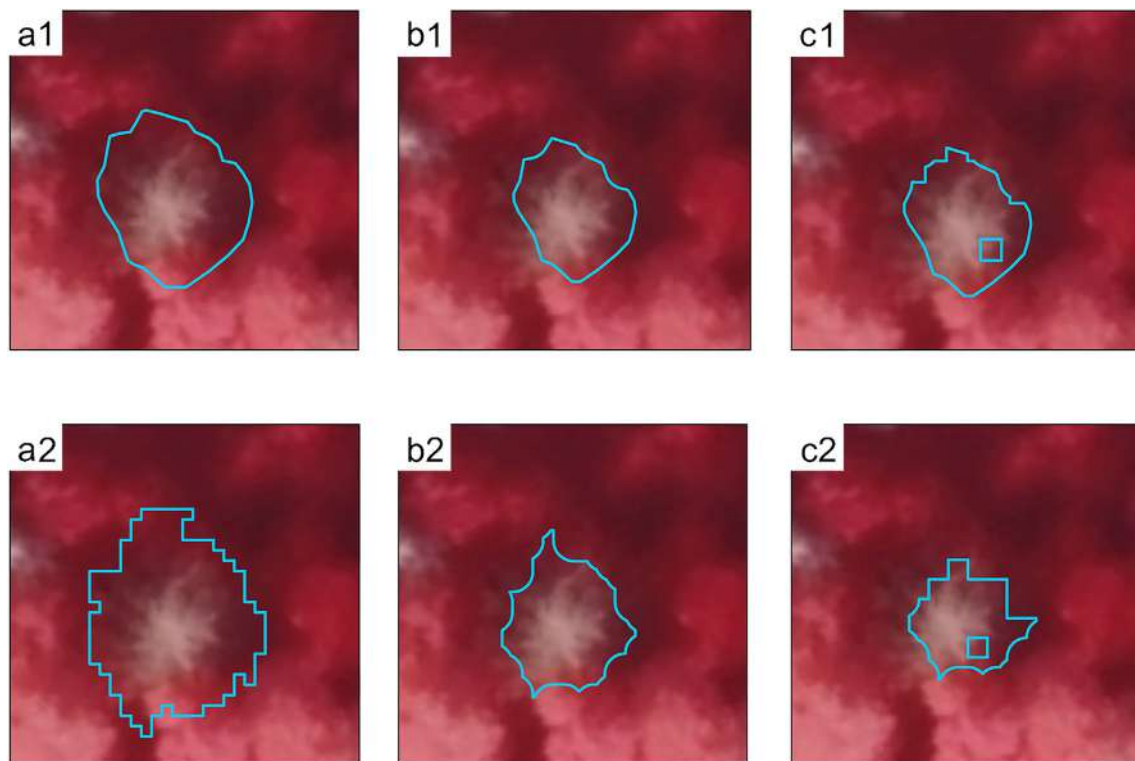


Fig. 6. Examples of tree canopy ranges. a1: sample of polygon range delineated manually based on Canopy Height Model, b1: polygon reduced by 1 m buffer, c1: polygon reduced by Gap Fraction, a2: sample segment delineated automatically based on Canopy Height Model (CHM), b2: segment reduced by 1 m buffer, c2: segment reduced by Gap Fraction. Basemap: Color-Infrared. (For interpretation of the references to color in this figure legend, the reader is referred to the Web version of this article.)

2.5. K-mean clustering method

ITC#1 was divided into test dataset and validation dataset. Trees from each health class condition were divided by stratified random sampling (in 50%/50% proportions) into these two sub-datasets (Fig. 7). In the validation dataset the same tree crowns are included in ITC#1 and ITC#2, which differ in a method of delineation (Fig. 6). Half of the gathered ground reference was taken to the test dataset and it was used to differentiate clusters from K-mean clustering method (see below). Other half of the ground reference was used as validation dataset, to compare and check results that were obtained in the test dataset (Fig. 7).

K-mean clustering method was used to divide test dataset into health class conditions. It is necessary to automate the process of detecting tree health status as it should be easy to repeat and performed in other study areas. K-mean clustering method was performed in ArcGIS without space restrictions. Only the average temperature of tree crowns was analyzed and on this basis the objects were grouped into 3 clusters ('healthy', 'poor condition', and 'dead'). Three clusters 'seeds' for each group were defined by the mean value of the temperature obtained from a given class from the ground reference. Ten iterations were executed. After performing the K-mean clustering, a division into three condition groups was created. Contour coefficient index was used to check the applicability of K-mean clustering results. Contour coefficient ranges from -1 to $+1$, where a high value indicates that the object is well matched to its own cluster and poorly matched to neighboring clusters (Zhang et al., 2018). To check if classes differ significantly from each other ANOVA and post-hoc tests were conducted. Then, the temperature ranges for the condition classes were created, taking the extreme values from each designated group from the clusters. Tree crown temperatures from the validation dataset were assigned in class condition ranges obtained from K-mean clustering separately for ITC#1 and ITC#2.

2.6. Accuracy metrics

The final step was to calculate the level of accuracy of the assignment of trees to the condition classes on the validation datasets (Fig. 6). The following metrics of accuracy were calculated: overall accuracy, producer's accuracy, and user's accuracy for each health condition class.

$$\text{Overall accuracy} = \frac{\text{True positive} + \text{True negative}}{\text{True positive} + \text{False positive} + \text{True negative} + \text{False negative}} \quad (1)$$

$$\text{Producer's accuracy} = \frac{\text{Correct impervious tree crowns}}{\text{Total impervious crowns}} \quad (2)$$

$$\text{Users' accuracy} = \frac{\text{Correct impervious tree crowns}}{\text{Correct} + \text{Misclassified crowns}} \quad (3)$$

3. Results

3.1. Determination of temperature ranges of condition categories

The ITC temperatures were used in the K-mean clustering method to split trees from the test dataset into three clusters, which represent different class conditions (Fig. 8). According to contour coefficient index results, the cluster with the highest value was the 'dead' (0.963), next they were the 'healthy' cluster (0.943) and the 'poor condition' cluster (0.930). High values indicate that objects (in this case canopy temperatures) were well matched to clusters. The cluster composed by 'healthy' trees has the lowest mean canopy temperature, while the mean temperature of trees from a cluster with dominant 'dead' trees is considerably higher (Fig. 9). The average temperature of a 'healthy' trees cluster

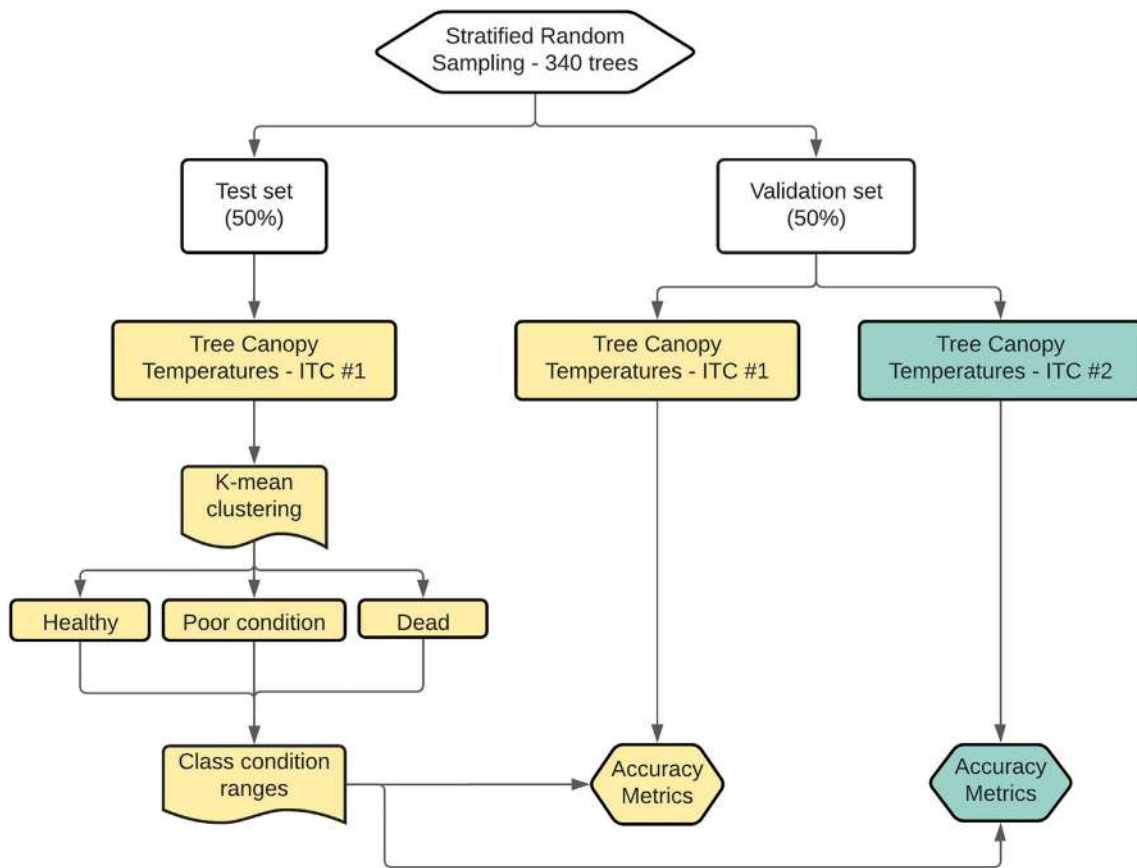


Fig. 7. Workflow of statistical analysis. ITC: Individual Tree Canopy.

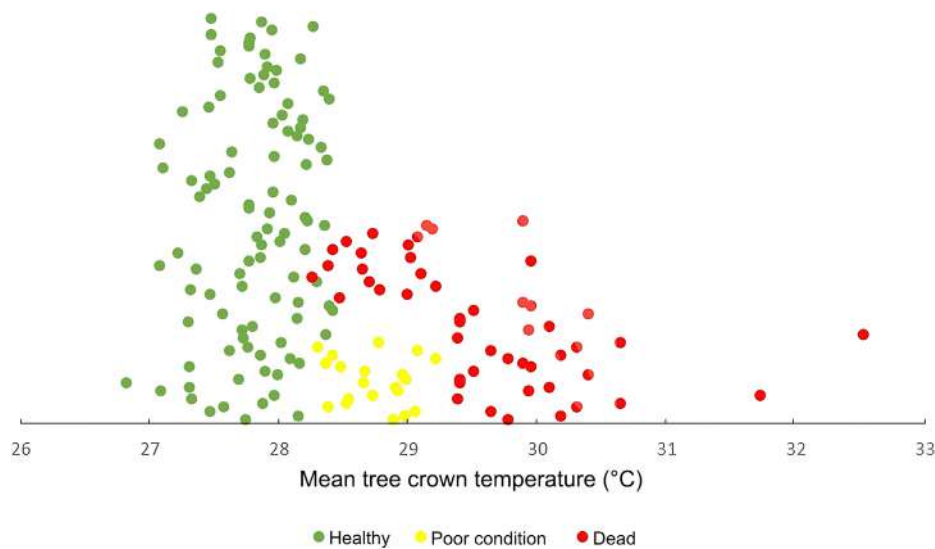


Fig. 8. K-mean clustering visualization of three clusters, which represent three condition classes of *P. abies* ('healthy', 'poor condition' and 'dead' classes determined by K-mean clustering). Each dot represents one trees' temperature.

is $27.70\text{ }^{\circ}\text{C} \pm 0.23\text{ }^{\circ}\text{C}$ and for trees in the 'poor condition' cluster it increases by $0.87\text{ }^{\circ}\text{C}$ to $28.57\text{ }^{\circ}\text{C} \pm 0.31\text{ }^{\circ}\text{C}$. The average temperature of 'dead' trees cluster is $30.17\text{ }^{\circ}\text{C} \pm 0.37\text{ }^{\circ}\text{C}$, resulting in a difference of $1.60\text{ }^{\circ}\text{C}$ between the 'poor condition' and the 'dead'. The difference in canopy temperature between the 'healthy' and 'dead' clusters is $2.47\text{ }^{\circ}\text{C}$.

ANOVA test confirmed that condition clusters of the test dataset were significantly different ($p < 0.001$). As a result, the average tree crown temperature of health condition is the factor that differentiates these

clusters by obtaining three post-hoc groups. Tukey's post-hoc test confirms that there were significant differences among all three condition states.

It was assumed that the extreme values of the ITC temperatures from individual clusters, separated by the K-mean method, would create compartments that allow to distinguish *P. abies* in three condition states (Table 3). According to this method, 'healthy' trees were assumed if the mean ITC temperature was less than or equal to $28.13\text{ }^{\circ}\text{C}$. Trees in 'poor

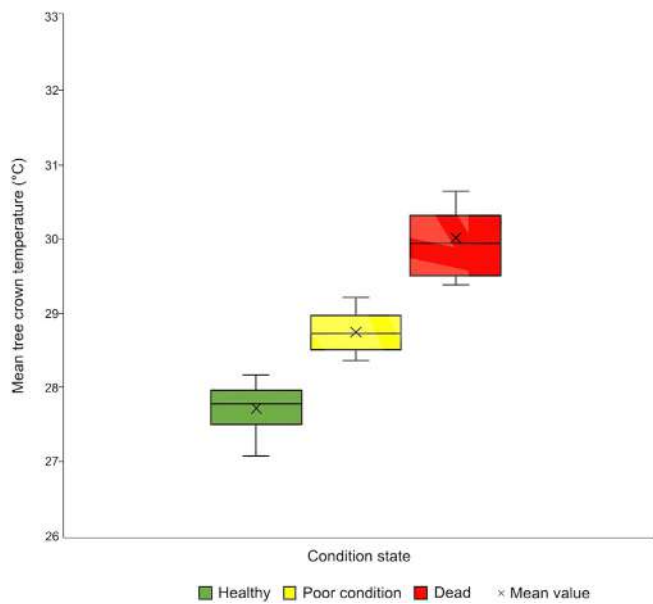


Fig. 9. Mean temperature values of *P. abies* canopies divided by their condition state, calculated from the clusters. Box: represents the first and the third quartile; plot: the highest and the lowest temperature values in a given class; × : mean value of a given class.

Table 3
Determination of temperature value ranges of condition categories.

Category	Range limits (°C)
Healthy	26.81–28.13
Poor condition	28.14–29.27
Dead	29.28–32.50

condition' class were trees with a mean ITC temperature from 28.14 °C to 29.27 °C. 'Dead' trees have mean ITC temperatures higher than 29.28 °C.

3.2. Result comparison of validation set created with two tree canopy delineated methods

Each tree from the validation dataset was assigned to the condition class according to its ITC temperature and thresholds from Table 3. Canopy temperature of each tree was calculated from two types of tree canopies creation method (ITC#1 and ITC#2) and because of that, two validations were performed.

Firstly, validation dataset created with ITC#1 method was performed. There were 100 tree canopies in the 'healthy', 20 in the 'poor condition' and 50 in the 'dead' classes, respectively. After the trees were grouped according to the assigned values of each category, the following results were acquired (Table 4): 67 were correctly classified as 'healthy' out of 100 healthy tree canopies, and 16 were accurately categorized as 'dead' out of 50 canopies of the 'dead' category; in 'poor condition' category 19 canopies from 20 were correctly classified.

A second validation was performed for the same trees used in Section 2.4., but this time the canopy range was determined on the basis of automatic segmentation (ITC#2). Each of these segments, after zonal statistics were computed, was assigned to the appropriate category (Table 3) based on the average tree canopy temperature determined. As a result of this analysis, 64 out of 100 tree canopies from this class were correctly classified to the 'healthy' category, while only 5 trees were correctly assigned to the 'dead' category (Table 5). 45 'dead' trees were classified as 'poor condition'. All trees from the 'poor condition' were assigned correctly.

As a part of the presented research, the possibility of identifying trees attacked by *I. typographus* was compared with two methods of delimiting the range of ITC. For the validation dataset, the value of correctly classified objects in accordance with the overall accuracy, producer's accuracy and user's accuracy for each class are presented in Table 6. Values of all metrics are similar to each other between ITC#1 and ITC#2. Despite obtaining statistically significant differences in temperature among all classes, validation results show values of overall accuracy 0.60 for ITC#1 and 0.52 for ITC#2. The highest values were obtained on producer's accuracy for 'poor condition'. Also, user's accuracy for 'healthy' and 'dead' classes are high. Very low values of producer's accuracy for the 'dead' and user's accuracy for the 'poor condition' were obtained. A large part of 'dead' trees, after creating clusters, were classified in the 'poor condition' category (Fig. 8), which may affect these results. Values of overall accuracy for both ranges are similar, albeit a slightly better ITC#1 than ITC#2. The visual representation of the results was presented in Fig. 10.

The applicability of the determined thresholds for classes on the basis of the tree canopy temperature values was checked on a selected fragment of the study area, where *P. abies* is the only growing tree species (Fig. 11). Information on mean temperature of each canopy was added to the segments, which were assigned to the appropriate class based on the thresholds in Table 3. The results were compared with CIR, CHM, and TIR basemaps.

Another analysis was also carried out for the entire study area, where each segment was assigned to the condition class based on their mean temperature and determined thresholds (Table 3). From 426,262 segments, automatically created in the study area, 414,757 segments (97.3%) were assigned to the 'healthy' class, 10,713 segments (2.5%) to 'poor condition' and 792 segments (0.2%) to the 'dead' class.

Table 4
Results for a validation set of ITC#1 assigned in accordance with the value of the mean tree canopy temperature. Numbers in green blocks represent True Positives.

Category assignment based on created ranges	Category assigned on the basis of ground reference set			Summary
	Healthy	Poor condition	Dead	
Healthy	67	0	0	67
Poor condition	31	19	34	84
Dead	2	1	16	19
Summary	100	20	50	170

Table 5
Results for a validation set of ITC#2 assigned in accordance with the value of the mean tree canopy temperature. Numbers in green blocks represent True Positives.

Category assignment based on created ranges	Category assigned on the basis of ground reference set			Summary
	Healthy	Poor condition	Dead	
Healthy	64	0	0	64
Poor condition	34	20	45	99
Dead	2	0	5	7
Summary	100	20	50	170

Table 6
Accuracy Metrics of validation set for ITC#1(Individual Tree Canopies #1) and ITC#2 (Individual Tree Canopies #2).

Accuracy metrics	ITC#1	ITC#2
Overall accuracy	0.60	0.52
Producer's accuracy – 'healthy'	0.67	0.64
User's accuracy – 'healthy'	1.00	1.00
Producer's accuracy – 'poor condition'	0.95	1.00
User's accuracy – 'poor condition'	0.23	0.20
Producer's accuracy – 'dead'	0.32	0.10
User's accuracy – 'dead'	0.84	0.71

4. Discussion

4.1. Effectiveness of tree crown temperature estimation with thermal infrared data

High spatial resolution of the acquired airborne multisensor data (GSD = 1 m) made it possible to analyze ITC and precisely determine their temperature. In this study we identified the average canopy temperature values of *P. abies* based on thermal infrared and airborne laser scanning data fusion, and confirmed that the temperature of the 'healthy' tree class was lower than the 'poor condition' and the 'dead' tree classes (Fig. 9). The biggest difference between individual 'healthy' and 'dead' trees reached above 5 °C. Higher temperatures of 'poor condition' and 'dead' tree classes may result from both high degree of defoliation (Clark et al., 2012) and low chlorophyll fluorescence emission in discolored needles (Calderón et al., 2013). Our research confirmed the assumption

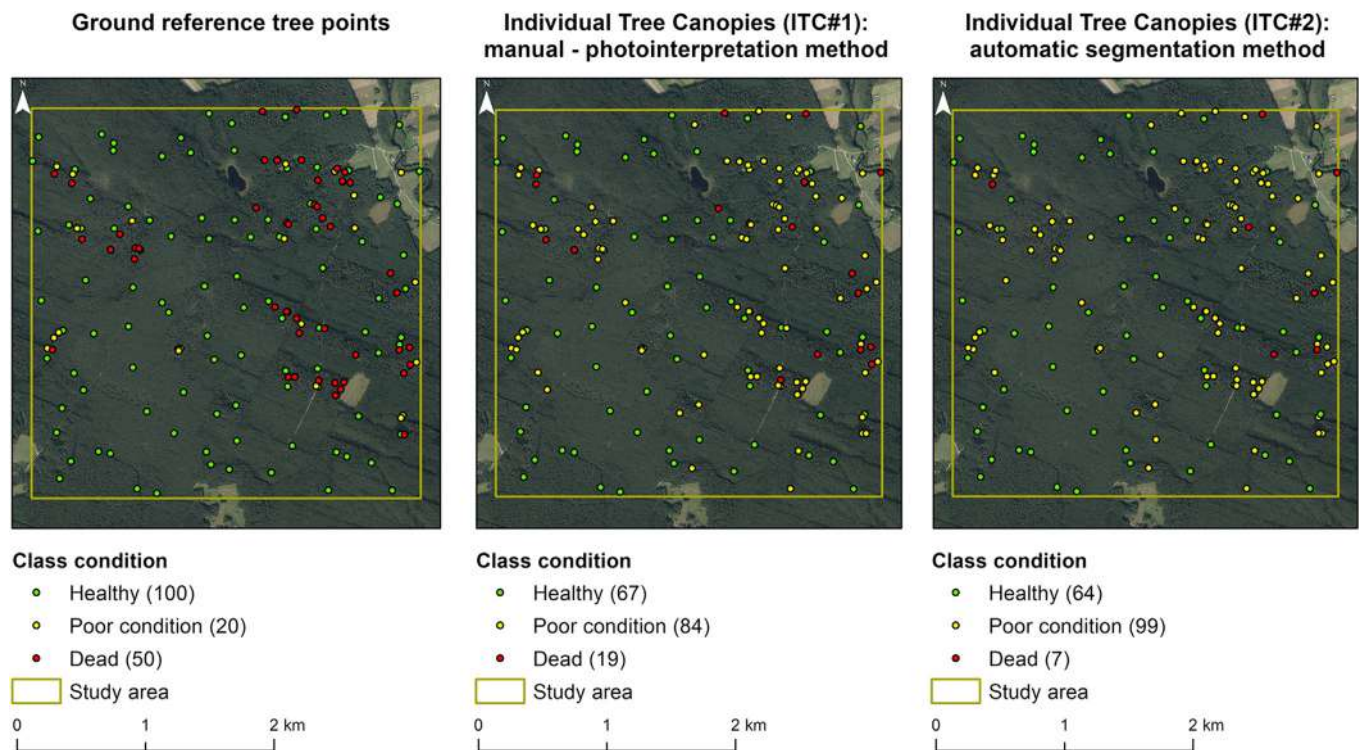


Fig. 10. Comparison of tree condition classes assigned in the study area (Ground reference tree points) with the results of manual-photo interpretation method of Individual Tree Canopies (ITC#1) and automatic segmentation method of Individual Tree Canopy (ITC#2). In brackets, the number of assigned tree individuals to a given class was provided.

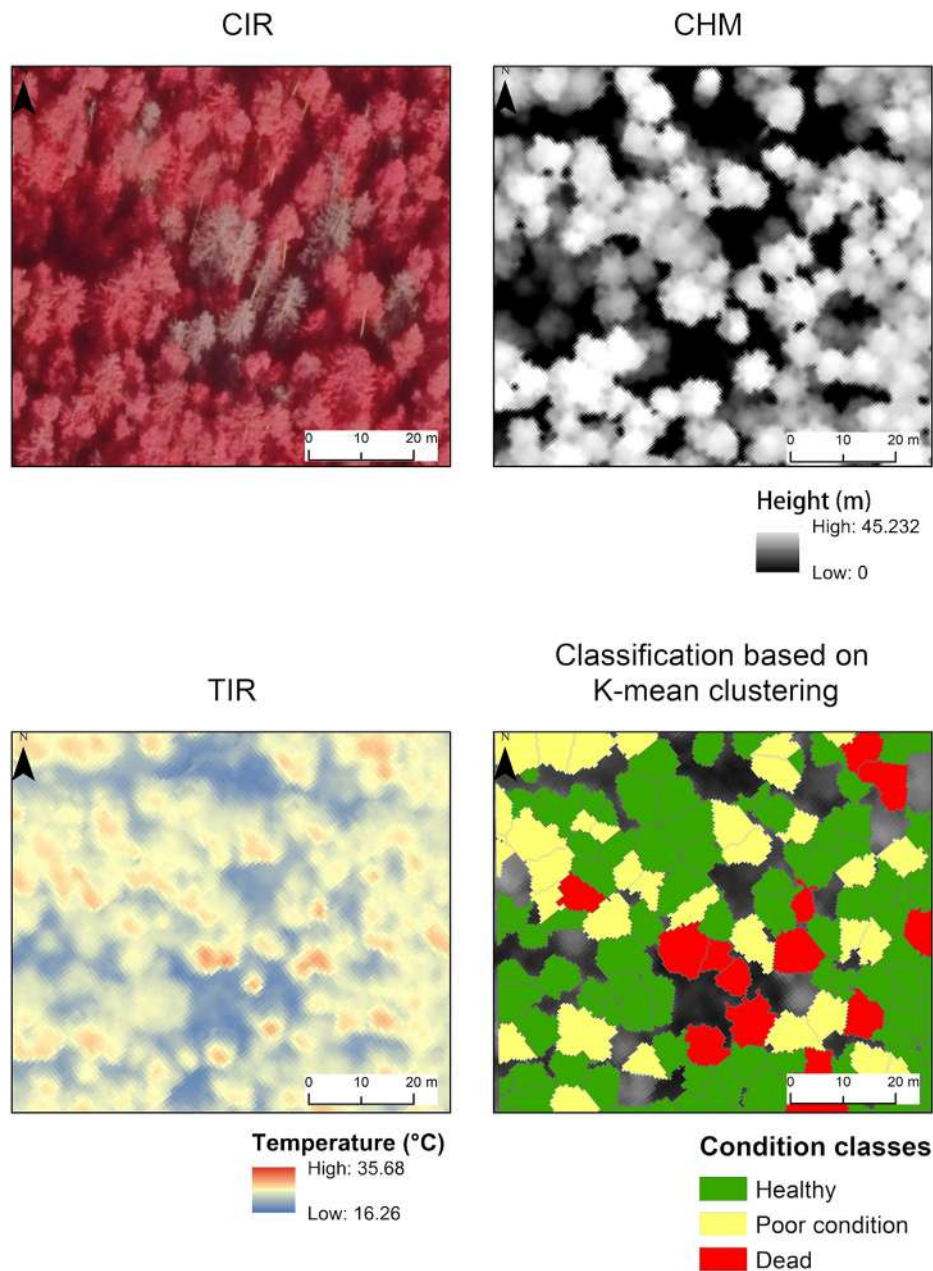


Fig. 11. Fragment of the study area where classification based on K-mean clustering method was made in accordance with the mean canopy temperature values of all trees. Information about the health condition of *P. abies* was added to each segment based on the temperature limits assumed and established for each class. CIR: Color-Infrared; CHM: Canopy Height Model; TIR: Thermal Infrared. (For interpretation of the references to color in this figure legend, the reader is referred to the Web version of this article.)

of Junttila et al. (2016) that high resolution thermal airborne data can be successfully used to distinguish dead and healthy *P. abies*. Moreover, a significant difference between the temperature of these classes was registered in the MWIR spectral range.

In this study, ITC temperatures were determined for condition classes in *P. abies* in homogeneous environment and under stable weather conditions, which made it possible to distinguish different health classes using thresholds (Table 3). The obtained values of the temperature ranges for the classes change depending on the weather conditions, the season and the illumination conditions. In order to be able to use them correctly to identify the health condition of *P. abies* health, the workflow proposed in this research should be used to create condition classes of trees, based on the field reference for the conducted research. It can be assumed that the temperature values of the classes may be different, but the relationship between them can be constant. For now, it is still an issue, which must be studied in future research.

An attempt was also made to determine the transition class ('poor condition'), which is the green attack phase. At this point, the 'poor

condition' class has become a separate group (statistically significant), most of which are trees in 'poor condition' and 'dead' (Fig. 8). Despite the low overall accuracy values, the results of the classification can be interpreted as creating a 'transition group', in which there is a high probability that there are 'dead' trees and trees in 'poor condition' attacked by the bark beetle (Table 6). It is up to the user to verify the designated individuals in the field. Determination of the 'poor condition' class of *P. abies* using only TIR data is difficult. In similar study, where thermal airborne data were used, the $p < 0.15$ value for trees in poor condition was obtained (Junttila et al., 2016). In studies where satellite data and also the clustering method (a principal components analysis) were used, fragments of the forest dominated by the green attack phase were successfully delineated (Abdullah et al., 2018, 2019). This confirms the possibility of using the workflow developed in this research for effective identification of, not the entire forest fragments, but individual *P. abies* trees, which are dead or in poor health condition. At the same time, it showed the advantage of using TIR data to determine *I. typographus* infestations in the 'green attack' phase. Determination of

correlation between water content and vegetation temperature is widely used in remote sensing techniques, especially in agriculture studies (Hernández-Clemente et al., 2019). MWIR can be particularly precise in determining water content in vegetation (Gerber et al., 2011). Our research confirmed this statement, by separating ‘healthy’ trees from ‘dead’ trees and trees in ‘poor condition’ (Fig. 7).

Even better results could be provided if TIR data would be collected together with other indices, which describes crown diameter and its structure, e.g., leaf area index. Wang et al. (2022) found high correlation between shoot damage ratio and canopy temperature (determination coefficients of 0.7890 and 0.5532), proving the significant influence of tree structure on its temperature. Many results and methodologies, which were obtained from UAVs level, could be repeated at aircraft level. However, a different scale of study area and different resolution of airborne data could be a limiting factor for implementing these solutions. Eventually a fusion of satellite, aircraft and UAV data can be another way for sophisticated monitoring (Kakooei and Baleghi, 2017).

4.2. Potential application of the results

Using an appropriate reference dataset and simple classification algorithms (such as K-mean clustering) available in programs like ArcGIS or Statistica, it is possible to isolate a group of trees with a high risk of attack by the bark beetle. It is still possible to process and identify this group quickly with the present method, contrary to *I. typographus* detection methods which use hyperspectral data, thus requiring more complicated data processing. The Kappa score of 0.60 was obtained in other studies using hyperspectral data from the UAV level, examining three condition states (healthy, infested and dead) of individual tree crowns (Näsi et al., 2015). A similar finding was also obtained for multi and hyperspectral data from UAV in Honkavaara et al. (2020), but their method was only good for small fragments of the forest. On the other hand, studies using satellite data also show high efficiency in detecting forest areas attacked by *I. typographus*, but with focuses on the analysis of entire forest fragments with limited presence and not on individual tree crowns (Filchev, 2012; Immitzer and Atzberger, 2014; Yang, 2019). Another method of highly effective detection of attacked *P. abies*, especially in the green stage, is the use of airborne hyperspectral data (Hellwig et al., 2021). Here we established a new method, which combines both hyperspectral and thermal data, believing it would improve the results even more. As suggested by previous publications, the selection of data and methods for determining outbreaks of *I. typographus* depends primarily on the size of the study area, disturbance case and end-user requirements. The method presented in this research can be especially useful in forest management if there are small groups of dead trees in the environment or single infested *P. abies* over a large area. It is particularly important to consider the life cycle of *I. typographus*, which may infest trees placed over 100 m away from earlier infested *P. abies* (Stereńczak et al., 2019). Dynamics of *I. typographus* development is crucial in examining its outbreaks in the study area. In our research, the lack of synchronization of TIR data with ALS and CIR did not affect our findings, because in the study area no outbreak of the bark beetle was found between August 2019 and June 2020. Still, all airborne data (in the case of the application of the described method) should be obtained synchronously, and it is especially important for areas with high dynamics of bark beetle development.

The benefit of airborne TIR data is that the results are easy to interpret. Moreover, data can be quickly processed using basic Geographic Information System (GIS) software and the results can be applied in the field (Fig. 11). An additional advantage of this method are lower acquisition costs. The drawbacks are difficulties in data processing (especially appropriate radiometric accuracy calibration), and problems with data acquisition under thermally stable conditions (Khanal et al., 2017). The temperature of the objects is a feature that changes over time, and it is difficult to be determined unequivocally. It depends primarily on the analyzed object and its emission properties (Bandfield and Smith, 2003).

Weather conditions (especially precipitation, average temperature, and air humidity) during the day and throughout the year are the second key factor. Canopy temperature depends on taxonomic affiliation, canopy architecture (its branching), ground, position in the field, and proximity of other objects (Zheng et al., 2018). For the study of mixed, multi-species forests, this method of canopy temperature assessment may work, because species have different canopy temperatures (Grace, 1988). With so many factors that need to be taken into account, there is a problem to obtain thermally stable data with accurate radiometry. The potential for the application of TIR data in environmental studies is very high, but further research in this area is required to examine different tree species in various environments and determine suitable acquisition parameters.

5. Conclusions

The results of the studies conducted in WNP are an initial phase of research into the analysis of airborne TIR data application for the detection of dead and in ‘poor condition’ trees in forest communities. Airborne data with very high spatial resolution (GSD = 1 m) made it possible to determine the canopy temperature of individual trees in various condition states and compare them. Based on the obtained result and reference to aims of this study, we draw the following conclusions:

- 1) TIR data registered in the spectral range of MWIR (3.6–4.9 μm) can be used to detect *P. abies* that are in ‘poor condition’ or dead due to *I. typographus* infestation. A statistically significant difference was obtained between the three conditional states (‘healthy’, ‘poor condition’, ‘dead’).
- 2) The comparison of the effectiveness of identifying the tree health condition based on two methods of determining the individual range of tree canopy indicates that the automatic segmentation method (ITC#2) lowers the accuracy of the identification of dead trees by 11% compared to the manual method (ITC#1), obtaining the overall accuracy = 0.52. The obtained results confirmed that TIR and ALS data fusion allow for creating a quick and simple workflow, which can successfully separate individual tree canopies and identify *I. typographus* invasion stages. The method based on the K-mean clustering algorithm and automatic segmentation of tree canopies based on CHM, allows to distinguish a class of ‘healthy’ trees with the producer’s accuracy = 0.64. The class of trees in ‘poor condition’ is distinguished by low user’s accuracy = 0.22 and ‘dead’ trees by producer’s accuracy = 0.10, because within these classes, individuals are mixed. Therefore, it can be concluded that the ‘poor condition’ class is a ‘transition group’ that contains trees from all condition classes with high probability of *I. typographus* infestation.

Further studies using TIR data are necessary, despite the fact that the ‘transition group’ has a high probability of making up individual *P. abies* trees that are either ‘dead’ or ‘in poor condition’. Increasing the precision of distinguishing trees depending on the invasive stage, should be prioritized in further studies, as identifying *I. typographus* infestation spots in the early stages of its attack and removing the infested tree is an effective method of reducing the bark beetle’s population.

Author contributions

Conceptualization, D.K.; Supervision, D.K.; Investigation, A.Z., Resources preparation, A.Z.; Statistical analysis, A.Z.; Data postprocessing, A.Z.; Results interpretation, A.Z., D.K.; Writing – original draft, A.Z.; Draft correction, D.K.

Funding

This work was co-financed by the European Union from the European Social Fund under the “InterDOC-START” project (POWR.03.02.00–00-

I033/16–00) and from the Operational Programme Infrastructure and Environment under the program 2.4.4d – assessment of the state of natural resources in national parks using modern remote sensing technologies, “Acquisition of multi-source remote sensing data and their analysis for the area of Wigry National Park with a part of Wigry lake and the Czarna Hańcza river” project.

Declaration of competing interest

The authors declare that they have no known competing financial interests or personal relationships that could have appeared to influence the work reported in this paper.

References

- Abdullah, H., Skidmore, A.K., Darvishzadeh, R., Heurich, M., 2018. Sentinel-2 accurately maps green-attack stage of European spruce bark beetle (*Ips typographus* L.) compared with Landsat-8. *Remote Sens. Ecol. Conserv.* 5 (1), 87–106. <https://doi.org/10.1002/rse2.93>.
- Abdullah, H., Darvishzadeh, R., Skidmore, A.K., Heurich, M., 2019. Sensitivity of Landsat-8 OLI and TIRS data to foliar properties of early stage bark beetle (*Ips typographus* L.) infestation. *Rem. Sens.* 11 (4), 398. <https://doi.org/10.3390/rs11040398>.
- Ali, A.M., Abdullah, H., Darvishzadeh, R., Skidmore, A.K., Heurich, M., Rooesli, C., Paganini, M., Heiden, U., Marshall, D., 2021. Canopy chlorophyll content retrieved from time series remote sensing data as a proxy for detecting bark beetle infestation. *Remote Sens. Appl. Soc. Environ.* 22, 100524. <https://doi.org/10.1016/j.rsase.2021.10052>.
- Bandfield, J.L., Smith, M.D., 2003. Multiple emission angle surface-atmosphere separations of Thermal Emission Spectrometer data. *Icarus* 161 (1), 47–65. [https://doi.org/10.1016/S0019-1035\(02\)00025-8](https://doi.org/10.1016/S0019-1035(02)00025-8).
- Calderón, R., Navas-Cortés, J.A., Lucena, C., Zarco-Tejada, P.J., 2013. High-resolution airborne hyperspectral and thermal imagery for early detection of Verticillium wilt of olive using fluorescence, temperature and narrow-band spectral indices. *Remote Sens. Environ.* 139, 231–245. <https://doi.org/10.1016/j.rse.2013.07.031>.
- Campbell, P.E., Rock, B.N., Martin, M.E., Neeffus, C.D., Irons, J.R., Middleton, E.M., Albrechtova, J., 2004. Detection of initial damage in Norway spruce canopies using hyperspectral airborne data. *Int. J. Rem. Sens.* 25 (24), 5557–5584. <https://doi.org/10.1080/01431160410001726058>.
- Cheng, T., Rivard, B., Sánchez-Azofeifa, G.A., Feng, J., Calvo-Polanco, M., 2010. Continuous wavelet analysis for the detection of green attack damage due to mountain pine beetle infestation. *Rem. Sens. Environ.* 114 (4), 899–910. <https://doi.org/10.1016/j.rse.2009.12.005>.
- Christiansen, E., Bakke, A., 1988. The spruce bark beetle of Eurasia. In: Berryman, A.A. (Ed.), *Dynamics of Forest Insect Populations*. Population Ecology. Springer, Boston MA, pp. 479–503. https://doi.org/10.1007/978-1-4899-0789-9_23.
- Clark, K.L., Skowronski, N., Gallagher, M., Renninger, H., Schäfer, K., 2012. Effects of invasive insects and fire on forest energy exchange and evapotranspiration in the New Jersey pineplands. *Agric. For. Meteorol.* 166, 50–61. <https://doi.org/10.1016/j.agrformet.2012.07.007>.
- Coops, N.C., Gillanders, S.N., Wulder, M.A., Gergel, S.E., Nelson, T., Goodwin, N.R., 2010. Assessing changes in forest fragmentation following infestation using time series Landsat imagery. *For. Ecol. Manag.* 259 (12), 2355–2365. <https://doi.org/10.1016/j.foreco.2010.03.008>.
- Danson, F.M., Hetherington, D., Morsdorf, F., Koetz, B., Allgower, B., 2007. Forest canopy gap fraction from terrestrial laser scanning. *Geosci. Rem. Sens. Lett. IEEE* 4 (1), 157–160. <https://doi.org/10.1109/LGRS.2006.887064>.
- Egea, G., Padilla-Díaz, C.M., Martínez-Guante, J., Fernández, J.E., Pérez-Ruiz, M., 2017. Assessing a crop water stress index derived from aerial thermal imaging and infrared thermometry in super-high density olive orchards. *Agric. Water Manag.* 187, 210–221. <https://doi.org/10.1016/j.agwat.2017.03.030>.
- Eichhorn, J., Szepesi, A., Ferretti, M., Durrant, D., Roskams, P., 2004. *Manual on methods and criteria for harmonized sampling, assessment, monitoring and analysis of the effects of air pollution on forests. Part II Visual Assessment of Crown Condition*. International Co-operative Programme on Assessment and Monitoring of Air Pollution Effects on Forests. United Nations Economic Commission for Europe Convention on Long-Range Transboundary Air Pollution, Germany.
- Fassnacht, F.E., Latifi, H., Koch, B., 2012. An angular vegetation index for imaging spectroscopy data—Preliminary results on forest damage detection in the Bavarian National Park, Germany. *Int. J. Appl. Earth Obs. Geoinf.* 19, 308–321. <https://doi.org/10.1016/j.jag.2012.05.018>.
- Fassnacht, F.E., Latifi, H., Ghosh, A., Joshi, P.K., Koch, B., 2014. Assessing the potential of hyperspectral imagery to map bark beetle-induced tree mortality. *Remote Sens. Environ.* 140, 533–548. <https://doi.org/10.1016/j.rse.2013.09.014>.
- Filchev, L., 2012. An assessment of European spruce bark beetle infestation using WorldView-2 satellite data. In: European SCGIS Conference “Best Practices: Application of GIS Technologies for Conservation of Natural and Cultural Heritage Sites.” Sofia, Bulgaria. <https://doi.org/10.13140/2.1.3005.2647>.
- Gandhi, G.M., Parthiban, B.S., Thummalu, N., Christy, A., 2015. N-dvi: vegetation change detection using remote sensing and GIS - a case study of Vellore District. *Procedia Comput. Sci.* 57, 1199–1210. <https://doi.org/10.1016/j.procs.2015.07.415>.
- Gerber, F., Marion, R., Olioso, A., Jacquemoud, S., Da Luz, B.R., Fabre, S., 2011. Modeling directional-hemispherical reflectance and transmittance of fresh and dry leaves from 0.4 µm to 5.7 µm with the PROSPECT-VISIR model. *Remote Sens. Environ.* 115 (2), 404–414. <https://doi.org/10.1016/j.rse.2010.09.011>.
- Grace, J., 1988. 3. Plant response to wind. *Agric. Ecosyst. Environ.* 22, 71–88. [https://doi.org/10.1016/0167-8809\(88\)90008-4](https://doi.org/10.1016/0167-8809(88)90008-4).
- Grodzki, W., 2013. *Kornik Drukarz I Jego Rola W Ekosystemach Leśnych*, first ed. Centrum Informacyjne Lasów Państwowych, Warsaw.
- Grodzki, W., McManus, M., Kniżek, M., Meshkova, V., Mihalciuc, V., Novotny, J., Turčani, M., Slobodyan, Y., 2004. Occurrence of spruce bark beetles in forest stands at different levels of air pollution stress. *Environ. Pollut.* 130 (1), 73–83. <https://doi.org/10.1016/j.envpol.2003.10.022>.
- Gutowski, J.M., 2002. *Problemy ochrony ekosystemów leśnych a gradacje kornika drukarza-wprowadzenie*. Prace Instytutu Badawczego Leśnictwa. Seria A 1, 5–15.
- Gutowski, J.M., 2004. Kornik drukarz-gatunek kluczowy. *Parki Narodowe* 1, 13–15.
- Gutowski, J.M., Krzysztofiak, L., 2005. Directions and intensity of migration of the spruce bark beetle and accompanying species at the border between strict reserves and managed forests in north-eastern Poland. *Ecol. Quest.* 6, 81–92.
- Hais, M., 2003. Changes in land cover temperature and humidity parameters resulting from spruce forests decay in the centre of the Sumava National Park. *Acta Univ. Carol. Geograph.* 2, 97–107.
- Hais, M., Kučera, T., 2008. Surface temperature change of spruce forest as a result of bark beetle attack: remote sensing and GIS approach. *Eur. J. For. Res.* 127 (4), 327–336. <https://doi.org/10.1007/s10342-008-0208-8>.
- Hanisch, B., Kitz, E., 1990. *Monitoring of forest damage: spruce and pine*. Verlag Eugen Ulmer, Stuttgart.
- Hedgren, P.O., Schroeder, L.M., 2004. Reproductive success of the spruce bark beetle *Ips typographus* (L.) and occurrence of associated species: a comparison between standing beetle-killed trees and cut trees. *For. Ecol. Manag.* 203 (1–3), 241–250. <https://doi.org/10.1016/j.foreco.2004.07.055>.
- Hellwig, F.M., Stelmaszczyk-Górska, M.A., Dubois, C., Wolsza, M., Truckenbrodt, S.C., Sagichewski, H., Chmara, S., Bannehr, L., Lausch, A., Schmutli, C., 2021. Mapping European spruce bark beetle infestation at its early phase using Gyrocopter-mounted hyperspectral data and field measurements. *Rem. Sens.* 13 (22), 4659. <https://doi.org/10.3390/rs13224659>.
- Hernández-Clemente, R., Hornero, A., Mottus, M., Peñuelas, J., González-Dugo, V., Jiménez, J.C., Suárez, L., Alonso, L., Zarco-Tejada, P.J., 2019. Early diagnosis of vegetation health from high-resolution hyperspectral and thermal imagery: lessons learned from empirical relationships and radiative transfer modelling. *Curr. For. Res.* 5 (3), 169–183. <https://doi.org/10.1007/s40725-019-00096-1>.
- Hlásky, T., Zajicková, L., Turčani, M., Holuša, J., Sitková, Z., 2011. Geographical variability of spruce bark beetle development under climate change in the Czech Republic. *J. For. Sci.* 57 (6), 242–249. <https://doi.org/10.17221/104/2010-JFS>.
- Honkavaara, E., Näsi, R., Oliveira, R., Viljanen, N., Suomalainen, J., Khoramshahi, E., Hakala, T., Nevalainen, O., Markelin, L., Vuorinen, M., Kankaanhuhta, V., Lyytikäinen-Saarenmaa, P., Haataja, L., 2020. Using multitemporal hyper- and multispectral UAV imaging for detecting bark beetle infestation on Norway spruce. *Int. Arch. Photogramm. Remote Sens. Spat. Inf. Sci. XLIII-B3-2020*. <https://doi.org/10.5194/isprs-archives-xliii-b3-2020-429-2020>.
- Immitzer, M., Atzberger, C., 2014. Early detection of bark beetle infestation in Norway spruce (*Picea abies* L.) using WorldView-2 data. *Photogramm. Fernerkund. Geoinf.* 73, 351367. <https://doi.org/10.1127/1432-8364/2014/0229>.
- Jaime, L., Battlori, E., Margalef-Marrase, J., Navarro, M.A.P., Lloret, F., 2019. Scots pine (*Pinus sylvestris* L.) mortality is explained by the climatic suitability of both host tree and bark beetle populations. *For. Ecol. Manag.* 448, 119–129. <https://doi.org/10.1016/j.foreco.2019.05.070>.
- Jiang, J., Tian, G., 2010. Analysis of the impact of land use/land cover change on land surface temperature with remote sensing. *Proc. Environ. Sci.* 2, 571–575. <https://doi.org/10.1016/j.proenv.2010.10.062>.
- Jönsson, A.M., Harding, S., Krokene, P., Lange, H., Lindelöw, Å., Økland, B., Ravn, H.P., Schroeder, L.M., 2011. Modelling the potential impact of global warming on *Ips typographus* voltinism and reproductive diapause. *Clim. Change* 109 (3), 695–718. <https://doi.org/10.1007/s10584-011-0038-4>.
- Journal of Laws of 1988. No. 25, Item 173. The regulation of the council of ministers considering the creation of the Wigry national park. <https://isap.sejm.gov.pl/isap.nsf/download.xsp/WDU19880250173/O/D19880173.pdf>. (Accessed 3 October 2022).
- Junttila, S., Vastaranta, M., Hämäläinen, J., Latva-Käyrä, P., Holopainen, M., Hernández Clemente, R., Hyypää, H., Navarro-Cerrillo, R.M., 2016. Effect of forest structure and health on the relative surface temperature captured by airborne thermal imagery – case study in Norway spruce-dominated stands in Southern Finland. *Scand. J. For. Res.* 32 (2), 154–165. <https://doi.org/10.1080/02827581.2016.1207800>.
- Kakooei, M., Baleghi, Y., 2017. Fusion of satellite, aircraft, and UAV data for automatic disaster damage assessment. *Int. J. Remote Sens. Appl.* 38 (8–10), 2511–2534. <https://doi.org/10.1080/01431161.2017.1294780>.
- Khanal, S., Fulton, J., Shearer, S., 2017. An overview of current and potential applications of thermal remote sensing in precision agriculture. *Comput. Electron. Agric.* 139, 22–32. <https://doi.org/10.1016/j.compag.2017.05.001>.
- Kim, Y., Still, C.J., Roberts, D.A., Goulden, M.L., 2018. Thermal infrared imaging of conifer leaf temperatures: comparison to thermocouple measurements and assessment of environmental influences. *Agric. For. Meteorol.* 248, 361–371. <https://doi.org/10.1016/j.agrformet.2017.10.010>.
- Kimball, B.A., Bernacchi, C.J., 2006. Evapotranspiration, canopy temperature, and plant water relations. In: Nösberger, J., Long, S.P., Norby, R.J., Stitt, M., Hendrey, G.R., Blum, H. (Eds.), *Managed Ecosystems and CO₂*. Ecological Studies, vol. 187. Springer, Berlin, Heidelberg. https://doi.org/10.1007/3-540-31237-4_17.
- Kliczkowska, A., 2004. *Siedliskowe Podstawy Hodowli Lasu: Załącznik Do Zasad Hodowli Lasu*. Ośrodek Rozwojowo-Wdrożeniowy Lasów Państwowych.

- Kraniotis, D., Nore, K., Brückner, C., Nyruud, A.Q., 2016. Thermography measurements and latent heat documentation of Norwegian spruce (*Picea abies*) exposed to dynamic indoor climate. *J. Wood Sci.* 62 (2), 203–209. <https://doi.org/10.1007/s10086-015-1528-1>.
- Krzysztofak, L., Olszewski, K., 1999. *Klimat Wigierskiego Parku Narodowego. X Lat Wigierskiego Parku Narodowego*. Wydawnictwo Włodzimierz Lapiński, Krzywe, p. 230.
- Kuchma, T., Shvydenko, I., Vysochanska, M., Yaremko, O., Raichuk, L., Symochko, L., Kuchma, M., Havryliuk, Y., 2021. Monitoring of the seasonal development of Ips bark beetle (*Ips acuminatus*) in Scots pine stands by remote sensing. *Int. J. Ecosys.* 11 (4), 931–938. <http://hdl.handle.net/123456789/8543>. (Accessed 3 October 2022).
- Latifi, H., Fassnacht, F.E., Schumann, B., Dech, S., 2014. Object-based extraction of bark beetle (*Ips typographus* L.) infestations using multi-date LANDSAT and SPOT satellite imagery. *Prog. Phys. Geogr.* 38 (6), 755–785. <https://doi.org/10.1177/0309133314550670>.
- Lausch, A., Heurich, M., Gordalla, D., Dobner, H.J., Gwilym-Margianto, S., Salbach, C., 2013. Forecasting potential bark beetle outbreaks based on spruce forest vitality using hyperspectral remote-sensing techniques at different scales. *For. Ecol. Manag.* 308, 76–89. <https://doi.org/10.1016/j.foreco.2013.07.043>.
- Leuzinger, S., Körner, C., 2007. Tree species diversity affects canopy leaf temperatures in a mature temperate forest. *Agric. For. Meteorol.* 146 (1–2), 29–37. <https://doi.org/10.1016/j.agrformet.2007.05.007>.
- Lin, Q., Huang, H., Wang, J., Huang, K., Liu, Y., 2019. Detection of pine shoot beetle (PSB) stress on pine forests at individual tree level using UAV-based hyperspectral imagery and lidar. *Rem. Sens.* 11 (21), 2540. <https://doi.org/10.3390/rs11212540>.
- Lin, Q., Huang, H., Chen, L., Wang, J., Huang, K., Liu, Y., 2021. Using the 3D model RAPID to invert the shoot dieback ratio of vertically heterogeneous Yunnan pine forests to detect beetle damage. *Rem. Sens. Environ.* 260, 112475. <https://doi.org/10.1016/j.rse.2021.112475>.
- Livache, C., 2019. *Quantum-confined nanocrystals for infrared optoelectronics: carrier dynamics and intraband transitions*. PhD Thesis. Sorbonne Université, France.
- Long, J.A., Lawrence, R.L., 2016. Mapping percent tree mortality due to mountain pine beetle damage. *For. Sci.* 62 (4), 392–402. <https://doi.org/10.5849/forsci.15-046>.
- Lu, B., Dao, P.D., Liu, J., He, Y., Shang, J., 2020. Recent advances of hyperspectral imaging technology and applications in agriculture. *Rem. Sens.* 12 (16), 2659. <https://doi.org/10.3390/rs12162659>.
- Łuczak, W., 2019. *Wigierski Park Narodowy – ochrona dziedzictwa przyrodniczego i kulturowego a turystyka*. Warsztaty z Geografii Turyzmu 9, 143–149. <https://doi.org/10.18778/8142-698-5.12>.
- Maltamo, M., Næsset, E., Vauhkonen, J., 2014. *Forestry Applications of Airborne Laser Scanning: Concepts and Case Studies*. Springer. <https://doi.org/10.1007/978-94-017-8663-8>.
- Minkina, W., Dudzik, S., 2009. Infrared thermography: errors and uncertainties. *John Wiley & Sons*. <https://doi.org/10.1002/9780470682234.fmatter>.
- Möller, M., Alchanatis, V., Cohen, Y., Meron, M., Tsipris, J., Naor, A., Ostrovsky, V., Sprintsin, M., Cohen, S., 2007. Use of thermal and visible imagery for estimating crop water status of irrigated grapevine. *J. Exp. Bot.* 58. <https://doi.org/10.1093/jxb/erl115>.
- Müller, J., Bußler, H., Goßner, M., Rettelbach, T., Duelli, P., 2008. The European spruce bark beetle *Ips typographus* in a national park: from pest to keystone species. *Biodivers. Conserv.* 17 (12), 2979–3001. <https://doi.org/10.1007/s10531-008-9409-1>.
- Näsi, R., Honkavaara, E., Lyytikäinen-Saarenmaa, P., Blomqvist, M., Litkey, P., Hakala, T., Viljanen, N., Kantola, T., Tanhuanpää, T., Holopainen, M., 2015. Using UAV-based photogrammetry and hyperspectral imaging for mapping bark beetle damage at tree-level. *Rem. Sens.* 7 (11), 15467–15493. <https://doi.org/10.3390/rs71115467>.
- Näsi, R., Honkavaara, E., Blomqvist, M., Lyytikäinen-Saarenmaa, P., Hakala, T., Viljanen, N., Kantola, T., Holopainen, M., 2018. Remote sensing of bark beetle damage in urban forests at individual tree level using a novel hyperspectral camera from UAV and aircraft. *Urban For. Urban Green.* 30, 72–83. <https://doi.org/10.1016/j.ufug.2018.01.010>.
- Ortiz, S.M., Breidenbach, J., Kändler, G., 2013. Early detection of bark beetle green attack using TerraSAR-X and RapidEye data. *Rem. Sens.* 5 (4), 1912–1931. <https://doi.org/10.3390/rs5041912>.
- Osińska-Skotak, K., 2007. *Znaczenie korekcji radiometrycznej w procesie przetwarzania zdjęć satelitarnych*. Archiwum Fotogrametrii, Kartografii i Teledetekcji 17.
- Popescu, S.C., Wynne, R.H., 2004. Seeing the trees in the forest: using lidar and multispectral data fusion with local filtering and variable window size for estimating tree height. *Photogramm. Eng. Rem. Sens.* 70 (5), 589–604. <https://doi.org/10.14358/PERS.70.5.589>.
- Prakash, A., 2000. *Thermal remote sensing: concepts, issues and applications*. Int. Arch. Photogramm. Rem. Sens. 33 (B1), 239–243.
- Rachwald, A., Ciesielski, M., Szurlej, M., Żmihorski, M., 2022. Following the damage: increasing western barbastelle bat activity in bark beetle infested stands in Białowieża Primeval Forest. *For. Ecol. Manag.* 503, 119803. <https://doi.org/10.1016/j.foreco.2021.119803>.
- Rohde, M., Waldmann, R., Lunderstädt, J., 1996. Induced defence reaction in the phloem of spruce (*Picea abies*) and larch (*Larix decidua*) after attack by *Ips typographus* and *Ips cembrae*. *For. Ecol. Manag.* 86 (1–3), 51–59. [https://doi.org/10.1016/S0378-1127\(96\)03802-9](https://doi.org/10.1016/S0378-1127(96)03802-9).
- Sprintsin, M., Chen, J.M., Czuryłowicz, P., 2011. Combining land surface temperature and shortwave infrared reflectance for early detection of mountain pine beetle infestations in western Canada. *J. Appl. Remote Sens.* 5 (1), 053566. <https://doi.org/10.1117/1.3662866>.
- Stereńczak, K., Mielcarek, M., Modzelewska, A., Kraszewski, B., Fassnacht, F.E., Hilszczański, J., 2019. Intra-annual *Ips typographus* outbreak monitoring using a multi-temporal GIS analysis based on hyperspectral and ALS data in the Białowieża Forests. *For. Ecol. Manag.* 442, 105–116. <https://doi.org/10.1016/j.foreco.2019.03.064>.
- Trigo, I.F., Monteiro, I.T., Olesen, F., Kabsch, E., 2008. An assessment of remotely sensed land surface temperature. *J. Geophys. Res. Atmos.* 113 (D17). <https://doi.org/10.1029/2008JD010035>.
- Wang, X., Yang, W., Wheaton, A., Cooley, N., Moran, B., 2010. Automated canopy temperature estimation via infrared thermography: a first step towards automated plant water stress monitoring. *Comput. Electron. Agric.* 73. <https://doi.org/10.1016/j.compag.2010.04.007>.
- Wang, J., Meng, S., Lin, Q., Liu, Y., Huang, H., 2022. Detection of Yunnan pine shoot beetle stress using UAV-based thermal imagery and LiDAR. *Appl. Sci.* 12 (9), 4372. <https://doi.org/10.3390/app12094372>.
- Wermelinger, B., 2004. Ecology and management of the spruce bark beetle *Ips typographus* — a review of recent research. *For. Ecol. Manag.* 202 (1–3), 67–82. <https://doi.org/10.1016/j.foreco.2004.07.018>.
- Wypych, A., Sulikowska, A., Ustrnul, Z., Czekierda, D., 2017. Variability of growing degree days in Poland in response to ongoing climate changes in Europe. *Int. J. Biometeorol.* 61 (1), 49–59. <https://doi.org/10.1007/s00484-016-1190-3>.
- Yang, S., 2019. *Detecting bark beetle damage with Sentinel-2 multi-temporal data in Sweden*. Master Thesis. Lund University, Sweden.
- Zakrzewska, A., Kopeć, D., Krajewski, K., Charyton, J., 2022. Canopy temperatures of selected tree species growing in the forest and outside the forest using aerial thermal infrared (3.6–4.9 μm) data. *Eur. J. Remote Sens.* 55 (1), 313–325. <https://doi.org/10.1080/22797254.2022.2062055>.
- Zhang, Y., Liu, N., Wang, S., 2018. A differential privacy protecting K-means clustering algorithm based on contour coefficients. *PLoS One* 13 (11). <https://doi.org/10.1371/journal.pone.0206832>.
- Zheng, S., Guldmann, J.M., Liu, Z., Zhao, L., 2018. Influence of trees on the outdoor thermal environment in subtropical areas: an experimental study in Guangzhou, China. *Sustain. Cities Soc.* 42, 482–497. <https://doi.org/10.1016/j.scs.2018.07.025>.



Original article

Can canopy temperature acquired from an airborne level be a tree health indicator in an urban environment?



Agata Zakrzewska^a, Dominik Kopec^{a,b,*}, Adrian Ochtyra^c, Markéta Potůčková^d

^a Department of Biogeography, Paleocology and Nature Protection, Faculty of Biology and Environmental Protection, University of Lodz, Łódź, Poland

^b MGGP Aero Sp. z o.o., Tarnów, Poland

^c Department of Geoinformatics, Cartography and Remote Sensing, Faculty of Geography and Regional Studies, Warsaw University, Warsaw, Poland

^d Department of Applied Geoinformatics and Cartography, Faculty of Science, Charles University, Czechia

ARTICLE INFO

Keywords:

Infrared thermography

Thermal imagery

Middle wave infrared

Urban environment

Urban trees

Tree discolouration

ABSTRACT

Nowadays, gathering information about tree health conditions in cities is necessary. Trees are essential in regulating urban microclimate and mitigating the urban heat island effect. Therefore, their health status should be crucial in urban vegetation monitoring. The growing number of new cameras, sensors and research methods allows for a broader application of thermal data in remote sensing vegetation studies. This research aimed to evaluate whether it is possible to use thermal infrared data to assess the health condition of selected species of deciduous trees in an urban environment. More specifically, the data must have a 3.6–4.9 μm spectral range, obtained during the day and the night. For this purpose, research was carried out in the city center of Warsaw (Poland) in 2020. During the airborne data acquisition, thermal data, laser scanning and RGB images were collected. Synchronously with airborne data, 617 ground references were obtained in different health condition classes (healthy, slightly poor condition, poor condition and dying) for five tree species: *Acer platanoides*, *Acer pseudoplatanus*, *Aesculus hippocastanum*, *Tilia cordata* and *Tilia \times euchlora*. The results were as follows: (i) healthy trees were cooler than trees in poor condition and dying both during the daytime and nighttime; (ii) the difference in the canopy temperatures between healthy and dying trees was 1.06 °C of mean value on the nighttime data and 3.28 °C of mean value on the daytime data; (iii) all condition classes significantly differ from each other on daytime thermal data. The aerial thermal data can be considered a new alternative to hyperspectral data. Thermal sensing represents another method of assessing the health condition of trees in an urban environment – especially data obtained during the day, which can differentiate condition classes better than data obtained at night. The method based on thermal infrared and laser scanning data fusion could be a quick and efficient solution for identifying trees in poor health.

1. Introduction

Over the years, researchers have studied trees' properties and their role in shaping the urban microclimate. First of all, they provide several ecosystem services, like lowering the air temperature (Vailshery et al., 2013), cleaning the air of pollutants (Tallis et al., 2011) and improving the general thermal comfort of the surroundings (Shashua-Bar et al., 2011; Su et al., 2022). All these factors lead trees to effectively reduce

the Urban Heat Island effect (UHI; Pauleit, 2003; Chen et al., 2022). Both large clusters of trees (Yu and Hien, 2006) and single trees, such as those growing alongside roads, significantly impact the city microclimate (Kong et al., 2016). Multiple studies have also confirmed that properly maintained urban greenery improves the well-being and psychological comfort of residents (Tzoulas et al., 2007; Jenerette et al., 2007) and even contributes to the decline in crime (Burley, 2018).

Trees in cities provide numerous ecosystem benefits, however, the

Abbreviations: TIR, thermal infrared; MWIR, middle wave infrared; LWIR, long wave infrared; ALS, airborne laser scanning; RGB, red-green-blue camera; HS, hyperspectral; UAV, unmanned aerial vehicles; VTA, visual tree assessment; UHI, urban heat island; ITC, individual tree canopy; CHM, canopy height model; AGI, above ground level.

* Corresponding author at: Department of Biogeography, Paleocology and Nature Protection, Faculty of Biology and Environmental Protection, University of Lodz, Łódź, Poland.

E-mail addresses: agata.zakrzewska@biol.uni.lodz.pl (A. Zakrzewska), dominik.kopec@biol.uni.lodz.pl (D. Kopec), adrian.ochtyra@uw.edu.pl (A. Ochtyra), marketa.potuckova@natur.cuni.cz (M. Potůčková).

<https://doi.org/10.1016/j.ufug.2022.127807>

Received 13 July 2022; Received in revised form 25 November 2022; Accepted 28 November 2022

Available online 30 November 2022

1618-8667/© 2022 The Author(s).

Published by Elsevier GmbH. This is an open access article under the CC BY license (<http://creativecommons.org/licenses/by/4.0/>).

impact of the urban environment on the health condition of trees should also be taken into account (Sanesi et al., 2007). It was investigated how trees, particularly large clusters of trees, affect the urban microclimate and reduce the UHI effect, but less attention was paid to how an urban environment negatively affects trees (Berrang et al., 1985). Dead or unhealthy trees, which manifest, among other ways, by discolouration of leaves (not caused by autumn), defoliation and dead branches in the tree crowns, can cause several serious consequences, i.e., dieback. Such trees do not provide – or have limited – ecosystem services (Dale et al., 2016). They can pose a risk to people, property and infrastructure, e.g., through broken and falling branches (Ball, 2011). Moreover, they reduce the visual and aesthetic values of the city (Roy et al., 2012). The UHI effect alone is not the only challenge that trees in the city have to defend themselves against. High levels of air pollution (especially in large alleys), mechanical damage, impermeable surfaces, heat waves, frequent droughts and low rainfalls are other obstacles to the proper development of trees, especially new plantings (Nowak et al., 2004).

One of the methods of assessing the trees' health condition is Visual Tree Assessment (VTA) and inspection in the field by appointed services and specialists (Matthack and Breloer, 1994). Despite the high efficiency in assessing the health condition of trees, this solution is not feasible in large cities (Degerickx et al., 2018). Unhealthy trees need to be detected quickly, so their health can be improved as early as possible, e.g., by irrigation (Roman, 2013).

Another method of assessing the health condition of trees in the city is by using remote sensing. One potential solution in this field is hyperspectral (HS) and Airborne Laser Scanning (ALS) data fusion. HS allows the use of spectral indices to study, for example, the water or chlorophyll content in leaves, which is related to the trees' health (Delegido et al., 2014). Acquiring ALS from planes, helicopters or Unmanned Aerial Vehicles (UAVs) allows for precise determination of individual tree crowns by manually creating their polygons or using automatic segmentation (Pyysalo and Hyyppä, 2002). This data fusion was used in the detection of damage in urban forests caused by the bark beetle at the level of individual tree crowns (Näsi et al., 2018). It was further used to determine the characteristics of urban forests structure (Alonzo et al., 2016) and to classify different tree species (Jensen et al., 2012; Mozgeris et al., 2016). Generally, airborne data has a pixel size close to 1 m (Staben et al., 2016), which allows for the examination of single tree crowns and shrubs (Morgan et al., 2010). High-resolution HS data were used to monitor trees' defoliation and discolouration by Degerickx et al. (2018). In detecting healthy and unhealthy trees, the authors achieved an accuracy of 93% for defoliation and 71% for discolouration, compared to the VTA method. In similar studies, Chi et al. (2020) used data fusion and the Random Forest algorithm to study trees' defoliation, discolouration and damage. Overall accuracy ranging from 0.81 to 0.89 was achieved, confirming the high possibility of assessing the trees' health using remote sensing techniques. On the contrary, the freely available satellite data have a more coarse spatial resolution where pixel size is around tens of meters, which precludes analysis of individual tree-type objects (Anderson et al., 2012). Most often, multi-spectral data are obtained from the satellite level, so their spatial resolution only allows the study and monitoring of forests (Wang et al., 2010) or large forest complexes and green areas in the city (Royle and Lathrop, 1997; Laforteza and Giannico, 2019). They do not obtain accuracy at the level of individual tree crowns.

Until now, thermal infrared data (TIR) have been used primarily to study the UHI (Price, 1979; Tran et al., 2006; Majkowska et al., 2017). However, an assessment of the trees' health condition using thermal data has already been carried out, mainly in agricultural research (Maes and Steppe, 2012; Ishimwe et al., 2014; Khanal et al., 2017). The relationship that exists between the temperature of the canopy and trees' condition, which is manifested, in particular, by the discolouration of the leaves, was used in that research. Healthy trees properly carry out the evapotranspiration process, which effectively cools the surface of the leaves and the entire crown (Kimball and Bernacchi, 2006). On the other

hand, trees with discoloured leaves, which may be caused by dieback, damage or the presence of pests or diseases, have a disturbed evapotranspiration process, which causes them to heat up faster when exposed to high temperatures and solar radiation (Leuzinger and Körner, 2007).

Several studies over the years have shown the possibility of using thermal infrared data, both from satellite and airborne levels. Most often, both levels were used to study the same phenomena – e.g., the detection of damaged trees caused by the bark beetle attack was studied using both satellite data (Hais and Kučera, 2008) and aerial data (Junttila et al., (2016)). However, data obtained from the airborne level are much more popular and used, including the determination of the canopy temperatures of individual species in the natural environment (Leuzinger and Körner, 2007; Kim et al., 2016). This thermal property of trees has also been extensively used in orchard and crop studies by checking their irrigation (Zhou et al., 2021). This allows for quick and precise determination of where the cultivated trees are insufficiently irrigated.

Earlier research, which used airborne thermal data, focused on individual trees and studied the temperature of their crowns according to species (Leuzinger et al., 2010). The authors could distinguish the temperature of the individual tree crowns, set the temperature ranges for selected species and compare them with each other. The differences between the temperature ranges depended on many factors, primarily on species-specific characteristics, such as the leaves' size and arrangement, crown architecture and stomatal conductance. Another factor was the location of the tree in the study area (trees in the park were significantly cooler by 1 °C than those by the street; Leuzinger et al., 2010). The studies by Meier and Scherer (2012) also examined the thermal properties of single tree crowns of various species in spatial and temporal terms, investigating the relationship between crown temperature and air temperature. The authors pointed out that the temperature differences between crowns result from species (including leaf size), a fraction of impervious surfaces and tree locations in the field.

So far, thermal data obtained in the spectral range of 7–15 µm, referred to as Long Wave Infrared (LWIR), have been used in remote sensing vegetation studies (Marešová et al., 2020; Richter et al., 2021). In our research, we use the spectral range of 3.6–4.9 µm, referred to as Middle Wave Infrared (MWIR), which has already been used in trees' canopy temperature assessment in a natural environment (Zakrzewska et al., 2022). The present research aimed to test the possibilities of using thermal infrared data in this new spectral range obtained during the day and the night as a new data source and an effective method of trees' health assessment in the city. This approach aimed to check the usability of TIR data in trees' health assessment for a vast city area without considering other factors. The purpose of acquiring thermal data at two different dates was to check whether the condition of trees is better to distinguish in the daytime, where the influence of reflected radiation on the canopy temperature was also important. The daytime data was contrasted against nighttime data, where reflected radiation had limited impact. In this research, the Middle Wave Infrared spectral range (3.6–4.9 µm) imagery obtained from an airplane was used for the first time to assess trees' health status in an urban environment. Optimizing costs is essential for large research areas, especially urban areas with a wide variety of land cover. Economic advantages of TIR data are relatively low costs, fast data processing and ease of interpretation of results. The assumption of this research is to develop a new, alternative method of trees' health assessment with remote sensing techniques. Results obtained from TIR data would be faster and easier to implement in urban greenery management than methods based on HS data.

2. Materials and methods

2.1. Study area

The study area spanned 50 km² in the center of Warsaw, Poland (Fig. 1). The analyzed area is characterized by a wide spectrum of land

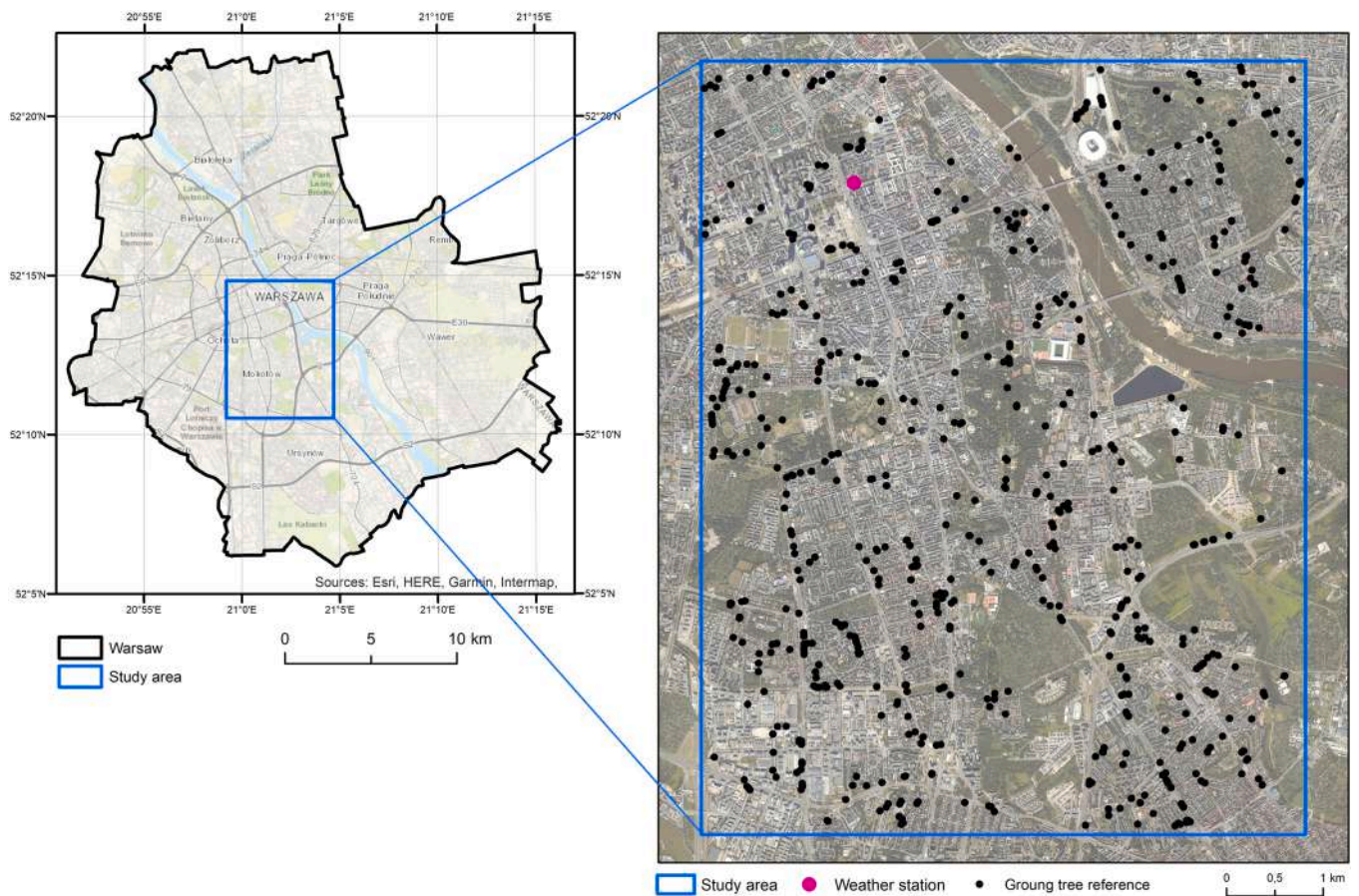


Fig. 1. Location of the study area, weather station and distribution of the ground tree reference. Basemap: orthophotomap in Red-Green-Blue (RGB) colors.

cover diversity: continuous and discontinuous dense urban fabric, industrial, commercial, public, military and private units, green urban areas, arable land, water and open spaces with little or no vegetation (Urban Atlas, 2018). The selected area was a representative part of the city in terms of surface diversity and dendroflora representation. The research was carried out in August 2020, when weather conditions were

as follows: average air temperature during the day 26.3 °C, average air temperature at night 15.1 °C, average rainfall 94.5 mm, average humidity 68% (Weather Underground, 2014–2022). August is considered one of the hottest months of the year, and also at this time, trees in poor health show their condition by leaf discoloration. The study area includes species native to Polish flora, but there are also, due to artificial

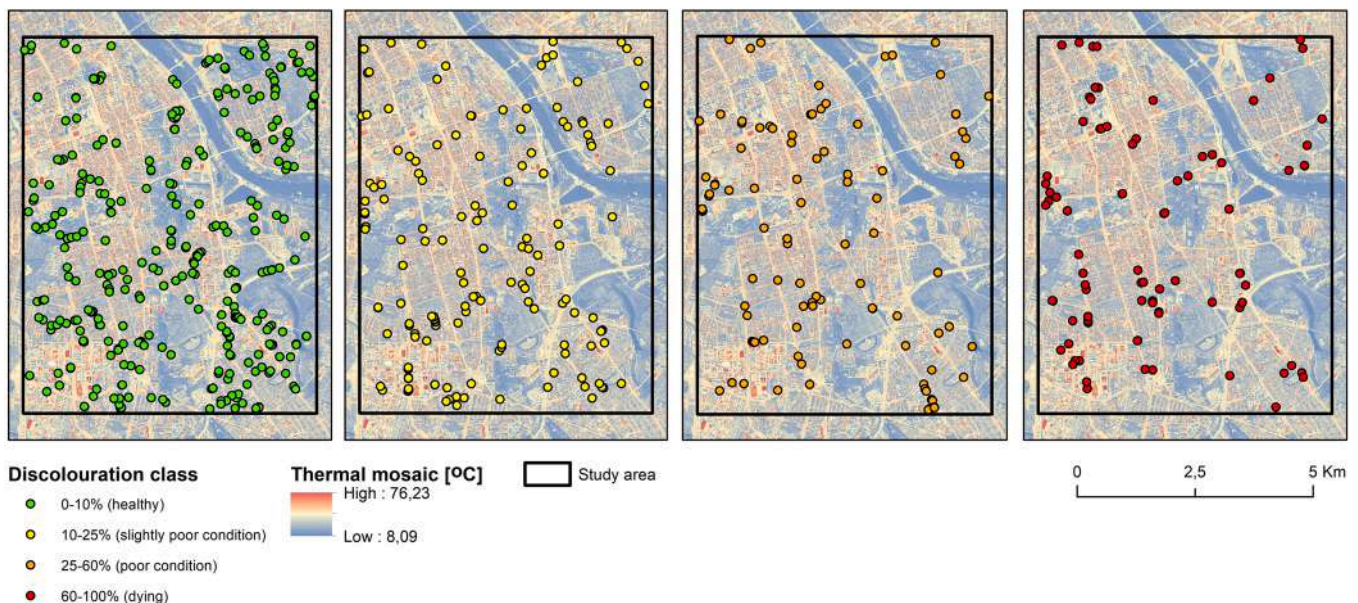


Fig. 2. Representation of discoloration classes in the study area. Basemap: Thermal infrared (TIR) obtained during the day.

plantings, species with breeding varieties, non-native and invasive non-native (Sikorska et al., 2019).

2.2. Ground reference data

On August 7–19, 2020, the reference data for 617 trees were collected synchronously with the flights. Data were collected using the MapIT application (MapIT GIS LTD, Wishaw, UK) as a point layer in GeoJSON format, where the base map was the current orthophotomap. Points were placed on tree crowns. All individuals were distributed as evenly as possible, taking into account their actual occurrence in the study area (Fig. 1). Representations of five tree species (see below) with dense crowns and not growing in the proximity of other trees were selected. In addition, the study species were characterized by their presence in different health classes in the study area, which made it possible to obtain an appropriate reference for the study (Fig. 2).

In the field, information was collected for each individual, assigning its species taxonomy and estimation of discolouration using the Hanisch and Kliz method (1990; Table 1). Leaf discolouration was considered a visual sign of a health condition. The higher the percentage of leaf discolouration in the tree crown, the worse its condition. It was necessary to use simplifications and to omit some other factors that could influence tree canopy temperature (see Discussion 4.1) during ground reference collection. Taking every such factor into account on such a large scale as the city would be impossible.

The research covered five tree species which are considered the most vulnerable to dieback in the study area: *Acer platanoides* L. (Norway maple), *Acer pseudoplatanus* L. (Sycamore maple), *Aesculus hippocastanum* L. (Horse chestnut), *Tilia cordata* Mill. (Littleleaf linden) and *Tilia × euchlora* K. Koch (Caucasian linden). Varied health conditions characterize selected species, and they are also often planted by streets. The collected ground data were divided into condition classes (Fig. 3).

2.3. Airborne data acquisition and processing

In 2020, two airborne data acquisitions were carried out. The first flight was made on the night of August 13th, when only TIR data were collected. The second flight was made on August 15th at daytime, with TIR, ALS and Red-Green-Blue data collection (RGB; Table 2).

2.3.1. Thermal Infrared

At night (August 13th, 2020), the air temperature was 17.22 °C, the relative humidity was 63%, and the wind speed did not exceed 0.89 m/s. During the daytime data acquisition (August 15th, 2020), the air temperature was 27.22 °C, the relative humidity was 34%, and the wind speed did not exceed 4.02 m/s. In both cases, weather conditions were necessary to obtain thermal data. These conditions included 0% cloud cover, no rainfall for at least three days, weak gusts of wind and general weather conditions that did not differ from the average for similar periods in the previous few years. In addition, the data from the day collection were obtained at noon, which reduced the influence of the shadows formed inside the tree crowns on the recorded temperature.

Data from the day and the night collection were acquired using the

Table 1

Assessment of the discolouration degree of the tree canopies prepared on the basis of the Hanisch and Kliz method (1990) and its division on condition classes.

Discolouration class	Degree of leaf discolouration in the tree canopy	Condition class
1	No discolouration: 0–10%	healthy
2	Slight discolouration: 10–25%	slightly poor condition
3	Moderate discolouration: 25–60%	poor condition
4	Severe discolouration or dead tree: 60–100%	dying

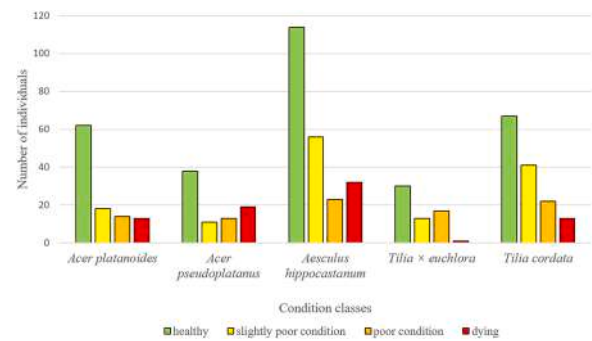


Fig. 3. The number of individuals in specific condition classes by species.

Table 2

Parameters of both collections. Abbreviations: AGL - Above Ground Level; TIR - Thermal Infrared; ALS - Airborne Laser Scanning; RGB - Red-Green-Blue camera.

Date of Flight	Hour of Flight	Aircraft	Flight Level [m]	Flight Airspeed	Data Type
13/08/2020	00:25–01:10	Partenavia P.68 Observer 2 (SP-FPM)	2460 AGL	120 [m/s]	TIR
15/08/2020	12:21–13:06	Partenavia P.68 Observer 2 (SP-FPM)	2460 AGL	120 [m/s]	TIR, ALS, RGB

ImageIR 9400 infrared camera by InfraTec GmbH (Dresden, Germany), which records in Middle Wave Infrared (3.6–4.9 μm) spectral range. During both collections, two types of on-ground measurements were taken synchronously to the collections: (1) with a Fluke 62 MAX pyrometer (spectral response 8–14 μm), the temperature of various types of substrate (asphalt, cobblestones, bushes, lawn) were measured and used for radiometric correction of airborne data; (2) the Weather Underground station recorded weather conditions, located in the study area (Fig. 1). The purpose of these measurements was to perform atmospheric correction and process thermal data.

The raw thermal data were checked for completeness and correctness of registration by comparing them with the measurements obtained from the meteorological station and the pyrometer in IRBIS Professional v.3.1. software (InfraTec GmbH, Dresden, Germany). Additionally, in this software, an atmospheric correction was made by the atmospheric transmittance model using ambient temperature and relative humidity (recorded during data acquisition), and flight altitude was taken into account (Minkina and Dudzik, 2009). Based on the literature reports, the average emissivity was determined as $\epsilon = 0.95$ (Ullah et al., 2012). One emissivity value was used because only a selected canopy of deciduous trees was examined, in which emissivity is very similar to each other. At the stage of geometric correction of thermal data, aerotriangulation was performed based on control points obtained from RGB orthomosaics in the Inpho Match-AT software (Trimble Inc., Sunnyvale, CA, USA). Thermal orthoimages were adjusted to the ALS data from the synchronous collection in Inpho OrthoMaster software (Trimble Inc., Sunnyvale, CA, USA). As a result, the thermal data and Canopy Height Model (CHM) created from the ALS were aligned. The orthoimages were combined into a thermal orthomosaic with a pixel size of 1 m for each collection in the automatic mosaic process in Inpho Orthovista software (Trimble Inc., Sunnyvale, CA, USA). Thermal orthomosaics were used to determine the canopy temperature of individual trees. The last stage of processing was to check the geometric and radiometric accuracy separately for each collection.

2.3.2. Airborne laser scanning

ALS data were acquired only during the day collection using a Riegl

VQ-780i scanner with a density of 4 pts/m². Data obtained from ALS were used to create CHM and to determine the Gap Fraction parameter. The raw ALS data were preprocessed in the RiProcess software (RIEGL Laser Measurement Systems GmbH, Horn, Austria). They were aligned and fitted with an accuracy of 0.1 m. The final step involved the point cloud classification conducted in the TerraScan software of the TerraSolid package (Terrasolid Ltd., Espoo, Finland).

Based on the generated point cloud, a CHM with a pixel size of 1 m resolution was created. CHM was used to adjust TIR and ALS data to each other by orthorectification. After that, the CHM was used to manually delineate canopy extents for trees recorded in the field.

ALS data were also used for creating a Gap Fraction map (Maltamo et al., 2014). The Gap Fraction indicates the rate of laser ray penetration through the canopy in relation to a spatial unit. The pixels in the Gap Fraction map have values from 0.0 for complete branching (laser beam absorbed by the canopy) to 1 in open areas (laser beam reaches the ground) (Danson et al., 2007). Gap Fraction allows for the rejection of pixels that most likely correspond to those parts of the tree crown which may be affected by the substrate due to their loose structure. Usage of this parameter allows removal of the analysis pixels from the mosaic of thermal data, which recorded the temperature of the tree crown and the ground beneath.

2.3.3. RGB data

RGB data were obtained only during the day collection using the PhaseOne IXM-100 camera with a spectral range of 0.4–0.7 µm and pixel size of 0.13 m. Furthermore, the obtained orthophotomap was used to visually verify the collected field data and as a base map for the figures. The source RGB images were processed in CaptureOne software (CaptureOne, Frederiksberg, Denmark). The geometrical accuracy of the orthophotomap was 0.2 m.

2.4. Data processing and statistical analysis

The purpose of the statistical analysis was to calculate the temperature of tree canopies precisely. For 617 ground reference points, an Individual Tree Canopy (ITC) extent was created as a vector layer, which was used to assess the mean temperature of tree canopies (Fig. 4). ITC was created in three steps which follow one another. In the first step, 617 tree canopies were manually delineated by photointerpretation of CHM (Fig. 4B). Then, a 1-meter inside buffer was used to exclude mixed pixels from further analysis (Fig. 4C). These pixels could potentially include a temperature of the ground, which could influence the whole mean canopy temperature. In the last step, a Gap Fraction map was applied to eliminate pixels with values higher than 0.5 (Fig. 4D). During this process, pixels that registered the ground temperature, because of the loose canopy parts, were excluded. After these three steps of processing, the final extent of ITC was ready to proceed.

For each ITC, zonal statistics (mean, standard deviation, minimum and maximum value, 5th and 95th percentile) were calculated from the thermal mosaics of daytime and nighttime data collections. Statistical calculations were made in ArcGIS 10.8.1 software (ESRI, Redlands, CA, USA). The data prepared in this way was then subjected to statistical

analysis.

To obtain reliable results, data randomization was performed. Using a stratified random sampling method (Acharya et al., 2013), in 30 subsampling randomizations, 50 trees from each condition class, out of 617 tree points, were selected for every randomization. Further, the mean values of all 30 randomizations were used to present the research results (Fig. 5).

In the statistical analysis stage, the sampling results from the previous stage were used to study differences between class conditions. Data were checked to see if they had a normal distribution. Then, the ANOVA and post-hoc Tukey's tests were used to determine the temperature differences between health condition classes. Data obtained during the day and the night were analyzed separately. The data set prepared was analyzed to answer the research question. All statistical calculations were performed in Statistica 13 software (TIBCO Inc., Palo Alto, CA, USA).

3. Results

3.1. Canopy temperatures at night as an indicator of trees' health condition

The ground reference and the night thermal mosaic were analyzed per the workflow (Fig. 5). The mean temperature of tree canopies acquired at night systematically increased (from 14.49 °C to 15.55 °C) when trees' condition declined and reached a difference of 1.06 °C between healthy and dying trees (Table 3). There is also a noticeable relationship in that the higher the leaf discoloration, the higher values of standard deviation inside ITC. The class with the highest value in the 'range of condition class' (a difference between the coolest and the hottest tree canopy in a class) was dying trees (1.83 °C; Table 3). The same relationship of systematically increased values was noticeable in the minimum and maximum temperature registered in the individual canopies. In individual canopies, the differences between healthy and dying trees in minimum temperature were 0.81 °C, and in maximum temperature, 1.21 °C. The same relation was observed in the 5th percentile and 95th percentile, with 0.98 °C and 1.21 °C differences, respectively, between the two extreme classes (Table 3).

The ANOVA test confirmed statistically significant differences in canopy temperatures between the condition classes ($p < 0001$). After the analysis of variance, statistical differences in mean, 5th and 95th percentiles, between condition classes were checked (Fig. 6). Only the healthy trees class created a separate, significantly distinguishable group and was possible to distinguish on the thermal data mosaic. Trees in slightly poor condition, in poor condition and dying mixed with each other and formed three overlapping post-hoc groups. The best differentiation results were observed for the mean tree canopy temperatures and for the 95th percentile (Fig. 6), where trees in slightly poor condition mixed with poor condition class, and poor condition class mixed with dying trees. The dying trees class is the most statistically different group after the healthy trees class. For other statistics – e.g., the 5th percentile (Fig. 6) – trees in slightly poor condition, in poor condition and dying formed one post-hoc group.

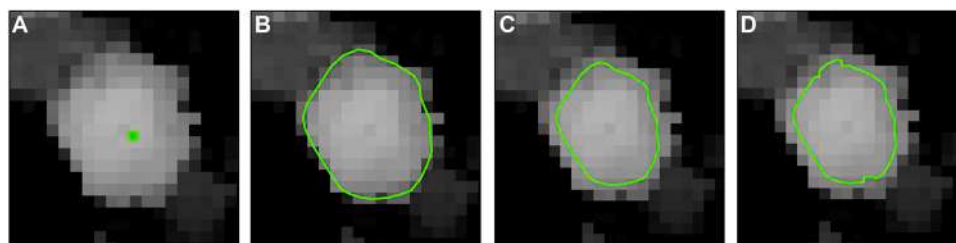


Fig. 4. Example of the Individual Tree Canopy (ITC) extents. A – tree point from ground reference data; B – polygon extent delineated manually based on Canopy Height Model; C – polygon reduced by 1 m buffer; D – polygon reduced by Gap Fraction higher than 0.5. Basemap: Canopy Height Model.

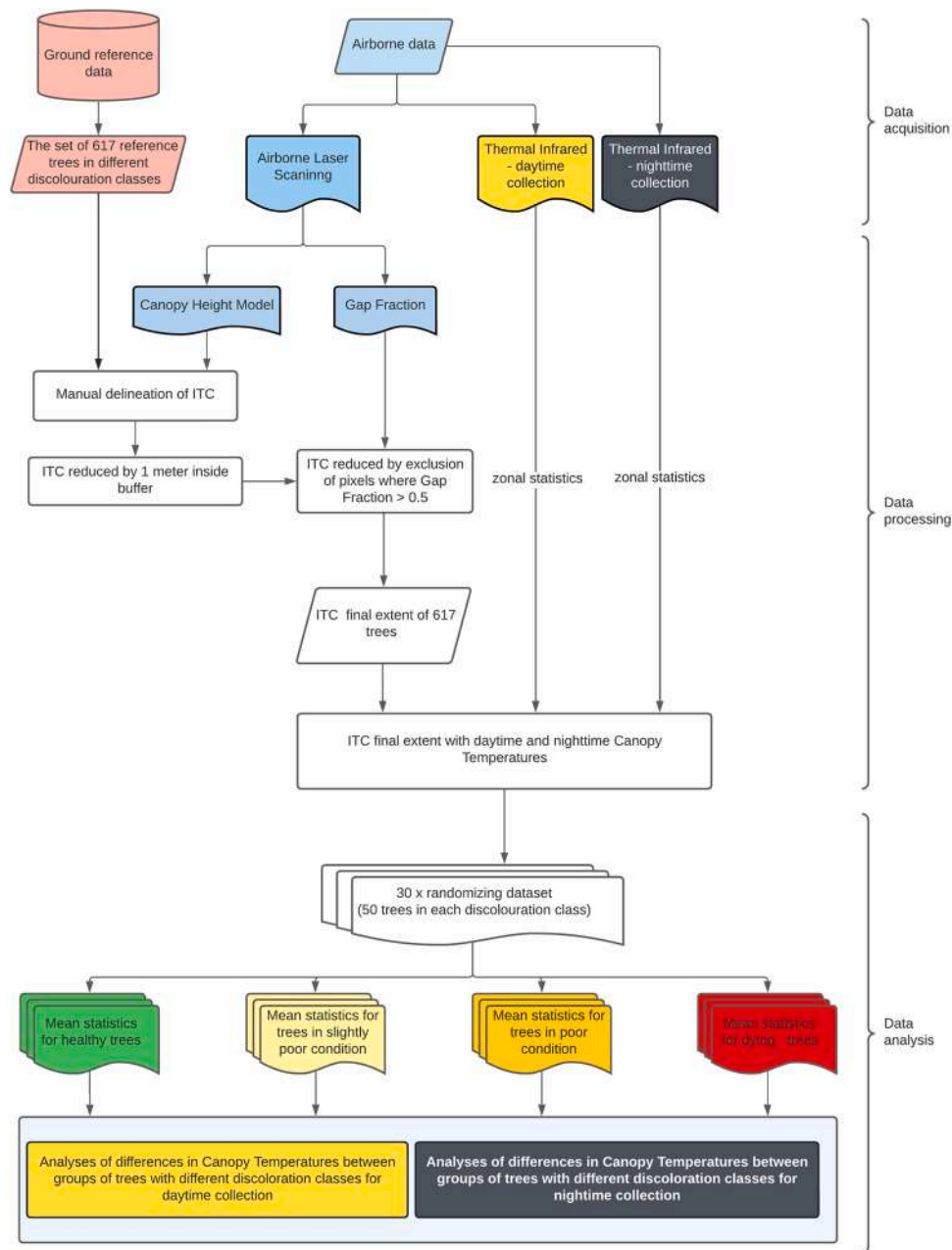


Fig. 5. Workflow of data processing. Creating Individual Tree Canopies (ITC) extent and assessment of canopy temperatures for discoloration classes.

Table 3

Zonal statistics obtained from 30 randomizing data sets for nighttime data divided into condition classes. ITC - Individual Tree Canopy.

Condition class	Mean pixel count for ITC extents	Mean canopy temperature for ITC extents [°C]	Mean standard deviation for ITC extents [°C]	Mean minimum pixel value for ITC extents [°C]	Mean 5th percentile of temperature for ITC extents [°C]	Mean 95th percentile of temperature for ITC extents [°C]	Mean maximum pixel value for ITC extents [°C]	Range of condition class [°C]
healthy	33	14.49	0.21	14.11	14.35	14.66	14.98	0.87
slightly poor condition	30	15.10	0.25	14.70	14.96	15.30	15.73	1.03
poor condition	26	15.41	0.34	14.90	15.12	15.56	16.23	1.33
dying	27	15.55	0.47	14.92	15.33	15.87	16.75	1.83

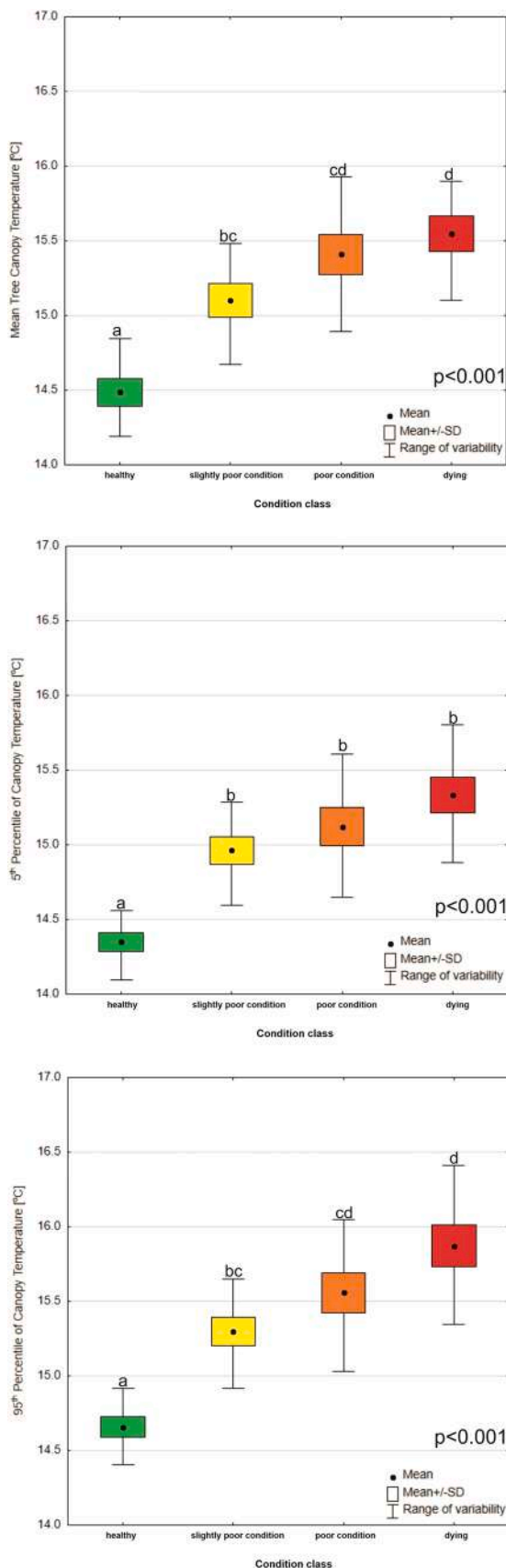


Fig. 6. Mean Canopy Temperatures, 5th percentile and 95th percentile with condition classes division for nighttime data. Letters (above the whiskers) represent Tukey's post-hoc groups.

3.2. Canopy temperatures in the day as an indicator of trees' health condition

The daytime mosaic thermal data and ground reference were analyzed the same way and on the same trees as the nighttime data with the same workflow (Fig. 5). The mean temperature of tree canopies increased with the degree of leaf discolouration from 25.31 °C to 28.59 °C. The greatest difference between the extreme classes (healthy and dying trees) was 3.28 °C (Table 4). The same relation as in nighttime data was in standard deviation in ITC and the range of the whole condition class. The largest value in 'range of condition class' was recorded in the dying trees class (above 7 °C; Table 4). In the same class, the mean standard deviation in single canopies had the highest value of 1.93 °C. Also, the minimum and maximum values of the pixels inside the canopy observed a gradual increase in temperature. Differences between extreme classes were 2.81 °C and 4.92 °C for minimum and maximum temperatures, respectively. Also, the same relation was observed for the 5th and 95th percentiles, where the differences between healthy and dying tree classes were, respectively, 2.89 °C and 3.56 °C (Table 4).

The analysis of the variance test confirmed statistically significant differences between the condition classes for the data obtained in the daytime collection ($p < 0001$). After analysis of variance, in Tukey's test for equal groups, the existence of statistically significant differences between all four condition classes was confirmed, dividing them into four post-hoc groups (Fig. 7). Statistical differences in mean, for 5th and 95th percentiles and between condition classes, were checked. In the mean for 5th and 95th percentiles of tree canopy temperatures, all condition classes were separated by the mean and standard deviation box (Fig. 7), which is not as clearly visible in nighttime statistics (Fig. 6).

4. Discussion

4.1. Differences in the canopy temperatures depending on trees condition class

This research shows that high-resolution thermal data made it possible to study the trees' health condition in an urban environment by analyzing their canopy temperatures. Our research showed a statistically significant difference in canopy temperatures between condition classes of tree groups, both in the daytime and nighttime data collection (Figs. 6 and 7).

Trees with a high degree of leaf discolouration heat up faster and more intensively due to the disturbed evapotranspiration process (Kimball and Bernacchi, 2006). According to this thesis, trees with a high percentage of discoloured leaves in their crowns have higher canopy temperatures. Our research confirms it was possible to register statistically significant differences in the canopy temperatures between groups of trees with varying degrees of leaf discolouration. In addition, Wakiyama (2002) also proved the influence of the chlorophyll content in leaves (and therefore the leaf color) on their temperature. Leaves with high chlorophyll content were 0.85 °C cooler than leaves with low chlorophyll content (Wakiyama, 2002). Our research confirmed the relationship between the degree of leaf discolouration and the canopy temperature of trees using remote sensing methods. Thus, it was possible to demonstrate this relationship in TIR data (both on daytime and nighttime data collections) and connect it with trees' health status. This concludes that the canopy temperature may be one of the indicators of health condition. The methodology developed during this study is a new way of using TIR data to study the health condition of trees in an urban environment. The novelty is not only the way of using the data, but also the spectral range itself, where most of the research is still carried out in the LWIR.

Low canopy temperatures and also smaller differences between health condition classes were observed in the nighttime data (Fig. 6). Dead leaves likely increase the tree's ability to store heat during the day and reduce the rate of heat loss during the night (Smith, 1979). Airborne

Table 4

Zonal statistics obtained from 30 randomizing data sets for daytime data divided into condition classes. ITC - Individual Tree Canopy.

Condition class	Mean pixel count for ITC extents	Mean canopy temperature for ITC extents [°C]	Mean standard deviation for ITC extents [°C]	Mean minimum pixel value for ITC extents [°C]	Mean 5th percentile of temperature for ITC extents [°C]	Mean 95th percentile of temperature for ITC extents [°C]	Mean maximum pixel value for ITC extents [°C]	Range of condition class [°C]
healthy	33	25.31	1.32	23.01	24.75	26.06	28.03	5.01
slightly poor condition	30	26.40	1.46	24.13	25.61	27.06	29.64	5.51
poor condition	26	27.03	1.54	24.75	26.24	27.86	30.41	5.65
dying	27	28.59	1.93	25.82	27.64	29.62	32.95	7.13

data was acquired four hours after sunset. Perhaps the data obtained earlier in relation to the sunset would be of greater value, because trees still retain more heat accumulated during the day. Bigger differences between discolouration classes were observed in daytime data (Fig. 7). Sunlight is a natural source of thermal contrast enhancement in various objects (Maldague et al., 2001; Crisóstomo and Pitarma, 2019). As a result, the crowns heat up more, especially the parts of the crowns with discoloured leaves. This enhances the contrast between healthy and discoloured leaves, which was reflected in the higher canopy temperatures of dying trees. It can lead to the conclusion that the cooling effect is not equal for trees of the same species. Healthy trees cope much better with the dynamic urban environment. Also, their cooling effect is stronger, which is manifested in UHI mitigation. Trees in poor condition have a limited impact on microclimate because of their disturbed evapotranspiration process.

When analyzing both collections (nighttime and daytime), the same relationships between health condition classes were noticed in the analyzed zonal statistics. Analyzing the data obtained at night, it is apparent that the higher the discolouration class, the higher the mean standard deviation inside the ITC and the higher range of the temperature within a given class. Particularly the highest standard deviation and the range were obtained for the dead and dying trees class (the mean standard deviation for ITC extents was 0.47 °C, and for the range 1.83 °C). The reason for this may be that some trees had unevenly distributed leaf discolouration in the canopy. This may be one of the main reasons for the increasing values of standard deviations for ITC extent in the higher discolouration classes, where discoloured leaves cooled more slowly than healthy leaves (Table 3). This also may be a reason for high temperature ranges between tree canopies in the same condition group. From the data obtained during the day, the largest range in the temperature difference of the tree canopies was recorded in the class of dying trees (over 7 °C), and the mean standard deviation for ITC extents was 1.93 °C. This may be due to larger proportions of discoloured leaves (60–100%) than in other groups, like healthy trees (0–10%).

The result of our research is the confirmation that the canopy temperature obtained from the airborne level can be an indicator of the health condition of trees in the city. The canopy temperatures recorded during the day allow for the determination of four condition classes of trees. This method still needs to be combined with VTA, but this research opens up new possibilities for applying TIR data and broadens the knowledge around tree temperatures. Also, this method could be used for regular tree monitoring if the acquisition of aerial thermal data were to be repeated in similar weather conditions.

The discolouration of the leaves is the factor that affects the temperature of individual tree crowns. We were aware that numerous other factors could significantly influence canopy temperature. The first factor, for example, is species taxonomy and what is associated with it – leaf size and stomatal conductance (Meier and Scherer, 2012). During the day, the shape and size of the leaves contribute to heat loss through convection (Vogel, 2009). A feature specific to each species is also the effect of heat transfer between the leaf and the atmosphere (Schuepp,

1993). Other factors include ground under the tree crown, when trees with impermeable surfaces have higher canopy temperatures due to upward long-wave radiation from fabricated surfaces (Mueller and Day, 2005; Meier and Scherer, 2012). The immediate surroundings and the location of the tree in the study area (park or street) also influence the canopy temperature (Melaas et al., 2016), as well as the branch spread and the crown architecture (Zheng et al., 2018). Other factors potentially affecting the canopy temperature are pests and fungi (Smigaj et al., 2019), which may be found frequently in an urban environment. All the factors mentioned above influence the crown temperature, whether the data is acquired during the day or at night. The last factor is the effect of a building's shadow cast on the tree canopy, which effectively lowers their temperature during the day (Meier et al., 2010). It remained possible to distinguish classes of health conditions on the thermal data obtained during the day without taking these factors into account.

4.2. Benefits of using thermal infrared data and their further development

The usage of thermal infrared data is becoming more popular in vegetation research, as evidenced by their wide application in agriculture (Sobrino et al., 1990) and urban studies (Lee (1993); Lo et al., 1997; Sobrino et al., 2013; Spronken-Smith and Oke, 1998; Dimoudi and Nikolopoulou, 2003). The results of our research prove the effectiveness of estimating the health condition of trees from an airborne level, particularly on data obtained during the day (Fig. 7).

It is worth researching and developing TIR methods, because they can support the detection of unhealthy trees. VTA methods cannot be fully replaced by TIR data alone. However, this method can be used as a systematic check of trees' health condition, as a new type of urban greenery monitoring. It can be used in two ways. The first way is regular health monitoring of trees already marked in the area. The second way is as a potential selection of ITC from obtained thermal data characterized by high canopy temperature. Those trees may be in the high stage of leaf discolouration, and such trees should then be checked in the field with the VTA method to confirm their condition.

VTA methods do not allow for quick and repetitive research for millions of trees in the city area. Our method can improve the process of detecting damaged trees by choosing selected trees that are probably in poor condition. The method presented in this research selects trees that need to be controlled in the first place. Frequent controls of trees are necessary in an urban environment. Dynamic changes of microclimate in cities are enhanced by global climate change. This influences the health condition of trees and leads to their faster dieback (Tubby and Webber, 2010).

Depending on the needs of urban greenery management, data can be obtained at night or during the day. Acquiring data at night may be more accessible due to limited air traffic, which can be high in urban areas during the day. However, the quality of night data makes it possible to distinguish only two classes: healthy trees and trees dying or in poor condition (Fig. 5). If the city management requires higher quality, the data would have to be obtained during the day as well. Additionally, when collecting data during the day, other types of data such as RGB or

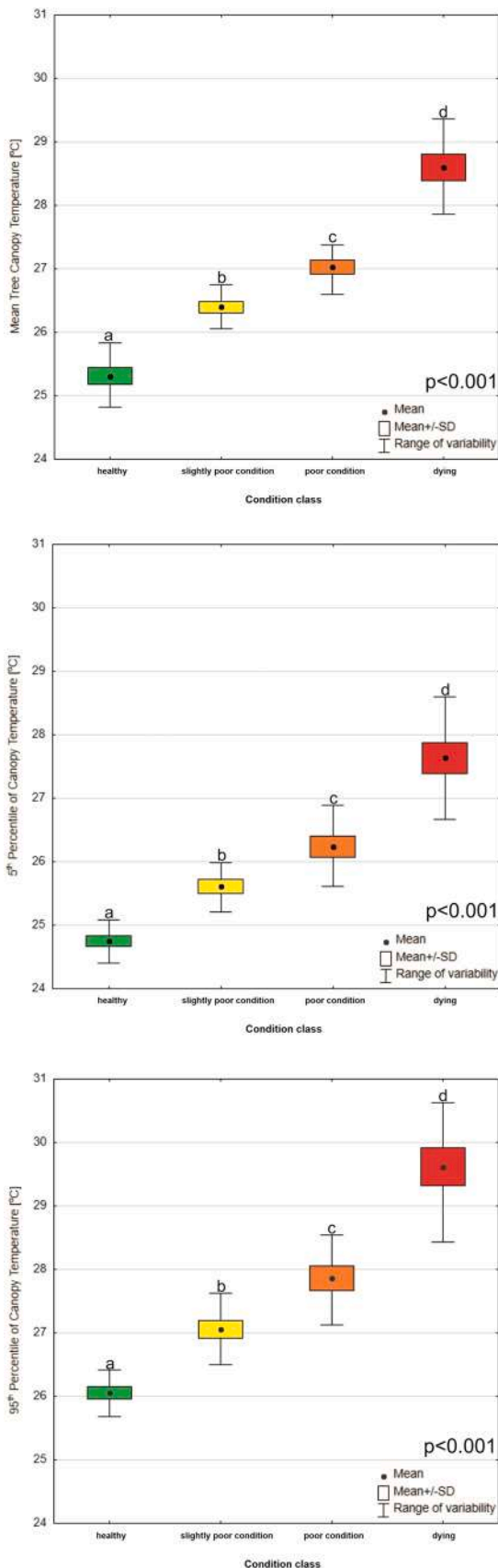


Fig. 7. Mean canopy temperatures, 5th percentile and 95th percentile with condition classes division for daytime data. Letters (above the whiskers) represent Tukey’s post-hoc groups.

HS can be synchronously obtained.

In our research, it was necessary to use data fusion (TIR, ALS) to extract ITC and assign the mean temperatures (Table 2). The advantage of this fusion was to automatically establish the boundaries of tree crowns and remove pixels that may have registered the temperature of the background or objects next to the canopy (Fig. 4). The developed method presents the possibility of using TIR data to determine the health condition of trees in an urban environment. TIR can be used to create a universal method for detecting unhealthy trees in a city based on the recorded canopy temperature alone. Not without reason, it did not include the division into species or location in the study area. Limiting the number of factors influencing the canopy temperature serves the speed of the reference data collection. Examining all species simultaneously made it possible to distinguish overall unhealthy trees. The most important advantage of TIR data over others, such as HS data, is the speed of the processing, analysis and interpretation of results. One of the products of TIR data is a temperature distribution map which can be easily understood and interpreted. Other studies that focused on estimating trees’ health status in a city using HS data also divide conditions into four classes (no damage, warning, slight to moderate damage and severe damage; Jarocińska et al., 2018). Comparing authors’ results with ours, both TIR and HS data gave similar results; therefore, it is possible to use them interchangeably depending on the user’s needs. Fusing these data may be an opportunity to create a new tree health monitoring system in cities.

There are several limitations of the method used, particularly related to the acquisition of thermal data. The first limitation is the dependence of the recorded canopy temperature on weather conditions (Moran et al., 1994). It was important, in this case, not to study the strictly recorded temperature of the canopy (which changes easily depending on the air temperature and air humidity), but the temperature differences between health conditions classes. This approach was also used to study the differences in canopy temperature among trees (Zakrzewska et al., 2022). The second limitation is the resolution with which thermal data are obtained. Taking into account the purpose of our method, it is impossible to use satellite data to study the health condition of ITC where the pixel of thermal data – obtained, for example, from the Landsat-8 satellite – has a size of 100 m (Anderson et al., 2012). Even after sharpening transformation up to 30 m of pixel size, it is still impossible to assess one single tree’s health condition (Anderson et al., 2004). This method could be used from data obtained from the UAV level, but it is spatially limited to only small parts of the cities. UAV can be a particularly useful method in the study of city parks, where the size of the park allows its entirety to be registered in a short period. Using the VTA method (performed from the ground level) is difficult when assessing discolouration in upper parts of a canopy, because of the height and density of trees.

It is still possible to improve the developed tree health assessment method based on the fusion of TIR and ALS data by testing it and comparing it with another data fusion (e.g., HS and ALS). Further improvement methods could include using another type of cameras with different spectral ranges (e.g., LWIR cameras) or obtaining data from different sensors (aircraft and UAV). This should be a priority in the next research if the aim is to develop monitoring of urban greenery based on thermal remote sensing methods.

5. Conclusions

The conclusion of our research is that thermal infrared data with a 3.6–4.9 μm spectral range obtained from the airborne level can be an indicator of the trees’ health condition in an urban environment. Based on the obtained result, the conclusions are as follows:

- (i) Statistically significant differences between different health conditions were proved on nighttime and daytime data

collections. Canopies of healthy trees were cooler than canopies of dying trees on both thermal mosaics;

- (ii) The difference in canopy temperature between healthy and dying trees was 3.28 °C during the day. The difference in canopy temperatures between these classes obtained from the nighttime data was 1.06 °C;
- (iii) Analyzing the data obtained at night, only the group of healthy trees was distinguished on the thermal data mosaic and formed a separate group. On daytime data, canopy temperatures between all condition classes were statistically significantly different;

In conclusion, only data obtained during the day may be used as an indicator to differentiate four health condition classes of deciduous trees. Nighttime data can be used to differentiate healthy trees from unhealthy trees but with less detail for unhealthy trees. Taking into account these guidelines, it is possible to create a new method of assessing the health condition of trees by their canopy temperature, only considering the degree of leaf discoloration.

CRedit authorship contribution statement

Agata Zakrzewska: Investigation, Resources, Visualization, Formal analysis, Writing – original draft. **Dominik Kopec:** Supervision, Conceptualization, Writing – review & editing. **Adrian Ochtyra:** Supervision, Writing – review & editing. **Markéta Potůčková:** Writing – review & editing.

Declaration of Competing Interest

The authors declare that they have no known competing financial interests or personal relationships that could have appeared to influence the work reported in this paper.

Acknowledgments

This work was supported by the European Union from the European Social Fund under the “InterDOC-START” project POWR.03.02.00–00–I033/16–00. We would like to thank MGGP Aero Sp. z o.o. for providing the remote sensing data used in the publication.

References

- Acharya, A.S., Prakash, A., Saxena, P., Nigam, A., 2013. Sampling: Why and how of it. *Indian Journal of Medical Specialties* 4(2), 330–333.
- Alonzo, M., McFadden, J.P., Nowak, D.J., Roberts, D.A., 2016. Mapping urban forest structure and function using hyperspectral imagery and lidar data. *Urban. For. Urban. Green.* 17, 135–147. <https://doi.org/10.1016/j.ufug.2016.04.003>.
- [3] Anderson, M.C., Norman, J.M., Mecikalski, J.R., Torn, R.D., Kustas, W.P., Basara, J. B., 2004. A multiscale remote sensing model for disaggregating regional fluxes to micrometeorological scales. *J. Hydrometeorol.* 5 (2), 343–363. [https://doi.org/10.1175/1525-7541\(2004\)005<0343:AMRSMF>2.0.CO;2](https://doi.org/10.1175/1525-7541(2004)005<0343:AMRSMF>2.0.CO;2).
- Anderson, M.C., Allen, R.G., Morse, A., Kustas, W.P., 2012. Use of Landsat thermal imagery in monitoring evapotranspiration and managing water resources. *Remote Sens. Environ.* 122, 50–65. <https://doi.org/10.1016/j.rse.2011.08.025>.
- Ball, D., 2011. *Common Sense Risk Management of Trees: Guidance on Trees and Public Safety in the UK for Owners, Managers and Advisers.* Forestry Commission, Edinburgh.
- Berrang, P., Karnosky, D.F., Stanton, B.J., 1985. Environmental factors affecting tree health in New York City. *J. Arboric.* 11 (6), 185–189.
- Burley, B.A., 2018. Green infrastructure and violence: Do new street trees mitigate violent crime. *Health Place* 54, 43–49. <https://doi.org/10.1016/j.healthplace.2018.08.015>.
- Chi, D., Degerickx, J., Yu, K., Somers, B., 2020. Urban tree health classification across tree species by combining airborne laser scanning and imaging spectroscopy. *Remote Sens.* 12 (15), 2435. <https://doi.org/10.3390/rs12152435>.
- Chen, Y., Chen, W.Y., Giannico, V., Laforteza, R., 2022. Modelling inter-pixel spatial variation of surface urban heat island intensity. *Landsc. Ecol.* 37 (8), 2179–2194. <https://doi.org/10.1007/s10980-022-01464-2>.
- Crisóstomo, J., Pitarna, R., 2019. The importance of emissivity on monitoring and conservation of wooden structures using infrared thermography. In: Hassan, M.H.M. (Ed.), *Advances in Structural Health Monitoring.* IntechOpen, London, p. 16.
- Dale, A.G., Youngsteadt, E., Frank, S.D., 2016. Forecasting the effects of heat and pests on urban trees: impervious surface thresholds and the ‘pace-to-plant’ technique. *Arboric. Urban* 42 (3), 181–191.
- Danson, F.M., Hetherington, D., Morsdorf, F., Koetz, B., Allgower, B., 2007. Forest canopy gap fraction from terrestrial laser scanning. *IEEE Geosci. Remote. Sens. Lett.* 4 (1), 157–160. <https://doi.org/10.1109/LGRS.2006.887064>.
- Degerickx, J., Roberts, D.A., McFadden, J.P., Hermy, M., Somers, B., 2018. Urban tree health assessment using airborne hyperspectral and LiDAR imagery. *Int. J. Appl. Earth Obs. Geoinf.* 73, 26–38. <https://doi.org/10.1016/j.jag.2018.05.021>.
- Delegido, J., Van Wittenberghe, S., Verrelst, J., Ortiz, V., Veroustraete, F., Valcke, R., Samson, R., Rivera, J.P., Tenjo, C., Moreno, J., 2014. Chlorophyll content mapping of urban vegetation in the city of Valencia based on the hyperspectral NAOC index. *Ecol. Indic.* 40, 34–42. <https://doi.org/10.1016/j.ecolind.2014.01.002>.
- Dimoudi, A., Nikolopoulou, M., 2003. Vegetation in the urban environment: microclimatic analysis and benefits. *Energy Build.* 35 (1), 69–76. [https://doi.org/10.1016/S0378-7788\(02\)00081-6](https://doi.org/10.1016/S0378-7788(02)00081-6).
- Hais, M., Kučera, T., 2008. Surface temperature change of spruce forest as a result of bark beetle attack: remote sensing and GIS approach. *Eur. J. For. Res.* 127 (4), 327–336. <https://doi.org/10.1007/s10342-008-0208-8>.
- Hanisch, B., Kitz, E., 1990. *Monitoring of Forest Damage: Spruce and Pine.* Verlag Eugen Ulmer, Stuttgart.
- Ishimwe, R., Abutaleb, K., Ahmed, F., 2014. Applications of thermal imaging in agriculture—A review. *Adv. Remote Sens.* 3 (3), 128. <https://doi.org/10.4236/ars.2014.33011>.
- Jarocińska, A., Białczak, M., Stawik, Ł., 2018. Application of aerial hyperspectral images in monitoring tree biophysical parameters in urban areas. *Misc. Geogr.* 22 (1), 56–62. <https://doi.org/10.1515/mgrsd-2017-0034>.
- Jenerette, G.D., Harlan, S.L., Brazel, A., Jones, N., Larsen, L., Stefanov, W.L., 2007. Regional relationships between surface temperature, vegetation, and human settlement in a rapidly urbanizing ecosystem. *Landsc. Ecol.* 22, 353–365. <https://doi.org/10.1007/s10980-006-9032-z>.
- Jensen, R.R., Hardin, P.J., Hardin, A.J., 2012. Classification of urban tree species using hyperspectral imagery. *Geocarto Int* 27 (5), 443–458. <https://doi.org/10.1080/10106049.2011.638989>.
- Junttila, S., Vastaranta, M., Hämäläinen, J., Latva-Käyrä, P., Holopainen, M., Hernández Clemente, R., Hyypä, H., Navarro-Cerrillo, R.M., 2016. Effect of forest structure and health on the relative surface temperature captured by airborne thermal imagery—Case study in Norway Spruce-dominated stands in Southern Finland. *Scand. J. For. Res.* 32 (2), 154–165. <https://doi.org/10.1080/02827581.2016.1207800>.
- Khanal, S., Fulton, J., Shearer, S., 2017. An overview of current and potential applications of thermal remote sensing in precision agriculture. *Comput. Electron. Agric.* 139, 22–32. <https://doi.org/10.1016/j.compag.2017.05.001>.
- Kim, Y., Still, C.J., Hanson, C.V., Kwon, H., Greer, B.T., Law, B.E., 2016. Canopy skin temperature variations in relation to climate, soil temperature, and carbon flux at a ponderosa pine forest in central Oregon. *Agric. For. Meteorol.* 226, 161–173. <https://doi.org/10.1016/j.agrformet.2016.06.001>.
- Kimball, B.A., Bernacchi, C.J., 2006. Evapotranspiration, canopy temperature, and plant water relations. *Managed Ecosystems and CO₂.* Springer-Verlag, Berlin, pp. 311–324. https://doi.org/10.1007/3-540-31237-4_17.
- Kong, F., Yan, W., Zheng, G., Yin, H., Cavan, G., Zhan, W., Zhang, L., 2016. Retrieval of three-dimensional tree canopy and shade using terrestrial laser scanning (TLS) data to analyze the cooling effect of vegetation. *Agric. For. Meteorol.* 217, 22–34. <https://doi.org/10.1016/j.agrformet.2015.11.005>.
- Laforteza, R., Giannico, V., 2019. Combining high-resolution images and LiDAR data to model ecosystem services perception in compact urban systems. *Ecol. Indic.* 96, 87–98. <https://doi.org/10.1016/j.ecolind.2017.05.014>.
- Lee, H.Y., 1993. An application of NOAA AVHRR thermal data to the study of urban heat islands. *Atmos. Environ. Part B. Urban Atmos.* 27 (1), 1–13. [https://doi.org/10.1016/0957-1272\(93\)90041-4](https://doi.org/10.1016/0957-1272(93)90041-4).
- Leuzinger, S., Körner, C., 2007. Tree species diversity affects canopy leaf temperatures in a mature temperate forest. *Agric. For. Meteorol.* 146 (1–2), 29–37. <https://doi.org/10.1016/j.agrformet.2007.05.007>.
- Leuzinger, S., Vogt, R., Körner, C., 2010. Tree surface temperature in an urban environment. *Agric. For. Meteorol.* 150 (1), 56–62. <https://doi.org/10.1016/j.agrformet.2009.08.006>.
- Lo, C.P., Quattrochi, D.A., Luvall, J.C., 1997. Application of high-resolution thermal infrared remote sensing and GIS to assess the urban heat island effect. *Int. J. Remote Sens.* 18 (2), 287–304. <https://doi.org/10.1080/014311697219079>.
- Maes, W.H., Steppe, K., 2012. Estimating evapotranspiration and drought stress with ground-based thermal remote sensing in agriculture: a review. *J. Exp. Bot.* 63 (13), 4671–4712. <https://doi.org/10.1093/jxb/ers165>.
- Majkowska, A., Kolendowicz, L., Pórolniczak, M., Hauke, J., Czernecki, B., 2017. The urban heat island in the city of Poznań as derived from Landsat 5 TM. *Theor. Appl. Climatol.* 128, 769–783. <https://doi.org/10.1007/s00704-016-1737-6>.
- [38] Maldague, X.P.V., Streckert, H.H., Trimm, M.W., 2001. *Introduction to Infrared and Thermal Testing.* In: Maldague, X.P.V., Moore, P.O. (Eds.), *Infrared and Thermal Testing. Nondestructive Testing Handbook.* American Society for Nondestructive Testing, Columbus, Ohio.
- Maltamo, M., Næsset, E., Vauhkonen, J., 2014. Forestry applications of airborne laser scanning. Concepts and case studies. *Manag. For. Ecosys.* 27, 460. <https://doi.org/10.1007/978-94-017-8663-8>.
- Marešová, J., Majdák, A., Jakuš, R., Hradecký, J., Kalinová, B., Blaženc, M., 2020. The short-term effect of sudden gap creation on tree temperature and volatile composition profiles in a Norway spruce stand. *Trees* 34 (6), 1397–1409. <https://doi.org/10.1007/s00468-020-02010-w>.

- Mattheck, C., Breloer, H., 1994. Field guide for visual tree assessment (VTA). *Arboric. J.* 18 (1), 1–23. <https://doi.org/10.1080/03071375.1994.9746995>.
- Meier, F., Scherer, D., Richters, J., 2010. Determination of persistence effects in spatio-temporal patterns of upward long-wave radiation flux density from an urban courtyard by means of Time-Sequential Thermography. *Remote Sens. Environ.* 114 (1), 21–34. <https://doi.org/10.1016/j.rse.2009.08.002>.
- Meier, F., Scherer, D., 2012. Spatial and temporal variability of urban tree canopy temperature during summer 2010 in Berlin, Germany. *Theor. Appl. Climatol.* 110 (3), 373–384. <https://doi.org/10.1007/s00704-012-0631-0>.
- Melaas, E.K., Wang, J.A., Miller, D.L., Friedl, M.A., 2016. Interactions between urban vegetation and surface urban heat islands: a case study in the Boston metropolitan region. *Environ. Res. Lett.* 11 (5), 054020 <https://doi.org/10.1088/1748-9326/11/5/054020>.
- Minkina, W., Dudzik, S., 2009. Infrared Thermography: Errors and Uncertainties. John Wiley & Sons. <https://doi.org/10.1002/9780470682234.fmatter>.
- Moran, M.S., Clarke, T.R., Inoue, Y., Vidal, A., 1994. Estimating crop water deficit using the relation between surface-air temperature and spectral vegetation index. *Remote Sens. Environ.* 49 (3), 246–263. [https://doi.org/10.1016/0034-4257\(94\)90020-5](https://doi.org/10.1016/0034-4257(94)90020-5).
- Morgan, J.L., Gergel, S.E., Coops, N.C., 2010. Aerial photography: a rapidly evolving tool for ecological management. *BioScience* 60 (1), 47–59. <https://doi.org/10.1525/bio.2010.60.1.9>.
- Mozgeris, G., Gadal, S., Jonikavičius, D., Straigyte, L., Ouerghemmi, W., Juodkienė, V., 2016. Hyperspectral and color-infrared imaging from ultralight aircraft: Potential to recognize tree species in urban environments. 8th Workshop on Hyperspectral Image and Signal Processing: Evolution in Remote Sensing (WHISPERS), Los Angeles, CA, USA. 10.1109/WHISPERS.2016.8071756.
- Mueller, E.C., Day, T.A., 2005. The effect of urban ground cover on microclimate, growth and leaf gas exchange of oleander in Phoenix, Arizona. *Int. J. Biometeorol.* 49 (4), 244–255. <https://doi.org/10.1007/s00484-004-0235-1>.
- Näsi, R., Honkavaara, E., Blomqvist, M., Lyytikäinen-Saarenmaa, P., Hakala, T., Viljanen, N., Kantola, T., Holopainen, M., 2018. Remote sensing of bark beetle damage in urban forests at individual tree level using a novel hyperspectral camera from UAV and aircraft. *Urban. For. Urban. Green.* 30, 72–83. <https://doi.org/10.1016/j.ufug.2018.01.010>.
- Nowak, D.J., Kuroda, M., Crane, D.E., 2004. Tree mortality rates and tree population projections in Baltimore, Maryland, USA. *Urban. For. Urban. Green.* 2 (3), 139–147. <https://doi.org/10.1078/1618-8667-00030>.
- Pauleit, S., 2003. Urban street tree plantings: identifying the key requirements. *Munic. Eng.* 156 (1), 43–50. <https://doi.org/10.1680/muen.2003.156.1.43>.
- [53] Price, J.C., 1979. Assessment of the urban heat island effect through the use of satellite data. *Mon. Weather Rev.* 107 (11), 1554–1557. [https://doi.org/10.1175/1520-0493\(1979\)107<1554:AOTUHI>2.0.CO;2](https://doi.org/10.1175/1520-0493(1979)107<1554:AOTUHI>2.0.CO;2).
- Pyysalo, H., Hyyppä, H., 2002. Reconstructing tree crowns from laser scanner data for feature extraction. *Int. Arch. Photogramm. Remote Sens. Spat. Inf. Sci.* 34 (3/B), 218–221.
- Richter, R., Hutengs, C., Wirth, C., Bannehr, L., Vohland, M., 2021. Detecting Tree Species Effects on Forest Canopy Temperatures with Thermal Remote Sensing: The Role of Spatial Resolution. *Remote Sens.* 13 (1), 135. <https://doi.org/10.3390/rs13010135>.
- Roman, L.A., 2013. *Urban Tree Mortality*. University of California, Berkeley.
- Roy, S., Byrne, J., Pickering, C., 2012. A systematic quantitative review of urban tree benefits, costs, and assessment methods across cities in different climatic zones. *Urban. For. Urban. Green.* 11 (4), 351–363. <https://doi.org/10.1016/j.ufug.2012.06.006>.
- Royle, D.D., Lathrop, R.G., 1997. Monitoring hemlock forest health in New Jersey using Landsat TM data and change detection techniques. *For. Sci.* 43 (3), 327–335. <https://doi.org/10.1093/forestscience/43.3.327>.
- Sanesi, G., Laforetza, R., Marziliano, P.A., Ragazzi, A., Mariani, L., 2007. Assessing the current status of urban forest resources in the context of Parco Nord, Milan, Italy. *Lands. Ecol. Eng.* 3 (2), 187–198. <https://doi.org/10.1007/s11355-007-0031-2>.
- Schuepp, P.H., 1993. Tansley review No. 59. Leaf boundary layers. *N. Phytol.* 125, 477–507.
- Shashua-Bar, L., Pearlmutter, D., Erel, E., 2011. The influence of trees and grass on outdoor thermal comfort in a hot-arid environment. *Int. J. Climatol.* 31 (10), 1498–1506. <https://doi.org/10.1002/joc.2177>.
- Sikorska, D., Sikorski, P., Archiciński, P., Chormański, J., Hopkins, R.J., 2019. You Can't See the Woods for the Trees: Invasive *Acer negundo* L. in Urban Riparian Forests Harms Biodiversity and Limits Recreation Activity. *Sustainability* 11(20), 5838. <https://doi.org/10.3390/su11205838>.
- Smigaj, M., Gaulton, R., Suárez, J.C., Barr, S.L., 2019. Canopy temperature from an Unmanned Aerial Vehicle as an indicator of tree stress associated with red band needle blight severity. *Ecol. Manag.* 433, 699–708. <https://doi.org/10.1016/j.foreco.2018.11.032>.
- Smith, A.P., 1979. Function of dead leaves in *Espeletia schultzii* (Compositae), and Andean caulescent rosette species. *Biotropica* 11 (1), 43–47. <https://doi.org/10.2307/2388171>.
- Sobrino, J.A., Caselles, V., Becker, F., 1990. Significance of the remotely sensed thermal infrared measurements obtained on a citrus orchard. *ISPRS J. Photogramm. Remote Sens.* 44 (6), 343–354. [https://doi.org/10.1016/0924-2716\(90\)90077-0](https://doi.org/10.1016/0924-2716(90)90077-0).
- [65] Sobrino, J.A., Oltra-Carrió, R., Soria, G., Jiménez-Muñoz, J.C., Franch, B., Hidalgo, V., Mattar, C., Julien, Y., Cuenca, J., Romaguera, M., Gómez, J.A., De Miguel, E., Bianchi, R., Paganini, M., 2013. Evaluation of the surface urban heat island effect in the city of Madrid by thermal remote sensing. *Int. J. Remote Sens.* 34 (9–10), 3177–3192. <https://doi.org/10.1080/01431161.2012.716548>.
- Spronken-Smith, R.A., Oke, T.R., 1998. The thermal regime of urban parks in two cities with different summer climates. *Int. J. Remote Sens.* 19 (11), 2085–2104. <https://doi.org/10.1080/014311698214884>.
- Staben, G.W., Lucieer, A., Evans, K.G., Scarth, P., Cook, G.D., 2016. Obtaining biophysical measurements of woody vegetation from high resolution digital aerial photography in tropical and arid environments: Northern Territory, Australia. *Int. J. Appl. Earth Obs. Geoinf.* 52, 204–220. <https://doi.org/10.1016/j.jag.2016.06.011>.
- [69] Su, Y., Wu, J., Zhang, C., Wu, X., Li, Q., Liu, L., Bi, Ch, Zhang, H., Laforetza, R., Chen, X., 2022. Estimating the cooling effect magnitude of urban vegetation in different climate zones using multi-source remote sensing. *Urban Clim.* 43, 101155. <https://doi.org/10.1016/j.uclim.2022.101155>.
- Tallis, M., Taylor, G., Sinnett, D., Freer-Smith, P., 2011. Estimating the removal of atmospheric particulate pollution by the urban tree canopy of London, under current and future environments. *Lands. Urban. Plan.* 103 (2), 129–138. <https://doi.org/10.1016/j.landurbplan.2011.07.003>.
- Tran, H., Uchihama, D., Ochi, S., Yasuoka, Y., 2006. Assessment with satellite data of the urban heat island effects in Asian mega cities. *Int. J. Appl. Earth. Obs. Geoinf.* 8 (1), 34–48. <https://doi.org/10.1016/j.jag.2005.05.003>.
- Tubby, K.V., Webber, J.F., 2010. Pests and diseases threatening urban trees under a changing climate. *Int. J. For. Res.* 83 (4), 451–459. <https://doi.org/10.1093/forestry/cpq027>.
- Tzoulas, K., Korpela, K., Venn, S., Yli-Pelkonen, V., Kazmierczak, A., Niemela, J., James, P., 2007. Promoting ecosystem and human health in urban areas using Green Infrastructure: A literature review. *Lands. Urban. Plan.* 81 (3), 167–178. <https://doi.org/10.1016/j.landurbplan.2007.02.001>.
- Ullah, S., Schlerf, M., Skidmore, A.K., Hecker, C., 2012. Identifying plant species using mid-wave infrared (2.5–6 μm) and thermal infrared (8–14 μm) emissivity spectra. *Remote Sens. Environ.* 118, 95–102. <https://doi.org/10.1016/j.rse.2011.11.008>.
- Urban Atlas, 2018. (<https://land.copernicus.eu/local/urban-atlas/urban-atlas-2018>) (accessed: 4th March 2022).
- Vaishery, L.S., Jaganmohan, M., Nagendra, H., 2013. Effect of street trees on microclimate and air pollution in a tropical city. *Urban. For. Urban. Green.* 12 (3), 408–415. <https://doi.org/10.1016/j.ufug.2013.03.002>.
- Vogel, S., 2009. Leaves in the lowest and highest winds: temperature, force and shape. *N. Phytol.* 183 (1), 13–26. <https://doi.org/10.1111/j.1469-8137.2009.02854.x>.
- Wakiyama, Y., 2002. Infrared remote sensing for canopy temperature in paddy field and relationship between leaf temperature and leaf color. *J. Agric. Meteorol.* 58 (4), 185–194. <https://doi.org/10.2480/agrmet.58.185>.
- Wang, J., Sammis, T.W., Gutschick, V.P., Gebremichael, M., Dennis, S.O., Harrison, R.E., 2010. Review of satellite remote sensing use in forest health studies. *Open Geogr. J.* 3 (1), 10.2174/1874923201003010028.
- Weather Underground, 2014–2022. (<https://www.wunderground.com/>) (accessed: 18th February 2022).
- Yu, C., Hien, W.N., 2006. Thermal benefits of city parks. *Energy Build.* 38 (2), 105–120. <https://doi.org/10.1016/j.enbuild.2005.04.003>.
- Zakrzewska, A., Kopec, D., Krajewski, K., Charyton, J., 2022. Canopy temperatures of selected tree species growing in the forest and outside the forest using aerial thermal infrared (3.6–4.9 μm) data. *Eur. J. Remote Sens.* 55 (1), 313–325. <https://doi.org/10.1080/22797254.2022.2062055>.
- Zheng, S., Guldmann, J.M., Liu, Z., Zhao, L., 2018. Influence of trees on the outdoor thermal environment in subtropical areas: an experimental study in Guangzhou, China. *Sustain. Cities Soc.* 42, 482–497. <https://doi.org/10.1016/j.scs.2018.07.025>.
- Zhou, Z., Majeed, Y., Naranjo, G.D., Gambacorta, E.M., 2021. Assessment for crop water stress with infrared thermal imagery in precision agriculture: A review and future prospects for deep learning applications. *Comput. Electron. Agric.* 182, 106019. <https://doi.org/10.1016/j.compag.2021.106019>.

**Oświadczenia współautorów
publikacji wchodzących w skład
rozprawy doktorskiej**

Łódź, 07.12.2022

miejsowość i data

Mgr. Agata Zakrzewska

Katedra Biogeografii, Paleoekologii i Ochrony Przyrody

Instytut Ekologii i Ochrony Środowiska

Stefana Banacha 1/3, 90-232 Łódź

Oświadczenie

Oświadczam, że w pracy:

Zakrzewska A., Kopeć D., Krajewski K. & Charyton J. (2022) *Canopy temperatures of selected tree species growing in the forest and outside the forest using aerial thermal infrared (3.6–4.9 μm) data. European Journal of Remote Sensing, 55:1, 313-325, DOI:10.1080/22797254.2022.2062055* mój udział polegał na przygotowaniu naziemnych danych referencyjnych do analiz, manualnym tworzeniu poligonów koron drzew, zaimplementowanie mapy zacielenia, wyznaczeniu z wykorzystaniem danych termalnych temperatur koron analizowanych drzew, analizie statystycznej i współudziale w interpretacji wyników, wykonaniu rycin 1, 2, 3 i 5, napisaniu rozdziałów: *Introduction, Materials and methods, Results, Discussion*, współtworzeniu rozdziałów: *Airborne data acquisition* i *Conclusions*, edytowaniu finalnej wersji manuskryptu, przygotowaniu większości odpowiedzi dla recenzentów i poprawie manuskryptu zgodnie z uwagami redakcji i recenzentów. Swój udział oceniam na 50%.

Zakrzewska, A., & Kopeć, D. (2022). *Remote sensing of bark beetle damage in Norway spruce individual tree canopies using thermal infrared and airborne laser scanning data fusion. Forest Ecosystems, 100068. <https://doi.org/10.1016/j.fecs.2022.100068>* mój udział polegał na zbiorze naziemnych danych referencyjnych, przygotowaniu naziemnych danych referencyjnych do analiz, manualnym tworzeniu poligonów koron drzew, zaimplementowanie mapy gap fraction, wyznaczeniu z wykorzystaniem danych termalnych temperatur koron analizowanych drzew, analizie statystycznej (przeprowadzenie analizy K-mean clustering) współudziale w interpretacji wyników, wyznaczeniu miar dokładności, wykonaniu rycin 1, 2, 3, 4, 6, 8, 9, 10 i 11, napisaniu wszystkich rozdziałów pracy: *Introduction, Materials and methods, Results, Discussion* i *Conclusions*, edytowaniu finalnej wersji manuskryptu, przygotowaniu większości odpowiedzi dla recenzentów i poprawie manuskryptu zgodnie z uwagami redakcji i recenzentów. Swój udział oceniam na 60%.

Zakrzewska A., Kopeć D., Ochtyra A. & Potůčková M. (2022). *Can canopy temperature acquired from an airborne level be a tree health indicator in an urban environment? Urban Forestry & Urban Greening, 127807. <https://doi.org/10.1016/j.ufug.2022.127807>* mój udział polegał na zbiorze naziemnych danych referencyjnych, przygotowaniu naziemnych danych referencyjnych do analiz, manualnym tworzeniu poligonów koron drzew, zaimplementowanie mapy gap fraction, wyznaczeniu z

wykorzystaniem danych termalnych temperatur koron analizowanych drzew, przeprowadzeniu wyboru losowego, opracowaniu wyników, analizie statystycznej i współudziale w interpretacji wyników, wykonaniu rycin 1, 2, 3, 4, 6 i 7, napisaniu rozdziałów pracy: *Introduction, Materials and methods, Results* i *Conclusions*, współudziale w pisaniu rozdziału *Discussion*, edytowaniu finalnej wersji manuskryptu, przygotowaniu większości odpowiedzi dla recenzentów i poprawie manuskryptu zgodnie z uwagami redakcji i recenzentów. Swój udział oceniam na 55%.

Agata Zakrzewska

podpis

.....
tcdz 07-12-2022

.....
miejsowość i data

dr hab. Dominik Kopeć, prof. UŁ

Katedra Biogeografii, Paleoekologii i Ochrony Przyrody

Instytut Ekologii i Ochrony Środowiska

Stefana Banacha 1/3, 90-232 Łódź


Oświadczenie

Oświadczam, że w pracy:

Zakrzewska A., Kopeć D., Krajewski K. & Charyton J. (2022) Canopy temperatures of selected tree species growing in the forest and outside the forest using aerial thermal infrared (3.6–4.9 μm) data, European Journal of Remote Sensing, 55:1, 313-325, DOI:10.1080/22797254.2022.2062055 mój udział polegał na sprawowaniu nadzoru merytorycznego i naukowego nad prowadzonymi badaniami, zdefiniowaniu hipotezy badawczej, udziale w projektowaniu analiz i interpretacji wyników, korekcie tekstu manuskryptu, współudziale w pisaniu rozdziału *Conclusions*, opracowaniu graficznym wyników przedstawionych na rycinach 4, 6 i 7, procedowaniu procedur w czasopiśmie naukowym, przygotowaniu części odpowiedzi dla recenzentów, zapewnienie finansowania dla prowadzonych badań. Swój udział oceniam na 40%.

Zakrzewska, A., & Kopeć, D. (2022). Remote sensing of bark beetle damage in Norway spruce individual tree canopies using thermal infrared and airborne laser scanning data fusion. Forest Ecosystems, 100068. <https://doi.org/10.1016/j.fecs.2022.100068> mój udział polegał na sprawowaniu nadzoru merytorycznego i naukowego nad prowadzonymi badaniami, zdefiniowaniu hipotezy badawczej, udziale w projektowaniu analiz i interpretacji wyników, wykonaniu oceny analizy K-mean clustering, korekcie tekstu manuskryptu, wykonaniu rycin 5 i 7, procedowaniu procedur w czasopiśmie naukowym, przygotowaniu części odpowiedzi dla recenzentów, zapewnienie finansowania dla prowadzonych badań. Swój udział oceniam na 40%.

Zakrzewska A., Kopeć D., Ochtyra A. & Potůčková M. (2022). Can canopy temperature acquired from an airborne level be a tree health indicator in an urban environment? Urban Forestry & Urban Greening, 127807. <https://doi.org/10.1016/j.ufug.2022.127807> mój udział polegał na sprawowaniu nadzoru merytorycznego i naukowego nad prowadzonymi badaniami, zdefiniowaniu hipotezy badawczej, udziale w projektowaniu analiz i interpretacji wyników, korekcie tekstu manuskryptu, wykonaniu ryciny 5, procedowaniu procedur w czasopiśmie naukowym, przygotowaniu części odpowiedzi dla recenzentów, zapewnienie finansowania dla prowadzonych badań. Swój udział oceniam na 30%.

.....


.....
podpis


.....Tarnów, 25.11.2022.....

miejsowość i data

Karol Krajewski
MGGP Aero Sp. z o.o.
Kaczkowskiego 6,
33-100 Tarnów

Oświadczenie

Oświadczam, że w pracy: *Zakrzewska A., Kopeć D., Krajewski K. & Charyton J. (2022) Canopy temperatures of selected tree species growing in the forest and outside the forest using aerial thermal infrared (3.6–4.9 μm) data, European Journal of Remote Sensing, 55:1, 313-325, DOI:10.1080/22797254.2022.2062055* mój udział polegał na utworzeniu mozaiki danych termalnych na podstawie surowych obrazów i współdziałałem w pisaniu rozdziału *Airborne data acquisition* polegający na opisanu procesu przetworzenia danych termalnych. Swój udział oceniam na 5%.



podpis

WARSZAWA 29.11.2022

miejsowość i data

Jakub Charyton

MGGP Aero Sp. z o.o.

al. Jerozolimskie 81

02-001 Warszawa

Oświadczenie

Oświadczam, że w pracy: *Zakrzewska A., Kopeć D., Krajewski K. & Charyton J. (2022) Canopy temperatures of selected tree species growing in the forest and outside the forest using aerial thermal infrared (3.6–4.9 μm) data, European Journal of Remote Sensing, 55:1, 313-325, DOI:10.1080/22797254.2022.2062055* mój udział polegał na wykonaniu mapy zacielenia (*illumination map*) na podstawie danych hiperspektralnych i współdziałałem w pisaniu rozdziału *Airborne data acquisition* polegający na opisanu przetworzenia danych hiperspektralnych i skaningu laserowego. Swój udział oceniam na 5%.

Jakub Charyton.....

podpis

Ostrówek, 12.12.2022

miejsowość i data

dr inż. Adrian Ochtyra

Uniwersytet Warszawski

Wydział Geografii i Studiów Regionalnych

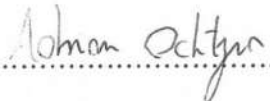
Zakład Geoinformatyki, Kartografii i Teledetekcji

ul. Krakowskie Przedmieście 30

00-927 Warszawa

Oświadczenie

Oświadczam, że w pracy: *Zakrzewska A., Kopeć D., Ochtyra A. & Potůčková M. (2022). Can canopy temperature acquired from an airborne level be a tree health indicator in an urban environment? Urban Forestry & Urban Greening, 127807. <https://doi.org/10.1016/j.ufug.2022.127807>* mój udział polegał na sprawowaniu nadzoru merytorycznego i naukowego nad prowadzonymi badaniami, współdziałale w analizie i interpretacji wyników, współdziałale w pisaniu rozdziału *Discussion*, korekcie tekstu manuskryptu i przygotowaniu części odpowiedzi dla recenzentów. Swój udział oceniam na 13%.


.....

podpis

Prague, 5th December 2022

Ing. Markéta Potůčková, Ph.D.

Department of Applied Geoinformatics and Cartography,

Faculty of Science,

Charles University,

Albertov 2038/6, 128 00 Praha, Czech Republic

e-mail: marketa.potuckova@natur.cuni.cz

Statement

I hereby declare that my contribution to the considered paper entitled: *Zakrzewska A., Kopeć D., Ochtyra A. & Potůčková M. (2022). Can canopy temperature acquired from an airborne level be a tree health indicator in an urban environment? Urban Forestry & Urban Greening, 12780, <https://doi.org/10.1016/j.ufug.2022.127807>* consisted of discussing the applied methodology and data processing, proofreading the text of the manuscript and preparing part of the responses for reviewers. My contribution is valued as 2%.



.....